Sensitivity enhancement in NMR by using parahydrogen induced polarization

Dissertation zur Erlangung des Grades
Doktor der Naturwissenschaften
am Fachbereich Chemie
der Johannes Gutenberg-Universität
in Mainz

Meike Roth
geboren in Mainz

Mainz 2010

Die vorliegende Arbeit wurde in der Zeit von September 2007 bis April 2010 am Max-Planck-Institut für Polymerforschung in Mainz angefertigt.

Dekan:
Erster Berichterstatter:
Zweiter Berichterstatter:

Tag der mündlichen Prüfung: 21.05.2010

"Es kommt nicht darauf an, mit dem Kopf durch die Wand zu rennen, sondern mit den Augen die Tür zu finden."

Albert Einstein

Contents

Abbreviations

ALTADENA	adiabatic longitudinal transport after dissociation engenders net alignment
BAC	biologically active compound
CACA	cis-4-amino-crotonic acid
CAS	chemical abstracts-number
COD	cyclooctadiene
COSY	correlation spectroscopy
d	doublet
dd	doublet of doublets
DNP	dynamic nuclear polarization
dppb	(diphenylphosphino)butane
dppbs	[diphenyl-sulfonate)phosphine]butane
e.g.	exempli gratia
FD	field desorption
FID	free induction decay
FT	fourier transformation
GABA	γ-aminobutyric acid
i.e.	id est
INEPT	insensitive nuclei enhancement by polarisation
IR	infrared
IUPAC	international union of pure and applied chemistry
LDA	lithium diisopropylamide
m	multiplet
MHz	megahertz
MRI	magnetic resonance imaging
MS	mass spectrum
NMR	nuclear magnetic resonance
NOE	nuclear Overhausen effect
nor	norbonadiene
NVP	N-vinyl-2-pyrrolidone

o-H_2	orthohydrogen
p-H_2	parahydrogen
PASADENA	parahydrogen and synthesis allow dramatically enhanced nuclear alignment
Pgp	permeability glycoprotein
PH-INEPT	parahydrogen-insensitive nuclei enhancement by polarisation
PHIP	parahydrogen induced polarization
Photo-CIDNP	photochemically induced dynamic nuclear polarization
ppbs	(phenyl-propane sulfonate)phosphine
ppm	parts per million
PVP	polyvinylpyrrolidone
pyr	pyridine
qu	quartet
rf	radio frequency
s	singlet
SE	signal enhancement
SNR	signal-to-noise ratio
SSRIs	selective serotonin reuptake inhibitors
t	triplet
TACA	trans-4-amino-crotonic acid
tchp	tricyclohexylphosphine
tdmpp	tris(dimethyl-phenylphosphine)
TPA	time point of acquisition
tpps	[triphenyl-sulfonate phosphine)
tppsm	triphenyl-sulfonate-methoxy phosphine)

1 Introduction

The origin of nuclear magnetic resonance (NMR) dates back to the experimental proof of the proton spin in 1933 by Otto Stern. Since its discovery in 1946 by two independent groups [1,2], nuclear magnetic resonance spectroscopy has turned out to be a powerful spectroscopic technique in analytical chemistry. Nowadays, its applications are spread over a huge range like for example the nondestructive detection of substances in a sample or the determination of the structure of small and big molecules (like proteins) and, furthermore, investigations of intra- and intermolecular interactions. However, unfortunately NMR spectroscopy is a rather insensitive technique due to only poor population differences between the Zeeman energy levels resulting in a minute polarization of the sample. This inherent handicap is caused by the low gyromagnetic ratio of the nuclear spins. Thus, the lack of sensitivity of nuclear magnetic resonance makes hyperpolarization techniques and their further development of great importance for NMR measurements.

Several possibilities are known to produce hyperpolarized molecules which means molecules obtaining an intense overpopulation of one of the Zeeman energy levels. Caused by this overpopulation a sensitivity enhancement of several orders of magnitude of nuclear magnetic resonance spectroscopy can be achieved. Well-known hyperpolarization techniques are e.g. dynamic nuclear polarization (DNP) [3–6], photochemically induced dynamic nuclear polarization (Photo-CIDNP) [7–9] and parahydrogen induced polarization (PHIP) [10–18].

Parahydrogen induced polarization is based on a chemical reaction which generates hyperpolarized product molecules. This chemical reaction is a homogeneously catalyzed hydrogenation of an unsaturated precursor with parahydrogen. Parahydrogen is one of the two spin isomers of thermal hydrogen, namely the antisymmetric spin isomer which forms a singlet state. As it is the low energy spin isomer its content can be enriched in thermal hydrogen by cooling. The spin isomer parahydrogen itself is nonmagnetic and thus NMR silent. However, the implementation of a hydrogenation reaction with parahydrogen can create two magnetically non-equivalent protons in the hydrogenation product. These two inserted protons populate only specific energy levels and hence exhibit a polarization far above the Boltzmann polarization. This leads to a theoretical signal increase in NMR spectroscopy of up to 10^5.

Due to the strong NMR signals produced via parahydrogen induced polarization, this method finds a lot of applications in chemistry e.g. the characterization of short-lived reaction intermediates or the investigation of catalytic mechanisms. Also in medicine it opens up the possibility to boost the sensitivity of medical diagnostics via magnetic labeling of active contrast agents enabling the examination of metabolisms of physiological relevant substances via magnetic resonance imaging (MRI) [19,20]. Thus, further examination and optimization of the PHIP technique with regard to these topics is of significant importance.

As this hyperpolarization method represents a unique combination between chemistry itself and NMR spectroscopy it offers a large range of physical, chemical, biological and spectroscopical applications. However, the aim of this work was not to explore one specific application but to investigate and improve the overall technique. Therefore, at the beginning of this work the basic theoretic background of the PHIP method is explained. The main part will discuss the PHIP method with regard to different experimental aspects and demonstrate their optimization. This more general investigation of PHIP bears the possibility to interact between certain topics and thus optimize the PHIP method as a whole. Taking this into account, the main part is divided in two chapters. The first part focuses on optimizing the parahydrogen technique on model compounds (Chapter 3). Thereby, the reaction conditions of the hydrogenation reaction display an important point of interest. This includes for example the implemented pressure and temperature during the reaction or the utilization of different catalyst systems for the homogeneous hydrogenation. Another aspect discussed in Chapter 3 deals with the measurement conditions during the hydrogenation with regard to the application setup of parahydrogen or the present magnetic field strength during the hydrogenation. Further examinations focus on a more spectroscopic part, namely the aim to transer the generated polarization from the protons to heteronuclei like especially ^{13}C nuclei.

The second part deals with the examination of physiological relevant substances taking the later application of PHIP in medicine into account (Chapter 4). Hence, the advantages identified in Chapter 3 are transferred to such molecules in order to achieve hyperpolarization of biological active compounds (BACs). One group of interesting substances in Chapter 4 is represented by metabolites or neurotransmitters in mammalian cells. Achieving significantly high signal enhancements on the protons and the carbons of these substances would offer the opportunity to investigate their metabolism and function in the body at the target tissue. Other interesting substances investigated in this chapter are clinically relevant drugs and pharmaceuticals. Thereby, depressants and narcotics like a barbituric acid derivative or antidepressant drugs like citalopram

are investigated with regard to their applicability for the PHIP technique and the possibility to achieve polarization transfer to ^{13}C nuclei exhibiting long spin-lattice relaxation times. This would open up the possibility to investigate the mechanism of action and the biotransformation of pharmaceutical compounds in vivo. The last investigated substrate belonging to this group is a polymerizable monomer whose polymer was used as a blood plasma expander for trauma victims after the first half of the 20th century. The idea in this case is to investigate the utility of the monomer for the PHIP technique as a basis for later investigations of a polymerization reaction using hyperpolarized monomers.

Thus, by combining different disciplines of research, the present thesis covers on one hand the optimization of the overall PHIP technique and on the other hand applies the achieved results to the utilization of PHIP for physiological relevant substances. In Chapter 5 the results of the different investigated aspects are merged and summarized in order to draw a conclusion of the accomplished effort.

2 Theory

2.1 Hyperpolarization

One drawback of nuclear magnetic resonance spectroscopy is its lack of sensitivity due to the low spin polarization at thermal equilibrium. This is caused by the low gyromagnetic ratio of the nuclear spins resulting in a small population difference between the Zeeman energy levels occupied according to the Boltzmann distribution (Equation 2.1).

$$\frac{N_+}{N_-} = e^{-\gamma\hbar B_0/k_B T} \approx 1 - \frac{\gamma\hbar B_0}{k_B T} \tag{2.1}$$

Here, the gyromagnetic ratio γ is a fundamental property of the nucleus in question. Therefore, the sensitivity can be increased via two means: either at the lowest possible temperature and/or at the highest possible magnetic field. In practice, both factors are limited to certain values depending on the properties of the investigated sample or technical problems. Driven by this reality, recent years have witnessed extensive efforts to devise alternatives that prepare nuclei in hyperpolarized states. Hyperpolarization, in a physical meaning, is the nuclear spin polarization of a material far beyond thermal equilibrium conditions. This means the intense overpopulation of one energy level with respect to the other as depicted in Figure 2.1 which results in a large net polarization of the sample. In comparison to the thermal polarization described in Equation 2.1, hyperpolarization is independent of the magnetic field strength and the temperature of the sample. Furthermore, the hyperpolarized state turns back into the state of equilibrium via spin-lattice relaxation. This returning process is irreversible and the hyperpolarization cannot be regained by normal relaxation processes.

Hyperpolarization is commonly applied to gases such as ^{129}Xe and ^{3}He which are used, for instance, in hyperpolarized magnetic resonance imaging (MRI) of the lungs

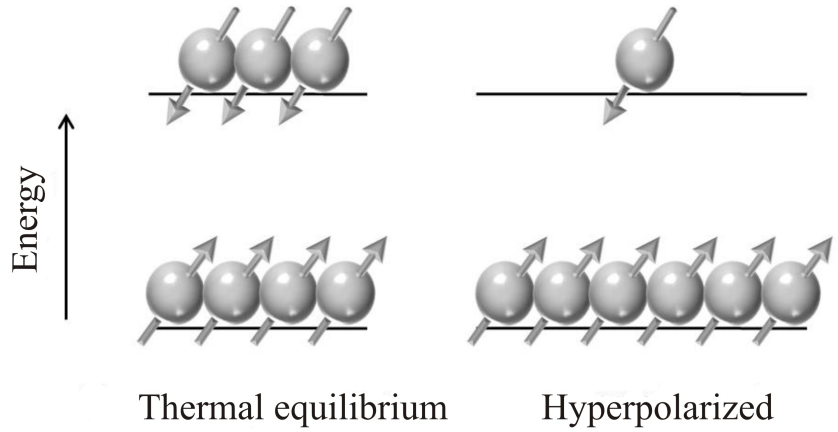

Figure 2.1: Scheme of the population of energy levels at thermal equilibrium and when hyperpolarized.

[21–23]. Hyperpolarization of ^{129}Xe and ^{3}He can be achieved by the spin exchange optical pumping method [24, 25]; in addition hyperpolarized ^{3}He can also be generated via metastable optical pumping [26–29]. As the overall application of hyperpolarized gases is limited, hyperpolarization techniques also working in the liquid or solid state are of great importance for NMR measurements and its applications in physics, chemistry, biology and medicine. These other techniques include for example dynamic nuclear polarization (DNP) for solids at cryogenic temperatures and liquids at room temperature [3–6, 30, 31], photochemically induced dynamic nuclear polarization (Photo-CIDNP) for liquids [7–9] and parahydrogen induced polarization (PHIP) used in the gas and in the liquid phase [10–18]. The latter is a versatile technique to generate hyperpolarized molecules via a chemical route and was applied in this work.

2.2 Parahydrogen Induced Polarization

The discovery of the PHIP effect dates back to the early eighties of the 20th century. Due to the world-wide energy crisis investigations whether the production of gasoline from coal might be an alternative were carried out. Therefore, Prof. Robert Bergman of the UC Berkeley asked his graduate student Henry Bryndza in 1979 to examine model systems for the FischerTropsch reaction, which requires a cobalt catalyst. By storing the samples over the weekend at liquid nitrogen temperature, the PHIP effect was first observed in 1980 by Bryndza and Bergmann and named the monday phenomenon [32]. The resulting NMR spectra showed characteristic, considerable en-

hanced antiphase signals. In 1986, the PHIP effect was theoretically predicted by Bowers and Weitekamp [33] and proved experimentally one year later by two independent groups [10, 12].

PHIP spectroscopy is based on a homogeneous hydrogenation reaction of an unsaturated molecule with parahydrogen. Bowers and Weitekamp obtained the characteristic antiphase signals during the hydrogenation of acrylonitrile with parahydrogen inside the spectrometer and called the effect PASADENA (parahydrogen and synthesis allow dramatically enhanced nuclear alignment) [33]. While implementing the PHIP experiment outside the magnet, different peak pattern as the PASADENA-pattern are generated which got the name ALTADENA (adiabatic longitudinal transport after dissociation engenders net alignment) in 1988 by Pravica and Weitekamp [11]. Nowadays, the abbreviation PHIP is used as the general term of the phenomenon in common, whereas the acronyms PASADENA and ALTADENA are used to distinguish the different possible reaction conditions. One limiting factor of the PHIP effect is the loss of hyperpolarization due to T_1 relaxation in the product. Therefore, transfer of the initially created proton polarization to heteronuclei, which on average have longer relaxation times, is of great importance.

The achieved signal enhancement with parahydrogen induced polarization permit the examination of reaction mechanisms and kinetics in situ, especially the detection and analysis of otherwise elusive reaction intermediates in hydrogenation reactions. With regard to medical applications, PHIP opens up the possibility to utilize active contrast agents in magnetic resonance imaging.

2.2.1 Ortho- and Parahydrogen

Under normal conditions, hydrogen gas is a mixture of two states exhibiting different relative orientations of their nuclear spins [34]. The symmetry properties of molecular hydrogen give rise to two spin isomers, namely the magnetic orthohydrogen and the non-magnetic parahydrogen. Both types are connected via the following temperature depending equation of equilibrium (Equation 2.2).

$$o - H_2 \rightleftharpoons p - H_2 \qquad \Delta H_0 = -0{,}08 \quad kJ/molR \tag{2.2}$$

Under standard conditions, normal hydrogen consists of 74.9% of ortho- and 25.1% parahydrogen [35]. Regarding their physical properties, the two spin isomers show only minor differences as for example a deviation of 0.1 K for their melting points.

Nuclear Spin of Hydrogen

Via linear combination of the individual nuclear spins of the hydrogen atoms in the molecule, two possible spin isomers are generated. In case of parallel alignment of the nuclear spins, the resulting spin isomer is called orthohydrogen (o-H_2), whereas, if the nuclear spins of the protons are arranged in an antiparallel way, parahydrogen (p-H_2) is the generated spin isomer (Figure 2.2).

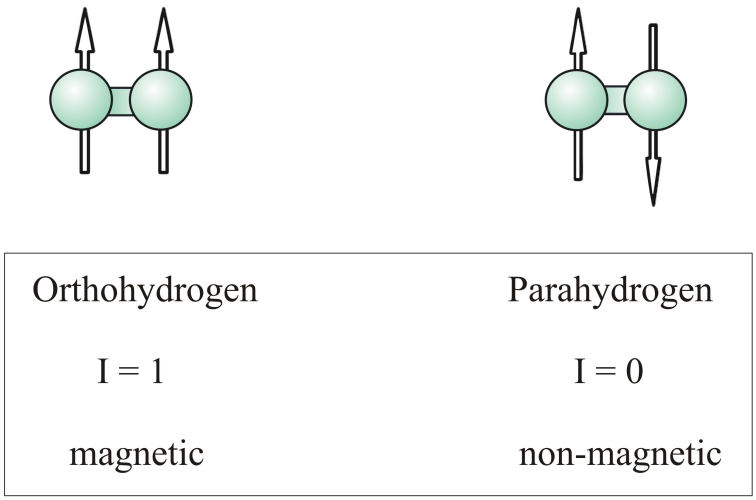

Figure 2.2: The two existing spin isomers of molecular hydrogen.

While the diamagnetic p-H_2 represents a singlet state with a corresponding total nuclear spin of I = 0, orthohydrogen is a degenerated triplet state which shows paramagnetic behavior with a resulting total nuclear spin of I = 1. The outcome of the threefold degeneration of o-H_2 in absence of a magnetic field is the above mentioned ratio between o-H_2 and p-H_2 of 3:1. At the presence of a magnetic field, the singlet state of p-H_2 is unaffected, whereas the triplet state of o-H_2 splits up as a result of the Zeeman-effect (Figure 2.3) [35].

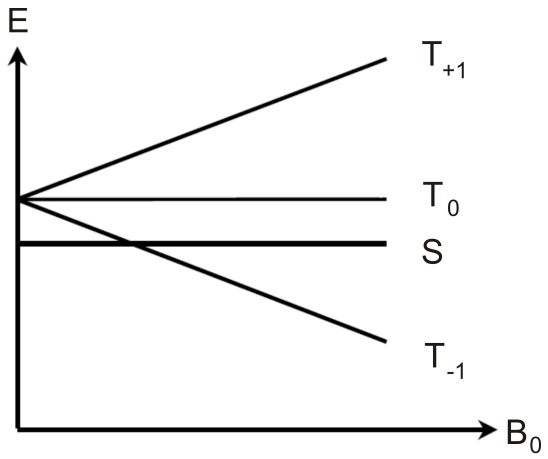

Figure 2.3: Energy levels of the triplet state orthohydrogen and the singlet state parahydrogen with respect to the magnetic field strength.

The three possible alignments with respect to the outer magnetic field, namely with, against or orthogonal to the field are characterized as the triplet states T_{+1}, T_{-1} and T_0 (Figure 2.4). The explanation for the energy difference between the two spin isomers is based on the total wave function of the molecule. The total wave function is represented by a product of independent parts originating from translation, vibration, electronical motion, rotation and nuclear spin (Equation 2.3) [13].

$$\Psi_{total} = \Psi_{translation} * \Psi_{vibration} * \Psi_{electronical} * \Psi_{rotation} * \Psi_{nuclearspin} \tag{2.3}$$

As the total system of hydrogen is classified as a fermion system, the symmetry of the total wave function has to be odd according to the Pauli principle. As the vibrational and electronical part are not excited at room temperature, they can be neglected for the further examination. The most relevant terms of the total wave function are the nuclear spin wave function and the rotational wave function. Therefore, the product of these two parts, namely of rotation and nuclear spin should be antisymmetric. By rotating the molecule around 180°, the two nuclei interchange their actual positions. This process is correlated to the rotational quantum number J = 1 and a change of sign of the rotational wave function. Via rotation of 0° or 360° the molecule is displayed on itself without any change of sign of the wave function. The corresponding quantum numbers

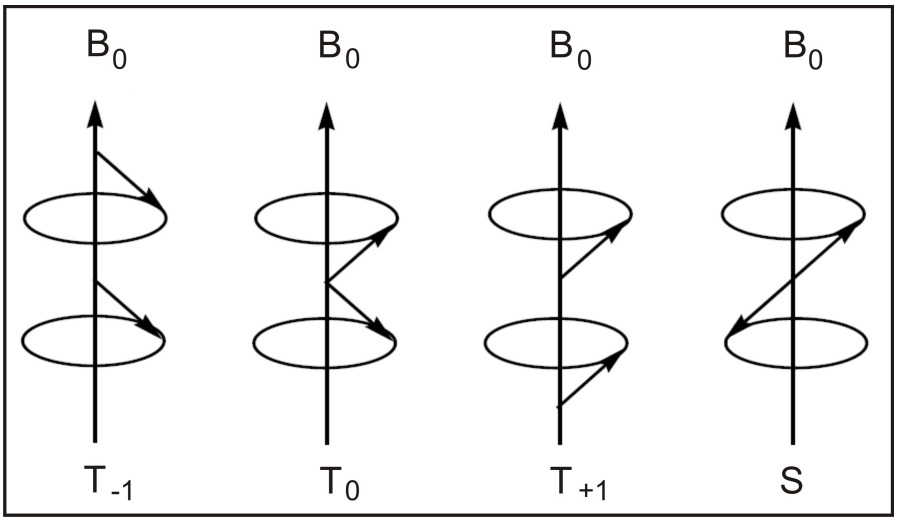

Figure 2.4: Alignment of the nuclear spin vectors of hydrogen in a magnetic field.

to this processes are J = 0 for the 0° rotation and J = 2 for the rotation of 360° [36,37]. In order to satisfy the antisymmetric conditions of the total wave function of parahydrogen, the antisymmetric singlet state of the nuclear part leads to a population of the even rotational quantum numbers coupled with symmetric states. In contrast, the symmetric triplet state of the nuclear part of orthohydrogen causes the population of the odd rotational quantum numbers belonging to antisymmetric states. Due to the fact that the corresponding states of even rotational quantum numbers are energetically preferred, it becomes obvious that parahydrogen is the low energy spin isomer.

Parahydrogen Enrichment

For the enrichment of p-H_2, Equation 2.3 plays an important role. Hence, an enrichment of the low-energy isomer p-H_2 can be achieved via cooling of the thermal hydrogen mixture. The exchange of the alignment of the nuclear spins into the antiparallel orientation occurs very slowly as a result of the symmetry forbidden transition between nuclear spin states of different multiplicities. For this reason, the use of an adequat catalyst systems during the enrichment of parahydrogen is important. By cooling normal hydrogen to 77 K with liquid nitrogen in the presence of active charcoal as the conversion catalyst, a content of 50% p-H_2 is achieved. Further cooling to 30 K leads to a content of more than 95% of p-H_2 in the mixture [38,39] (Figure 2.5). Due to the symmetry forbidden transition between ortho- and parahydrogen in the absence of a catalyst system, the latter is stable and can be stored for several days.

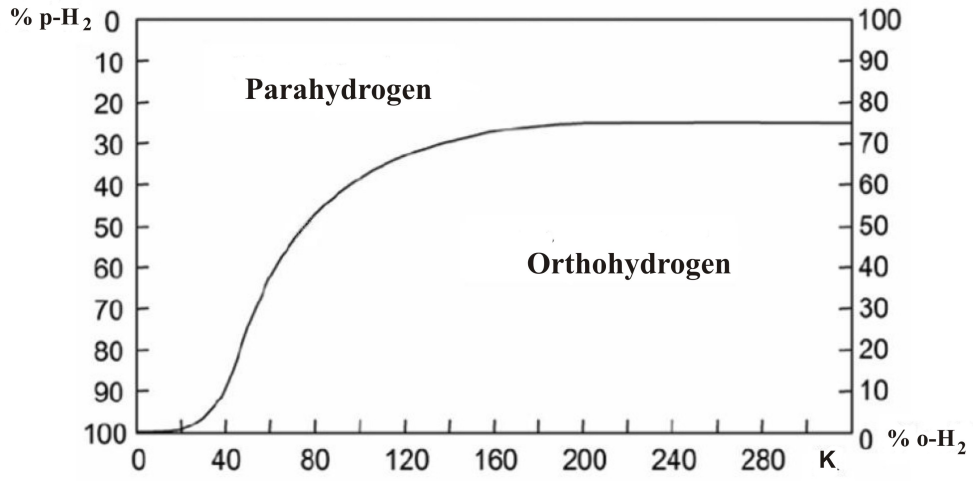

Figure 2.5: Plot of the equilibrium equation of ortho- and parahydrogen in dependence of the temperature.

2.2.2 The Chemical Reaction behind the PHIP Method

Parahydrogen induced polarization is a chemical method, which makes use of the correlation between nuclear spins in parahydrogen to create hyperpolarized molecules. The key feature of this technique is the pairwise and simultaneous transfer of the two hydrogen atoms of parahydrogen to a double or triple bond resulting in a population of the Zeeman energy levels different from the Boltzmann equation. The obtained hyperpolarization results in antiphase peaks in the NMR spectrum with high intensities. The whole PHIP process is depicted in Figure 2.6.

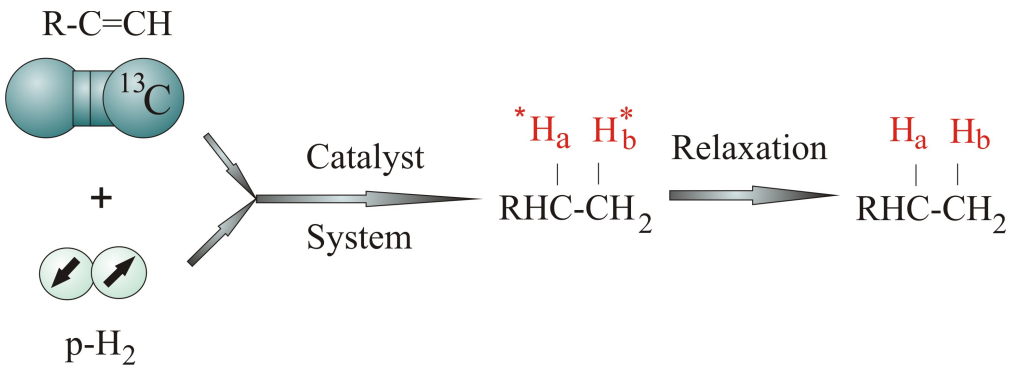

Figure 2.6: Scheme of the parahydrogenation.

After the creation of the hyperpolarized system, this excited state returns into the state of equilibrium via relaxation processes. This results in a decay of the generated enhanced signals during a system-dependent time frame (T_1-relaxation rate). As this relaxation process starts directly after breaking the symmetry of p-H_2 by transfering it to different positions of the catalyst system, the transfer of the hydrogen atoms to the substrate molecule has to occur faster than the relaxation process. Otherwise, part of the polarization will be lost during the reaction and eventually no PHIP signal will remain detectable.

Homogeneous Hydrogenation

The transfer of para-enriched hydrogen to an unsymmetric, unsaturated substrate is the basic requirement for the generation of hyperpolarized product molecules. In practice, this transfer is implemented via a catalyzed homogeneous hydrogenation reaction. One important point in matters of the hydrogenation mechanism with parahydrogen is the pairwise transfer of both atoms of the hydrogen molecule to the substrate molecule. Of utmost importance is that the correlation between the former p-H_2 atoms does not break during the reaction. The underlying mechanism of the homogeneous hydrogenation can follow two different pathways depending on the properties of the used catalyst system and the hydrogenation substrate. With respect to the nature of the first reaction steps, the homogeneous hydrogenation can be divided into the so-called “dihydride” and the ”unsaturated” routes [35].

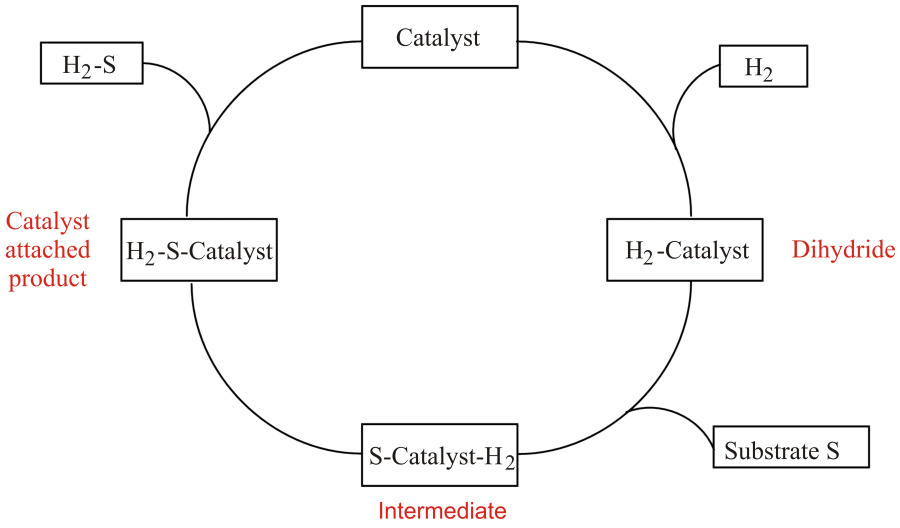

Figure 2.7: Dihydride route of homogeneous hydrogenation.

In compliance with Jack Halpern's step-wise analysis [40], the well-known "Wilkinson's catalyst" follows the "dihydride" route depicted in Figure 2.7 [37]. In the first step, this cycle includes the oxidative addition of H_2 to the metal center. Afterwards the reaction of the dihydride rhodium complex with an unsaturated precursor leads to a dihydride substrate complex as a short-lived reaction intermediate. After insertion of the substrate into the metal-hydride-bonding, the catalyst is released via reductive elimination of the hydrogenated product.

In comparison, the DIPHOS catalyst as an cationic rhodium complex containing a chiral phosphine ligand reacts following the "unsaturated" route shown in Figure 2.8 [41, 42].

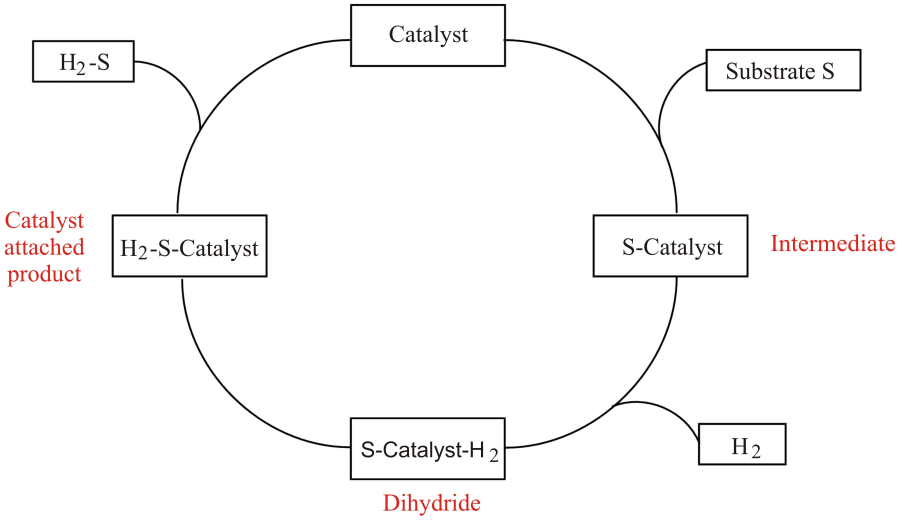

Figure 2.8: Unsaturated route of homogeneous hydrogenation.

In both reaction routes the catalyst is activated via dissociation of a former ligand and subsequent ligation of the present solvent. This means for the Wilkinson's catalyst, that one of the three phosphine ligands is replaced by a solvent molecule. In contrast, the DIPHOS catalyst is normaly generated by a precatalyst system containing a diene as a ligand. After hydrogenation of the diene to an alkane, it is eliminated from any subsequent reaction scheme as it has no known coordination chemistry and a solvent molecule acts as a further ligand to the metal [41]. The hereby activated catalyst forms an intermediate by ligation of the substrate in exchange with the solvent molecule. This intermediate undergoes a reaction with H_2 leading to a dihydride-substrate-complex. After transferring both hydrogen atoms from the metal center to the substrate, the hydrogenated product is reductively eliminated and leaves the catalyst system.

Depending on the dominating reaction route, different mechanisms underly the homogeneous hydrogenation and variable reaction intermediates are generated. Not only the properties of the catalyst system play an important role in this case, but also the steric and electronic properties of the unsaturated substrate molecule. Different properties of the utilized substrates bear the need of choosing matching catalyst systems, which led to the examination of several catalyst systems in this work. Because the signal enhancement strongly depends on the conversion rate of the hydrogenation reaction, high-performance catalysts have to be implemented to speed up the reaction. The catalyst systems used for our experiments are homogeneous, cationic rhodium or iridium complexes which show high activity in combination with low substrate specivity. Furthermore, stereoselective hydrogenation via embedding stereoinformation into the phospine ligand-system is in principle possible [43]. One drawback of homogeneous catalyst systems regarding to the application of PHIP in medicine is their toxicity and their general water insolubility. Therefore, many catalyst systems have been investigated for their PHIP applicability during the last years [44, 45]. Current research is the immobilization of homogeneous catalysts to a polymer or silica gel to facilitate the separation of the toxic catalyst species from the reaction mixture [46]. Further investigations of the PHIP effect in heterogeneous hydrogenations were performed in 2008 using Pt/Al_2O_3 and Pd/Al_2O_3 as heterogeneous catalyst systems [47]. A big disadvantage of the implementation of heterogeneous catalyst systems for PHIP are the much smaller achieved signal enhancements in comparison to the homogeneous catalysts. Therefore, this work focuses on homogeneous catalyst systems.

PASADENA versus ALTADENA

Depending on the experimental setup parahydrogenation results in two different NMR signal patterns named either adiabatic longitudinal transport after dissociation engenders net alignment (ALTADENA) [11], in case of parahydrogenation at low magnetic field or parahydrogen and synthesis allow dramatically enhanced nuclear alignment (PASADENA) [33] for parahydrogenation at high magnetic field.

During the addition of molecular hydrogen to an unsymmetric unsaturated molecule a symmetry reduction or break of the former p-H_2 occurs. Due to the non-magnetical euqivalence of the two hydrogen nuclei, the coupling between both proton nuclear spins to a total nuclear spin vanishes. This leads to new nuclear spin levels of the unsymmetric product molecule which are generated by partial mixture of the former nuclear spin levels of the symmetric hydrogen. Because of this superposition of the spin levels, the

quantum mechanical transition prohibition between the different spin states of hydrogen disappears. This is due to the no longer existing, strictly symmetric and separated energy levels. The former A_2 type spin system is converted, depending on the magnetic field strength, into an AX spin system. Four possible transitions in an AX spin system give rise to the usual two doublets centered at the corresponding resonance frequencies given by the chemical shifts (Figure 2.9) [14].

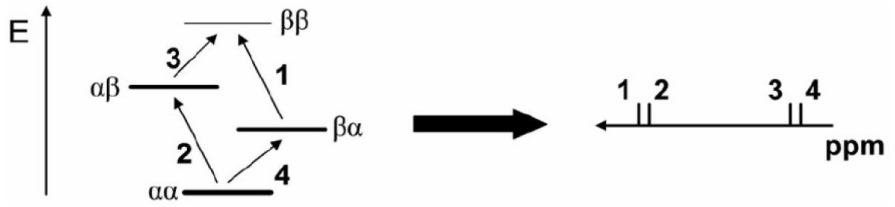

Figure 2.9: AX proton spin system at thermal equilibrium and the resulting NMR spectrum.

At thermal equilibrium, the energy levels are almost equally populated according to the Boltzmann distribution (Equation 2.1). The nuclear spin states $|\alpha\alpha>$ and $|\beta\beta>$ correlate with the triplet states T_{+1} and T_{-1} which were present before the symmetry break. The superposition of S and T_0 generates the spin states $|\alpha\beta>$ and $|\beta\alpha>$, representing a mixture of the same amount of singlet and triplet state (Figure 2.10).

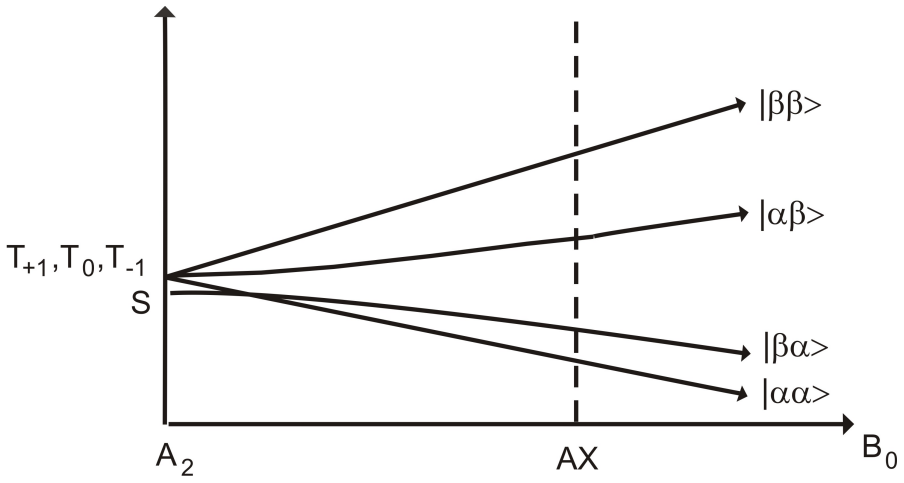

Figure 2.10: Classification of the nuclear spin states of the product after the symmetry break depending on the magnetic field strength.

Hydrogenation with para-enriched hydrogen results in a selective population of defined nuclear spin states in the product molecule. Because in pure p-H_2 only the singlet state is populated, only spin states with partial singlet character are occupied in the resulting product molecule. For this reason, the $|\alpha\beta>$ and $|\beta\alpha>$ states are occupied one half each in the generated AX spin system by the use of 100% p-H_2. Levels representing pure triplet states remain unoccupied. In contrast to the energy level population according to Boltzmann at thermal equilibrium, in this case a massive overpopulation of certain energy levels occurs, which leads to a significant signal increase in the resulting PHIP spectrum. Figure 2.11 shows the population of the energy levels if the hydrogenation is carried out in the high field of the magnet (PASADENA conditions). According to the overpopulation of high energy levels, the resulting NMR spectrum shows not only signals in absorption (transition 1 and 3), but also signals in emission (transition 2 and 4) [14].

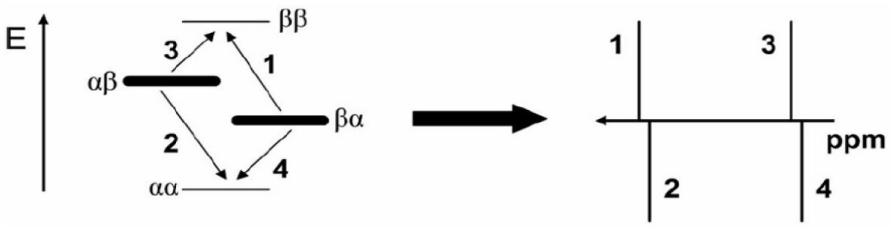

Figure 2.11: Population of the energy levels after hydrogenation under PASADENA conditions and resulting NMR spectrum.

For a reaction procedure under ALTADENA conditions, the hydrogenation and the so associated symmetry break takes place at low magnetic field (earthfield) and subsequent transfer of the reaction sample into the magnet to acquire a spectrum. This leads to selective population of one energy level and its corresponding absorption and emission peaks in the NMR spectrum (Figure 2.12).

Moreover, the superposition of the singlet state occurs during the symmetry break. However, the generated spin system of the product is, due to the low magnetic earthfield, a strongly coupled system, which in approximation can be treated as an A_2 spin system (Figure 2.10). Only the S energy level, which features singlet symmetry under the present conditions, becomes populated during the hydrogenation with p-H_2.

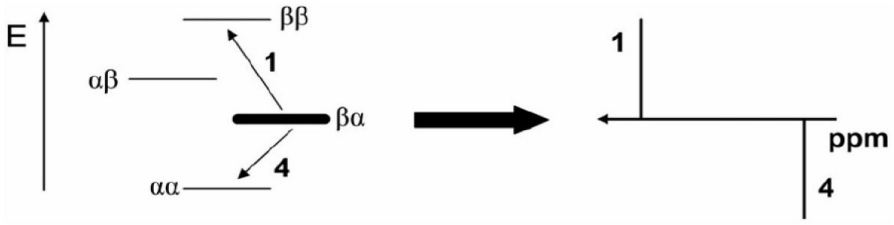

Figure 2.12: Population of the energy levels after hydrogenation under ALTADENA conditions and resulting NMR spectrum.

For an adiabatic transfer of the sample into the spectrometer, the AX system is generated by analogous splitting of the nuclear spin states without changing their populations. Consequently, only the $|\beta\alpha>$ state becomes populated under ALTADENA conditions. Therefore, only two characteristic signals, one in absorption and one in emission, appear in the spectrum [13].

In order to understand the whole process of the parahydrogen induced polarization method and the herefrom obtained results, it is necessary to have a closer look at the density matrix approach in the following chapter.

2.2.3 Density Matrix Approach

The density operator ρ of parahydrogen is given by

$$\rho_{\text{para}} = |\Psi\rangle\langle\Psi| = 1/2|\alpha\beta - \beta\alpha\rangle\langle\alpha\beta - \beta\alpha| = I_1 I_2 = I_{1x}I_{2x} + I_{1y}I_{2y} + I_{1z}I_{2z} \tag{2.4}$$

I_1I_2 is invariant under pulses and gradients, which explains that parahydrogen itself does not have an NMR signal. The evolution of this density operator into a two spin system averaged over the hydrogenation time $t \gg 1/k$ results in Equation 2.5,

$$\bar{\rho} = I_{1z}I_{2z} + \frac{1}{\xi^2+1}(I_{1x}I_{2x} + I_{1y}I_{2y}) + \frac{\xi}{2(\xi^2+1)}(I_{1z} - I_{2z}) \tag{2.5}$$

with $\xi = \delta\nu/J$. It follows that for an A_2 type of spin system ξ becomes zero and the density operator remains unaffected. In conclusion, for the occurence of a PHIP NMR signal the symmetry of parahydrogen has to be broken. Direct transfer of parahydrogen into an AX spin system where $\xi \gg 1$, as it is the case under PASADENA conditions, generates the following density operator:

$$\rho_{\text{PASADENA}} = I_{1z} I_{2z} \tag{2.6}$$

This result could also be derived by considering the populations in the AX spin system where the density operator is simply

$$\rho_{\text{PASADENA}} = |\alpha\beta\rangle\langle\alpha\beta| + |\beta\alpha\rangle\langle\beta\alpha| \tag{2.7}$$

which of course leads to the same result as Equation 2.6. The density operator of the ALTADENA experiment is more complex and its analysis is only possible if the two former parahydrogen nuclei form an isolated, weakly coupled two spin system in the product molecule. Under ALTADENA conditions, only one of the four energy levels of the AX spin system gets populated, namely $\alpha\beta$ or $\beta\alpha$. Thus, the density operator is:

$$\rho_{\text{ALTADENA}} = |\alpha\beta\rangle\langle\alpha\beta| \quad or \quad \rho_{\text{ALTADENA}} = |\beta\alpha\rangle\langle\beta\alpha| \tag{2.8}$$

depending on which of the energy levels is energetically favored. This gives rise to the following equation:

$$\rho_{\text{ALTADENA}} = I_{1z} I_{2z} \pm 1/2(I_{1z} - I_{2z}) \tag{2.9}$$

By applying a pulse with a flip angle ϕ and phase γ, the density operator of the PASADENA experiment (Equation 2.6) evolves into

$$\rho_{\text{PASADENA}}(\phi) = cos^2(\phi) I_{1z} I_{2z} + cos(\phi) sin(\phi)(I_{1z} I_{2x} + I_{1x} I_{2z}) + sin^2(\phi) I_{1x} I_{2x} \tag{2.10}$$

Only the middle term $I_{1z}I_{2x} + I_{1x}I_{2z}$ evolves into detectable magnetization during the FID. Consequently, two antiphase doublets are obtained, which are largest for $\phi = 45°$. After applying a pulse with a flip angle ϕ and phase γ to the density operator of the ALTADENA experiment (Equation 2.9) the following density operator is obtained, listing only the detectable terms.

$$\rho_{\mathrm{ALTADENA}}(\phi) = cos(\phi)sin(\phi)(I_{1z}I_{2x}) \pm 1/2sin(\phi)(I_{1x} - I_{2x}) \tag{2.11}$$

The first term is the same as in the PASADENA density operator and generates two antiphase doublets, whereas the last term causes to inphase doublets. As a result, applying small flip angles to an ALTADENA experiment leads to a partial cancellation of the inner lines of the antiphase and inphase doublets. Meanwhile, for a flip angle of $\phi = 90°$ the antiphase doublets disappear and the inphase doublets with opposite sign survive. Further information regarding the density matrix approach can be found in [13].

2.2.4 Theorectical Signal Enhancement

The calculation of the theoretical signal enhancement is performed with regard to the intensity of the signal at thermal equilibrium. With respect to the Boltzmann distribution, the thermal signal intensity depends on the present magnetic field strength, whereas the created hyperpolarization is field independent. Thus, the ratio of the intensities of thermal and hyperpolarized peaks change with magnetic field strength. Hence, higher signal enhancements can be achieved by working at low field where the intensity of the thermal signals is lower. Furthermore, in order to predict the signal enhancement, it is essential to know the enrichment factor of the nuclear spin isomer of parahydrogen utilized for the hydrogenation. Assuming the usage of pure p-H_2 under ALTADENA conditions, where only one energy level is occupied, the maximum signal enhancement can be calculated as the reciprocal value of the Boltzmann distribution at thermal equilibrium. The population excess of the lowest energy level at thermal euqilibrium is 2.40 $\cdot$ 10 $^{-5}$ by working at a magnetic field strength of 7 Tesla according to equation 2.1. Calculating the reciprocal value of this results in a theoretical signal enhancement of 41667 for the ALTADENA experiment. While in the PASADENA experiment the population is distributed over two energy levels, the resulting signal enhancement is one half of the ALTADENA, namely 20834.

In practice, the theoretical signal enhancement is limited by several factors due to the dependency of its hyperpolarized signal on the quality of the shim and the relaxation time T_1 . Moreover, the signal intensities of the characteristic peaks in the spectra decrease by a slow reaction process. For this reason, hydrogenation products with long T_1 times as well as an optimal choice of reaction conditions are of high importance for the generation of highest signal enhancements.

2.2.5 Relaxation

As mentioned above, the theoretical signal increase of the detectable PHIP pattern in the spectrum is in practice restricted by several factors. Especially relaxation processes which start directly after the generation of the hyperpolarized molecule play a major role in this case.

Relaxation in general is the process by which the bulk magnetization returns to its equilibrium value over time. This process is based on various mechanisms, depending on the physio-chemical features of the considered system [48]. Two different types of relaxation exist: On the one hand the longitudinal or spin-lattice-relaxation (T_1) and on the other hand the transverse or spin-spin-relaxation (T_2). Transverse relaxation is a pure entropic effect, which displays the loss of phase coherence between the magnetic moments of the nuclei. There are two contributions to tranverse relaxation: The non-secular contribution is brought about by the transverse components of local fields which are oscillating at the Larmor frequency; the secular contribution is caused by the existence of a distribution of the z-components of the local fields. Increasing the rate of random motion descreases the rate of this secular contribution. These effects lead to a decomposition of the transversal magnetization without transferring energy. In comparison, via the spin-lattice-relaxation an energy transfer occurs between the excited system and the nuclei in the neighborhood called ”lattice”. The local fields provide thermal contact between the spins and the random thermal motion of the molecules. This drives the magnetization back to its equilibrium value [49]. So, the longitudinal relaxation describes the build-up of magnetization along the B_0 field after an interference like e.g. a radio frequency excitation pulse. For the PHIP experiments performed in this work, the spin-lattice relaxation times T_1 of the hydrogenation products are of high interest because they display the time frame in which the hyperpolarized system turns back into the state of equilibrium described by Boltzmann and the signal enhancement is lost. In contrast to short T_1 times desired in standard NMR experiments, in PHIP experiments case hydrogenation products with long T_1 times are benificial in order to create long lasting hyperpolarization.

Relaxation Mechanisms

A particular source of a local magnetic field is called a relaxation mechanism. The total relaxation rate observed is additively composed of its single relaxation contributions depicted in Equation 2.12. Often one single mechanism of these is predominant.

$$\frac{1}{T} = \frac{1}{T_{\mathrm{DD}}} + \frac{1}{T_{\mathrm{CSA}}} + \frac{1}{T_{\mathrm{SR}}} + \frac{1}{T_{\mathrm{Q}}} \tag{2.12}$$

The dipole-dipole relaxation (T_{DD}) represents the dominating mechanism for spin-half nuclei like ^{1}H. In addition, the ^{13}C relaxation is not due solely to dipolar couplings. Also the chemical shift anisotropy relaxation (T_{CSA}) and the spin-rotation interaction T_{SR} can give comparable contributions to the total relaxation rate of this nucleus [50].

The Dipolar Mechanism

The local field in this mechanism is disturbed by another spin nearby, which has a magnetic moment and therefore is generating its own magnetic field. The local field due to the neighboring spin depends on a number of parameters like the distance between the two spins, the gyromagnetic ratio of the spin and the orientation of the vector joining the two spins relative to the applied magnetic field [49]. Dipolar relaxation is unique in giving rise to cross relaxation, a process which leads to the transfer of magnetization from one spin to another and hence the nuclear Overhausen effect (NOE). The cross relaxation rate rapidly falls off with distance, so in practice it occurs at distances of less than 5 Å.

Relaxation via Chemical Shift Anisotropy

When placed in a strong magnetic field B_0, a local field at a certain nucleus is generated as a result of the interaction between the electrons and B_0. This local field is responsible for the chemical shift. However, on account of the anisotropy of the electron distribution, the local field varies in direction and size as the molecule tumbles in solution. The resulting variation in the local field can be a source of relaxation. The local field is proportional to the applied field. Additionally, the interaction of this field with the nucleus depends on the gyromagnetic ratio of the nucleus [49]. Hence, this mechanism gives considerbale contibution only for ^{13}C nuclei in high magnetic fields.

Long-lived States

Another interesting feature in means of relaxation is the extension of hyperpolarized spin lifetimes by singlet states [51]. As long as the field does not break the symmetry between the spins, singlet states in general have no substantial interactions with external magnetic fields and are protected from the interactions that cause T_1 relaxation. The simplest example is the singlet state of H_2 itself, the parahydrogen. As explained in the former sections, the symmetry of parahydrogen has to be broken during the hydrogenation reaction, ending up with two inequivalent protons in the product for which the singlet state is no longer a true eigenstate. Therefore, without intervention the created hyperpolarized state would rapidly evolve into unprotected states. However, recently it was shown that singlet states in isolated spin pairs are long-lived under suitable conditions [52–54]. In addition, this lifetime enhancements require magnetic equivalence between the two isolated spins. Removing the frequency differences can be achieved by either keeping the sample in such a low field that the resonance frequencies are essentially the same or via application of a suitable RF pulse train. Under these conditions, quantum mechanical symmetry considerations imply that the singlet state is immune to the major mechansim of relaxation, namely the dipole-dipole interactions.

With regard to parahydrogen induced polarization, the two hydrogen atoms that are added to the molecule during the reaction represent a singlet state immediately after the hydrogenation. This created singlet state, however, is NMR silent and in order to successfully record a hyperpolarized spectrum the protons should become magnetically inequivalent. These conditions are ”naturally” implemented in the ALTADENA experiment, where the two added protons are equivalent at low field during and after the reaction and become inequivalent after transporting them adiabatically to high field. Thus, creation of isolated spin pairs with the ALTADENA technique offers the possibility to observe and study long-lived states originating from singlet states and thereby store the hyperpolarization for a period of time at low field prior to NMR measurements.

The mechanisms of lifetime prolongation in multi spin systems is still under investigation. For example, an isolated three spin system as the smallest non-trivial multispin system was studied, namely ethylpropiolate, yielding relaxation times two times longer as the longest T_1 observed in the high field [55].

2.2.6 Transfer of Polarization to Heteronuclei

An important precondition for the medical application of PHIP for MRI is the transfer of polarization to heteronuclei, thereby enabling the acquisition of MRI images without disturbing background signal. The generated polarization is not limited to protons and can be transferred to other nuclei like ^{13}C or ^{15}N [35], which is beneficial because these nuclei exhibit longer T_1 times than protons and larger chemical shift dispersions. Polarization transfer to heteronuclei naturally occurs when performing the hydrogenation at low magnetic field. Strong coupling of the nuclei at low magnetic field causes similar precession frequencies for the involved nuclei, which seems to bear an important role for spontaneous polarization transfer. However, the underlying mechanism of polarization transfer in parahydrogen experiments is not yet fully understood. In this context several possible mechanisms were discussed in the last years [35] e.g. polarization transfer via scalar couplings or dipolar relaxation. A general transfer scheme of the proton polarization to a ^{13}C nucleus is demonstrated in Figure 2.13. During the hydrogenation the spins keep their relative orientation which is then transferred in the next step to the heteronuclei.

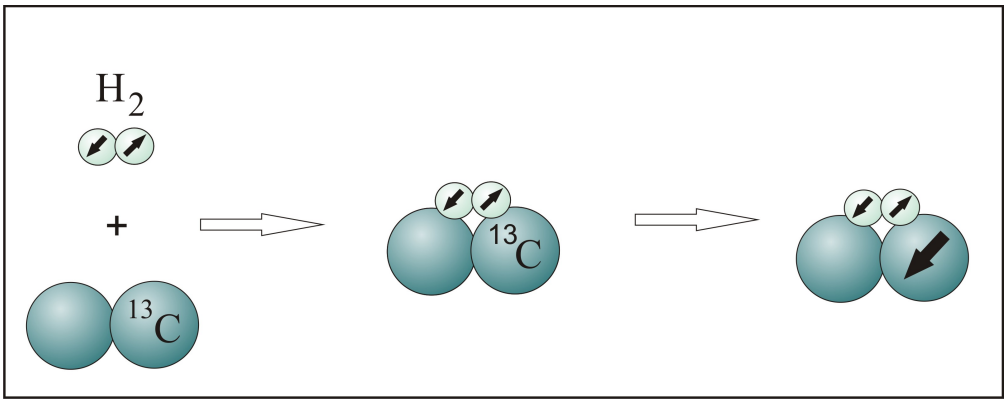

Figure 2.13: Scheme of the general polarization transfer.

Already in 1989, polarization transfer to ^{31}P under ALTADENA conditions was examined by the group of Eisenberg [56]. In this case, a dipolar transfer mechanism of the polarization from the protons to ^{31}P was assumed. In 1995, Barkemeyer et al. presented important polarization transfer experiments to ^{13}C nuclei. The highest signal enhancement in the resulting ^{13}C spectrum of the hydrogenation of acetylenedi-

carboxylic acid dimethyl ester under ALTADENA conditions yielded 2580 [57]. The characteristic antiphase peaks were not only present for the olefinic carbons, but as well for the carbonyl group. The authors presented a convincing description of the transfer mechanism based on analysis of the phase location and signal intensity of the regarded system. Only by consideration of all three nuclei of the presumably present AAX spin system, the signal pattern in the spectrum can be described. Thus, the dipolar relaxation represents a huge part of the total mechanism, but it is not sufficient for a complete explanation of the observed signals. In 2001, the same substance was used for succesful mapping of a ^{13}C angiogram of a rat [58].

Furthermore, polarization transfer to heteronuclei can be achieved via certain pulse sequences in low or in high magnetic field. In low field Goldman et. al. presented polarization transfer to ^{13}C through a sequence of rf pulses at the resonance frequencies of both spin species [59]. In 1993 the INEPT+ (insensitive nuclei enhanced by polarization transfer) pulse sequence was implemented together with an ALTADENA experiment for polarization transfer to ^{13}C and ^{31}P nuclei [60]. The achieved signal enhancement for ^{13}C in this case amounted to 25 meanwhile the signal of ^{31}P was 61 times higher than for hydrogenation with normal hydrogen. In 1996, the formerly implemented INEPT+ sequence was developed further with regard to the PASADENA spin system [61]. Hence, three INEPT analogous pulse sequences were examined in order to achieve polarization transfer to heteronuclei, namely the PH-INEPT, the PH-INEPT+ and the INEPT($+\pi/4$) sequence. Throughout all experiments, the PH-INEPT family of sequences performed considerably better than the standard INEPT+ sequence. As a result, this new INEPT derived pulse sequences led to signal enhancements of around 300 for ^{13}C in the prodcut molecule 1,4-diphenylbut-1-en-3-yne. In addition, polarization transfer to the heteronuclei ^{29}Si could be observed in the molecule trimethylvinylsilane via the PH-INEPT and the INEPT($+\pi/4$) sequence yielding signal enhancements estimated to amount to 500. Polarization transfer experiments to other heteronuclei such as ^{19}F [62] and ^{15}N [63] also have been prerformed in the last years.

As in nearly all organic compounds ^{13}C are the prevalent nuclei, most polarization transfer experiments in this work focus on this heteronucleus. Therefore, spontaneous polarization transfer under ALTADENA conditions to ^{13}C as well as the PH-INEPT family of sequences together with a PASADENA experiment were investigated resulting in ^{13}C hyperpolarization of our model compounds and the examined physiological relevant substances.

3 Optimizing the Parahydrogen Technique on Model Compounds

Enhancing the sensitivity of nuclear magnetic resonance measurements via parahydrogen induced polarization is of high interest for spectroscopic investigations. In order to achieve the highest possible sensitivity gain it is of great importance to optimize the conditions of the parahydrogenation technique. The PHIP technique represents a unique combination of magnetic resonance spectroscopy with chemistry itself. In order to influence the outcome of the PHIP method, one has to optimize certain interacting points which concern either chemical or spectroscopic aspects of the experiment as shown in Figure 3.1. As the whole technique offers a huge field to work in, most known theses treat only one special part, e.g. the spectroscopic topic of transferring the polarization to heteronuclei or the chemical performance of the implemented catalyst systems [64, 65].

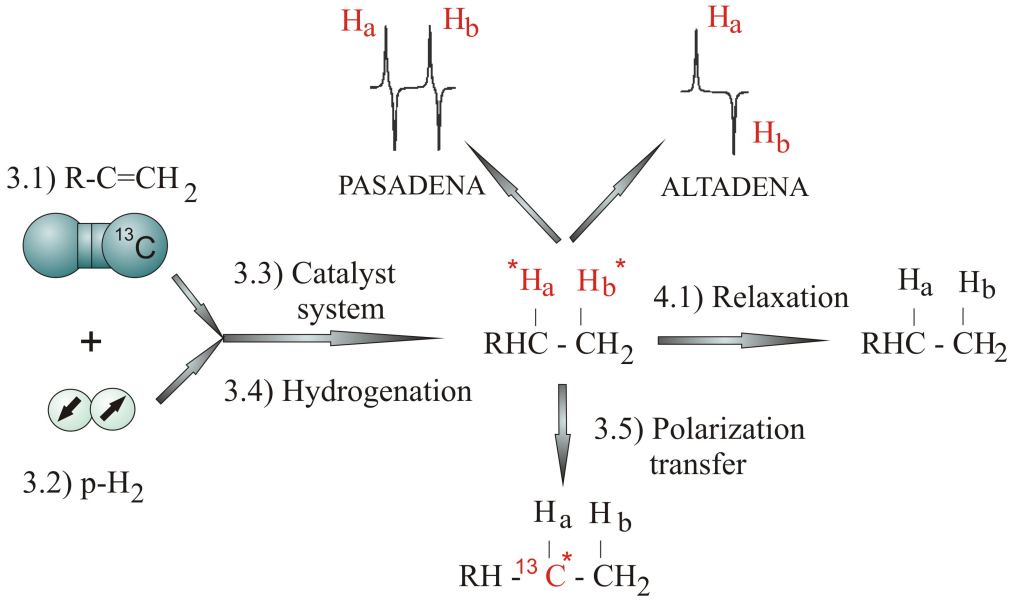

Figure 3.1: Identified aspects for optimization of the parahydrogenation technique, labeled with the corresponding chapters in this work.

In this work, Chapter 3 will deal systematically with all identified interacting aspects and display the obtained results of the overall optimization procedure. To ensure appropriate comparisons, all investigations were realized using two model compounds as described in the next section, namely 1-hexyne for reactions in organic solvents and 2-hydroxyethyl acrylate for reactions under aqueous conditions. Thus, the following sections deal with the topics: 3.2) generation of parahydrogen, 3.3) different investigated catalyst systems, 3.4) variable reaction conditions for the hydrogenation reaction and 3.5) with the possibility to transfer the polarization to heteronuclei. The last important point (labeled with 4.1) in Figure 3.1) concerns the relaxation from the hyperpolarized state to the ground state. This severe limitation factor can be reduced in some special cases as already mentioned in the theory part. Therefore, this topic is discussed at the beginning of chapter 4 dealing with an appropriate substance to investigate the life-time prolongation of the hyperpolarized state.

3.1 Model Compounds

Two substrates served as model compounds in order to investigate the PHIP technique, namely 1-hexyne for reactions in acetone-d_6 and 2-hydroxyethyl acrylate for reactions in D_2O. Both substrates are commercially available in sufficient amounts to implement a series of experiments. Furthermore, they show high signal enhancements under parahydrogenation which in the first place enables the investigation of this technique. However, both substrates are not physilogical relevant but harmful for the human body. Here a closer look to the various mechanisms of the PHIP technique is the matter of interest. Therefore, the aspect of toxicity will be neglected for the time being. Regarding the application of parahydrogen induced polarization in medicine, several physiological substrates are treated in Chapter 4.

3.1.1 1-Hexyne

1-Hexyne is a highly flammable liquid with a boiling point between $71 - 72\,^{\circ}C$. Its CAS registry number is 693-02-7. Hydrogenation of the terminal triple bond results in the product 1-hexene, displayed in Figure 3.2. 1-Hexyne represents an attractive model compound as it is barely sterical hindered giving rise to a favorable interaction with various catalyst designs. Another important aspect are the long spin-lattice relaxation times of the resulting hydrogenation product 1-hexene. The measured T_1 times of the protons of 1-hexene are summarized in Table 3.1.

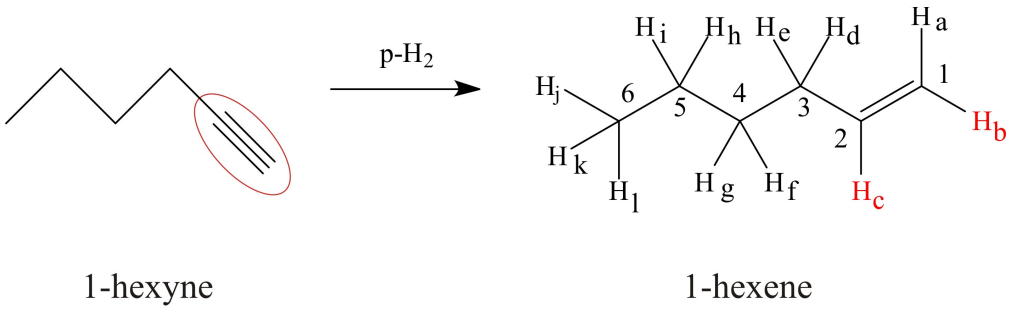

Figure 3.2: Scheme of the parahydrogenation of 1-hexyne.

Especially the protons of the hyperpolarized double bond show long T_1 times between 25 – 33 seconds, whereas all other protons in the molecule show T_1 times of about 15 seconds. Therefore, the hyperpolarization of 1-hexene lasts long enough to be detected several seconds after its generation.

Regarding the possibility to transfer the polarization to heteronuclei, the spin-lattice relaxation times of the carbons are interesting for later investigations. Thus, the experimental T_1 times of the carbons of 1-hexene are shown in Table 3.2. Due to the long carbon spin-lattice relaxation times of about 20 seconds, 1-hexyne also represents a good model compound in order to study the polarization transfer from ^{1}H to ^{13}C as realized later in Chapter 3.5.

Protons	$H_{a,b}$	H_c	$H_{d,e}$	$H_{f,g}$	$H_{h,i}$	$H_{j,k,l}$
T_1 time [s]	25.3	33.4	16.4	14.4	14.4	12.8

Table 3.1: Measured T_1 times of the proton atoms of the hydrogenation product 1-hexene.

Carbons	C_1	C_2	C_3	C_4	C_5	C_6
T_1 time [s]	14.8	23.1	19.0	19.0	19.2	14.4

Table 3.2: Measured T_1 times of the carbon atoms of the hydrogenation product 1-hexene.

3.1.2 2-Hydroxyethyl acrylate

The application of parahydrogen induced polarization in medicine requires to work at physiological conditions. Hence, the hydrogenation should be carried out in aqueous solutions in order to ensure a fast application of the hyperpolarized substrate into the target of interest without harming it. Another important point in this matter is the removal of the toxic catalyst from the reaction mixture.

As 1-hexyne only shows good solubility in organic solvents, another model compound is needed to examine the PHIP method in aqueous solutions. Therefore, in this study the water soluble model compound 2-hydroxyethyl acrylate is used to realize these investigations. 2-Hydroxyethyl acrylate is a toxic liquid with a boiling point of $210 - 215\,^{\circ}C$ and a CAS registry number of 818-61-1. In order to avoid polymerization it has to be stabilized. The parahydrogenation of 2-hydroxyethyl acrylate leads to 2-hydroxyethyl propionate shown in Figure 3.3.

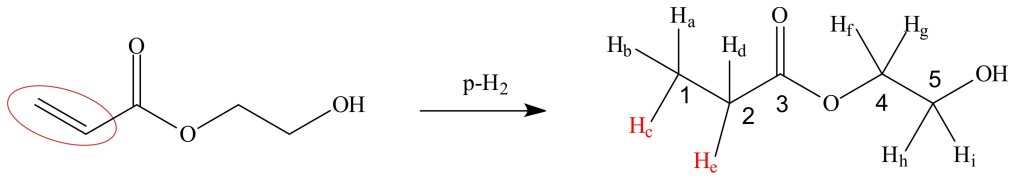

2-hydroxyethyl acrylate 2-hydroxyethyl propionate

Figure 3.3: Scheme of the parahydrogenation of 2-hydroxyethyl acrylate.

Like for 1-hexyne, the hydrogenation of the terminal group is not sterical hindered. However, hydrogenation of the double bond of 2-hydroxyethyl acrylate leads to a single bond wich generally shows shorter T_1 times. The measured T_1 times of the protons and carbons of 2-hydroxethyl propionate are summarized in Table 3.3. In comparison to 1-hexene, the T_1 times of the protons of 2-hydroxyethyl propionate are in a much shorter range of 2 – 5 seconds.

Nuclei	$H_{a,b,c}$	$H_{d,e}$	$H_{f,g}$	$H_{h,i}$	C_1	C_2	C_3	C_4	C_5
T_1 time [s]	5.8	5.0	2.6	2.3	6.2	5.6	47.2	2.1	2.5

Table 3.3: Measured T_1 times of the proton and carbon atoms of the hydrogenation product 2-hydroxyethyl propionate.

Besides from the generation of a single bond rather than a double bond, the fact that the T_1 times are measured in aqueous environment gives rise to this result. Hence, the signal enhancements for parahydrogenation of 2-hydroxyethyl acrylate is likely to be less than for 1-hexyne. Regarding the carbon atoms in the molecule, this model compound offers a very interesting basis to study the polarization transfer due to the existence of a carbonyl group next to the double bond which has a T_1 time of nearly 50 seconds.

3.2 Parahydrogen Generation

The most basic requirement for PHIP is an optimized parahydrogen enrichment. The setup described in the literature implies cooling thermal hydrogen to 77 K with the help of liquid nitrogen. In addition, active charcoal as a catalyst for the symmetry forbidden conversion from ortho- to parahydrogen is needed in order to achieve a content of 50% parahydrogen [35]. This content can be optimized by cooling to lower temperatures with helium to achieve higher para-H_2 ratios as shown in Figure 3.4.

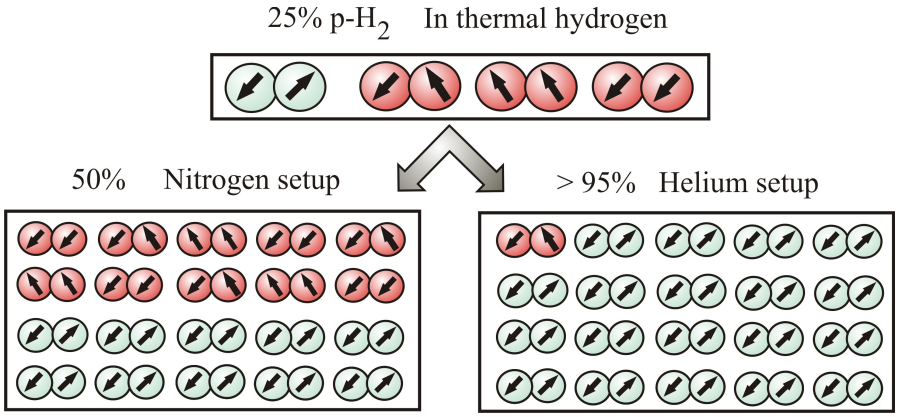

Figure 3.4: Scheme of two different enrichment strategies by cooling with liquid nitrogen to 77 K or with helium to 30 K.

Thus, 98% enriched parahydrogen was generated by cooling thermal hydrogen to 30 Kelvin with a closed-cycle cryostat setup in the presence of active charcoal as a catalyst for the symmetry forbidden conversion from ortho- to parahydrogen. Afterwards, the para-H_2 can be stored for several days in transportable aluminium cylinders at 3.5 bar.

In order to evaluate both setups, two spectra were recorded under the same conditions, i.e. both at room temperature with the model compound 1-hexyne under standard

PASADENA conditions which will be described more precisely in Chapter 3.4. The first spectrum was recorded during a hydrogenation reaction with a content of 50% parahydrogen meanwhile for the second spectrum a content of 98% of parahydrogen was used (Figure 3.5). In order to determine the achieved conversion rates of the hydrogenation, immediately after the measurement a thermally polarized spectrum was recorded. In both cases, the conversion rate at the time point of acquisition (TPA) was estimated to 1%.

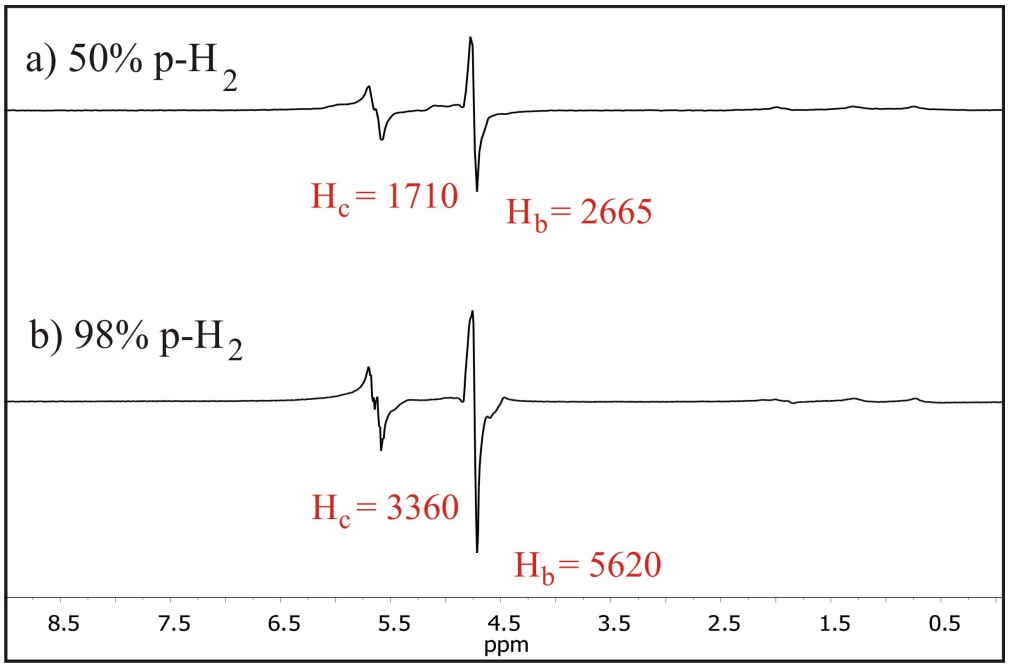

Figure 3.5: Parahydrogenation of 1-hexyne carried out under standard PASADENA conditions with a content of a) 50% p-H_2 and b) 98% p-H_2.

Both spectra show high signal enhancements for the hyperpolarized protons at the double bond of 1-hexene at 5 and 6 ppm respectively, in comparison to the thermal peaks of 1-hexyne in the high-field range between 0.5 and 2.5 ppm. Despite the longer T_1 time of proton H_c a smaller signal enhancement was observed for it. This is due to higher cancellation of antiphase parts stemming from more present couplings [66]. The application of 98% parahydrogen yielded a signal enhancement of 5620 for H_b and 3360 for H_c which is twice as high as the achieved signal enhancements for the usage of 50% enirched parahydrogen. This result is in good agreement with the theory; under equal reaction and measurement conditions, the utilization of a doubled content of p-H_2 should result in a doubled signal enhancement as demonstrated in the experiment.

3.3 Catalytic Systems

The investigated catalytic systems in this work are homogeneous catalyst complexes with Rhodium or Iridium as metal centers. Furthermore, they are all cationic in order to prevent isomerization as a side reaction. In general, commercial homogeneous catalyst systems are soluble in polar solvents like acetone or methanol but not in water. Thus, the presented water-insoluble catalyst systems in this work were all purchased from a commercial source. Unfortunately, only a few water-soluble catalyst systems are commercially available and thus must be synthesized. To achieve solubility in aqueous solvents, polar groups e.g. sulfonate groups have to be inserted into the ligand system of the catalyst. One drawback of this intervention into the electron density of the ligand system is the possible deactivation of the total catalyst. Hence, several water-soluble catalysts were synthesized in order to investigate their solubility and their activity with regard to the introduced groups in the ligand system.

3.3.1 Water-insoluble

Overall, seven commercially available catalyst systems were investigated; they are summarized on the next page. Most of them are Rhodium complexes, apart from catalyst 5 which contains an Iridium metal center. With exception of catalyst 6 which exhibits norbonadiene as a protection ligand, all other catalysts possess cyclooctadiene as a protection ligand. These two types of dienes will be hydrogenated and substituted with solvent molecules in the first reaction step of any hydrogenation in order to create the activated catalyst.

In order to compare the activity of these seven catalyst systems, all were used in a PASADENA experiment at elevated temperature and under pressure at identical reaction parameters. Therefore, seven times 130 mg of the model compound 1-hexyne was dissolved in 3 g acetone-d_6 in 10 mm NMR tubes under argon atmosphere. To each of the samples, 6 mg of the particular catalyst system 1 to 7 was added. All samples were treated in the same way before the measurement: After heating the samples up for one minute in a water bath at 60 °C, the tubes were pressurized with 3 bar of 98% parahydrogen. Then, the tubes were shaken 5 seconds above the bore of the magnet, immediately inserted into the spectrometer and measured 15 seconds after starting the reaction via shaking the tube. Each sample was shaken twice and each reference spectrum was measured of the actual reaction mixture 15 minutes after shaking the tube for the second time.

1) [Rh(COD)(dppb)]BF_4

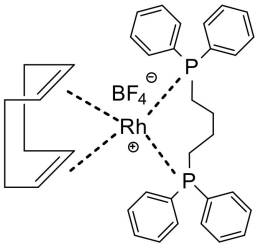

CAS: 79255-71-3

1,4-Bis(diphenylphosphino)butane]
(1,5-cyclooctadiene)rhodium(I)tetrafluoroborate

2) [Rh(COD)($C_{28}H_{28}O_2P_2$)BF_4

CAS: 56977-92-5

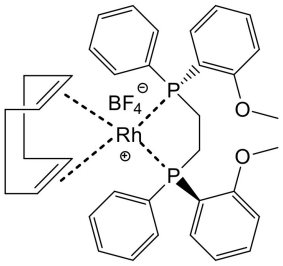

(R,R)-(-)-1,2-Bis[(o-methoxyphenyl)
phenylphosphino]ethane](1,5-cyclo-
octadiene)rhodium(I)tetrafluoroborate

3) [Rh(COD)($C_{22}H_{36}P_2$)CF_3SO_3

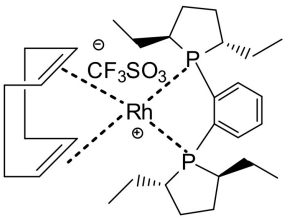

CAS: 142184-30-3

(+)-1,2-Bis[(2S,5S)-diethylphospholano]
benzene(1,5-cyclooctadiene)rhodium(I)triflate

4) [Rh(COD)($C_{16}H_{24}O_3P_2$)BF_4

CAS: 507224-99-9

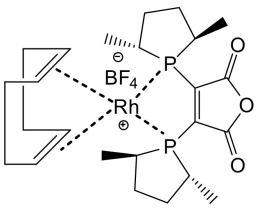

(-)-2,3-Bis[(2R,5R)-2,5-dimethylphos-
pholanyl]maleic anhydride(1,5-cyclo-
octadiene)rhodium(I)tetrafluoroborate

5) [Ir(COD)(pyr)(tchp)]PF_6

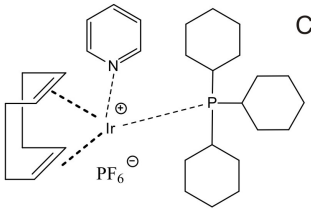

CAS: 64536-78-3

(Pyridine)(tricyclohexylphosphine)(1,5-
cyclooctadiene)iridium(I)hexafluorophosphate]

6) [Rh(nor)(tdmpp)]PF_6

CAS: 32761-50-5

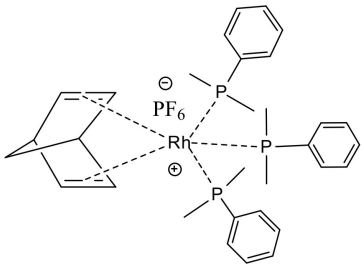

Tris(dimethyl-phenylphosphine)
(2,5-norbonadiene)rhodium(I)
hexafluorophosphate

7) [Rh(COD)($C_{22}H_{36}P_2$)CF_3SO_3

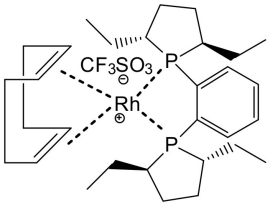

CAS: 142184-30-3

(-)-1,2-Bis[(2R,5R)-diethylphospholano]benzene
(1,5-cyclooctadiene)rhodium(I)triflate

In order to determine the conversion rates of the hydrogenation, small samples were taken with a needle through the septum immediately after each measurement. The hereby obtained hydrogenation rates of all reaction samples are summarized in Table 3.4. As a result, catalyst 2 and catalyst 3 showed only very small conversion rates, similar to the Iridium containing catalyst 5. The other catalyst systems performed better and achieved total hydrogenation rates between 5 – 6% after shaking the sample twice.

Procedure	cat. 1	cat. 2	cat. 3	cat. 4	cat. 5	cat. 6	cat. 7
1st shake	4%	0%	0%	1%	2%	5%	2%
2nd shake	5%	1%	2%	6%	3%	6%	5%

Table 3.4: Conversion rates during the hydrogenation reaction with different catalyst systems 1 – 7.

It is remarkable that catalyst 6, the only one with norbonadiene as a protection ligand, showed the highest conversion rate after the first shake. This leads to the conclusion that the hydrogenation of norbonadiene which is important for the activation of the catalyst system takes place in a shorter time scale than hydrogenation of cyclooctadiene. In order to avoid mistakes and ensure the reproducibility of the results, the whole experiment was repeated. The measured conversion rates of the second experiment are displayed in Table 3.5.

Procedure	cat. 1	cat. 2	cat. 3	cat. 4	cat. 5	cat. 6	cat. 7
1. shake	6%	0%	3%	6%	3%	10%	4%
2. shake	12%	3%	8%	12%	4%	13%	9%

Table 3.5: Conversion rates during the hydrogenation reaction with different catalyst systems 1 – 7, second run.

Overall, the second run provides the same trends as the first run, although all conversion rates are higher. An explanation for this phenomenon could be the fact, that for the second experiment each sample tube only contained 100 mg of the unsaturated precursor and therefore, the conversion rate in percentage is higher. Like in the first experiment, catalyst 6 showed the highest activity for the first shake and afterwards a

much lower conversion rate for the second shake. On the one hand, this confirms the estimation that the activation of norbonadiene takes place in a shorter time than the one of cyclooctadiene. On the other hand, the decrease of the conversion rate after the second shake leads to the conclusion that the catalyst system is partially deactivated, eventually due to the attachment of another ligand which hinders the whole catalytic activity. As already concluded from the first run of this experiment, catalysts 1, 4, 6 and 7 are most suited under the implemented conditions.

The recorded proton PHIP spectra of shaking the sample for the first time are shown in Figure 3.6. All spetra were obtained under the same reaction conditions, i.e. same receiver gain, same flip angle and within a single scan. In good agreement with the measured conversion rates, catalyst 6 showed the highest signal enhancement, but catalysts 1, 4, and 7 also showed the typical enhanced peak pattern. Due to the small conversion rates of catalysts 2, 3 and 5 they nearly did not cause any enhanced signals.

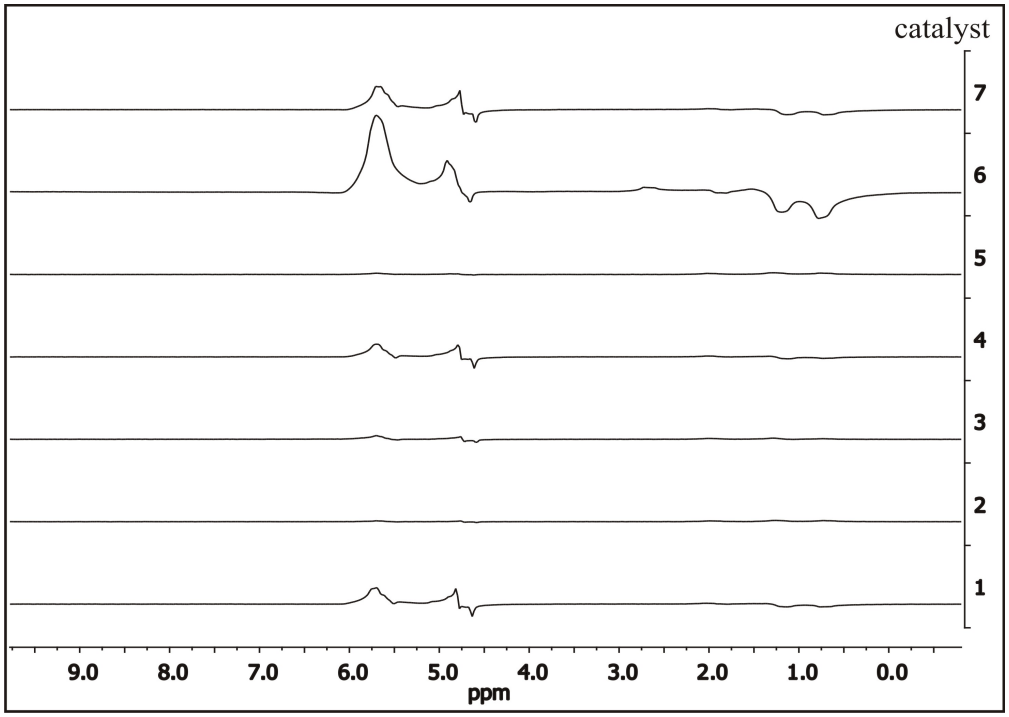

Figure 3.6: ^{1}H NMR spectra of the parahydrogenation of 1-hexyne with different catalyst systems 1– 7, first shake.

The spectra acquired after shaking the sample once again are displayed in Figure 3.7. In good agreement with the decreasing hydrogenation rate of catalyst 6 the signal enhancement decreases together with its conversion. Apart from catalyst system 6, all other catalyst systems showed higher signal enhancements for the second shake. The highest signal enhancements are observed for catalysts 1, 4 and 7. This emphasizes once again the correlation of the conversion rate and the obtained signal enhancement.

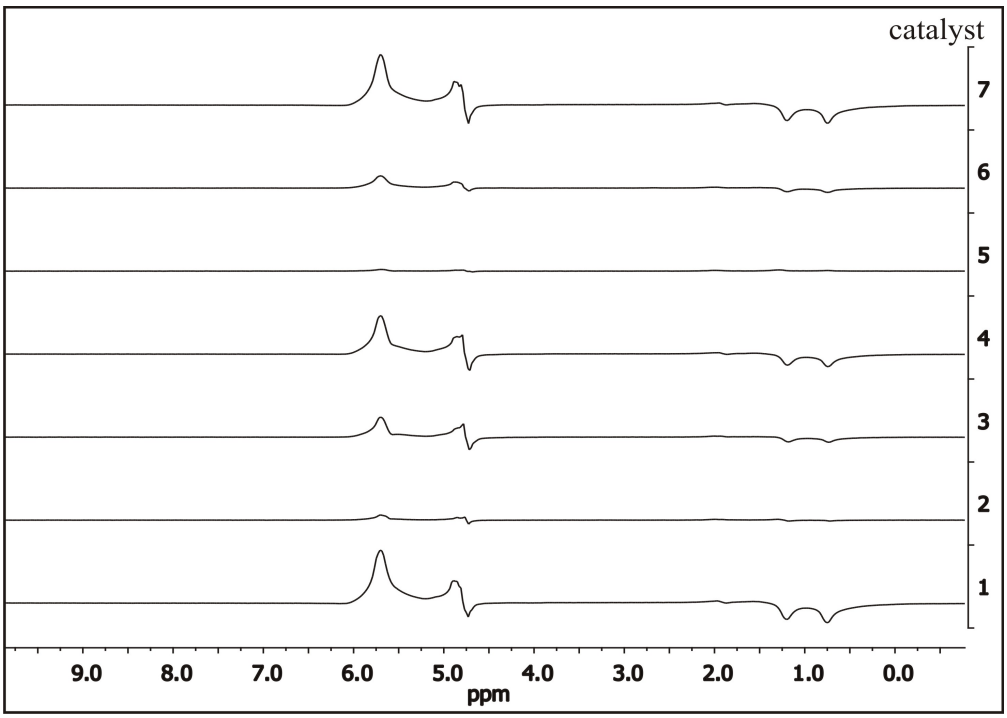

Figure 3.7: ^{1}H NMR spectra of the parahydrogenation of 1-hexyne with different catalyst systems 1–7, second shake.

A peculiar fact should be mentioned with regard to the calculated signal enhancements of these experiments summarized in Table 3.6: In the hyperpolarized spectrum, the observed signal enhancement occurs as an absolute value, meanwhile the later calculated signal enhancements depend on the intensity of the thermal peaks at the point of acquisition. Thus, the higher the conversion rate of the parahydrogenation, the higher are the thermal peaks of the reference spetrum and the smaller are the calculated amounts for the signal enhancements. As a conclusion, the calculated signal enhancements are relative values with regard to the present conversion rate of the hydrogenation reaction.

In Table 3.6 only the signal enhancements of the most promising catalyst systems 1, 4, 6 and 7 are summarized. After its activation, catalyst system 1 generated the highest signal enhancement of more than 3500. Hence, this catalyst was chosen for the following investigations with 1-hexyne in this chapter. However, catalyst 6 also yielded high signal enhancements up to 3365 and furthermore provided a faster reaction rate due to the ligand norbonadiene, but its activity seems to decrease after the first shake.

Procedure	catalyst 1	catalyst 4	catalyst 6	catalyst 7
1. shake	H_b=525 H_c=1110	H_b=985 H_c=1205	H_b=955 H_c=3365	H_b=1095 H_c=1725
2. shake	H_b=1485 H_c=3690	H_b=916 H_c=1620	H_b=420 H_c=1155	H_b=1095 H_c=3340

Table 3.6: Calculated signal enhancements of the hydrogenation reaction with different catalyst systems depending on the hydrogenation rate at the time point of acquisition.

To complete this examination one should keep in mind that the intensity gain of the signal not only depends on the conversion rate of the hydrogenation reaction. More precisely, a good or sufficient conversion rate is the basic requirement to obtain hyperpolarized signals. However, the height of the intensity gain also depends on the underlying mechanism of the hydrogenation reaction. Important points in this regard are the pairwise transfer of the hydrogen atoms and a fast transfer reaction. In conclusion, if the transfer of the hydrogen atoms to the substrate occurs on a longer time frame than the relaxation process, or the underlying mechanism of the hydrogenation does not support a pairwise transfer, it is possible that no signal enhancement is detected in spite of a good conversion rate.

3.3.2 Water-soluble

Physiologically relevant processes take place in aqueous surroundings. Thus, the implementation of a water-soluble ligand system in order to generate water-soluble homogeneous catalyst systems suggests itself. Therefore, two ligand systems were synthesized, both containing sulfonate groups in order to enhance their solubility in water. A more detailed description of their synthesis is given in Chapter 6. Additionally, one low priced ligand system from Alfa Aesar (CAS 63995-70-0) and one expensive ligand

system described in the literature [67] from Sigma Aldrich were purchased and connected to a Rh containing precursor. All water-soluble catalyst systems investigated in this work are summarized in the box depicted below.

8) [Rh(COD)(dppbs)]CF_3SO_3

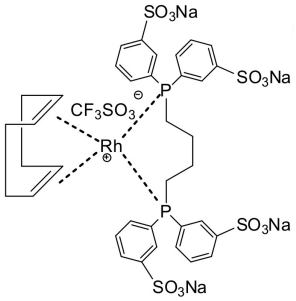

1,4-Bis[sodium 3,3'-(diphenyl-3,3'-sulfonate)phosphine] butane (1,5 cyclooctadiene)rhodium(I)triflate

9) [Rh(COD)(tpps)]CF_3SO_3

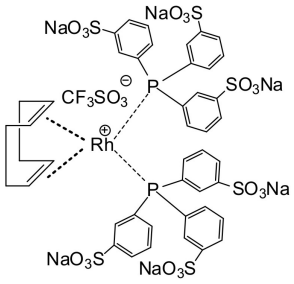

Bis[sodium 3,3',3''-(triphenyl-3,3',3''-sulfonate phosphine)] (1,5 cyclooctadiene)rhodium(I)triflate

10) [Rh(COD)(tppsm)]CF_3SO_3

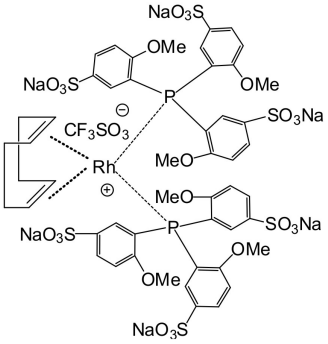

Bis[sodium-3,3',3''-(triphenyl-3,3',3''-sulfonate-6,6'6''-methoxy phosphine)] (1,5 cyclooctadiene)rhodium(I)triflate

11) [Rh(nor)(ppbs)]BF_4

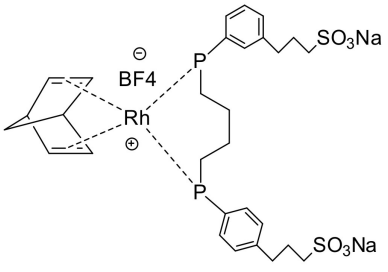

1,4-Bis[sodium 3-(phenyl-3-propane sulfonate)phosphine] butane (2,5-norbonadiene) rhodium(I)tetrafluoroborate

The denoted water soluble catalyst systems were synthesized from these ligand systems via a simple reaction step, namely by adding a commercial precatalyst as depicted in Figure 3.8 [35].

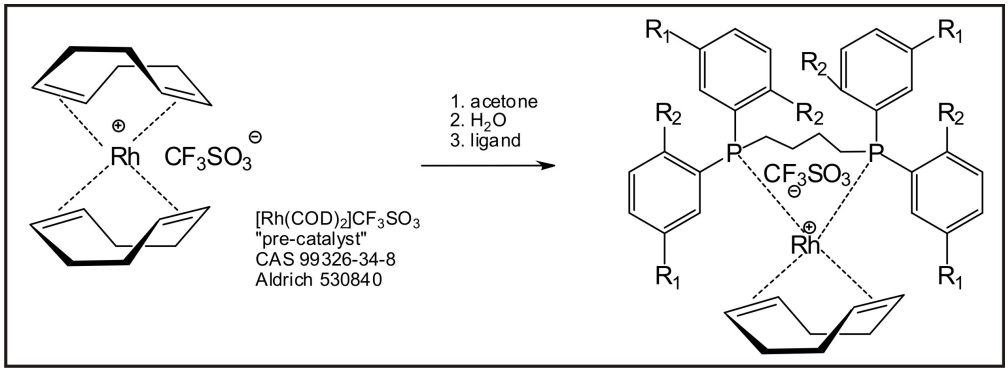

Figure 3.8: Scheme of the general procedure to synthesize a catalyst system out of a ligand and a prectalyst [35].

The presented precatalyst system in this figure only displays one possible precatalyst system to realize the reaction. For example, in order to follow the description in the literature [67] the commercially purchased ligand system from Sigma Aldrich was converted into the catalyst system 11 together with a precatalyst containing twice the amount of norbonadiene. In comparison to this, the second purchased and low priced ligand system implies triphenylphosphine as the basic structure and was converted to catalyst 9. For the first synthesized ligand system of catalyst 8, the original diphenylphosphine butane ligand system (dppb) of catalyst 1 served as a basis. The four phenyl groups in the ligand were sulfonated in order to combine the high activity of catalyst 1 together with a good water solubility. One disadvantage of the introduced sulfonate groups is the reduced electron density in the aromatic ring and, furthermore, at the catalytic metal center itself. This leads to a definite decrease of the catalytic activity. This negative effect can be compensated by an additional group adjacent to the sulfonate group in order to adjust the density. Therefore, the ligand system of catalyst 10 was synthesized in order to investigate the outcome of this measure. Thus, the structure of the ligand system of catalyst 9 was modified via additional introduction of methoxy groups to the aromatic ring system. The purchased ligand system of catalyst 11 does not include methoxy groups. In this case the problem of deactivation due to the sulfonate groups is solved in another way: The sufonated groups are located at the end of a carbon chain and therefore do not have such a strong influence on the electron density of the aromatic ring. This supersedes the need of the activating methoxy groups and, moreover, makes the catalyst system less sterically hindered.

The investigation of the water-soluble catalyst systems was carried out in a similar way as the investigation of the water-insoluble catalyst systems. Hence, all were implemented in a parahydrogenation reaction at elevated temperature and under pressure. Thus, all samples were heated up before the measurement for one minute in a water bath at 60 °C and afterwards pressurized with 3 bar of 98% parahydrogen. Every reaction sample contained 100 mg of the model compound 2-hydroxethyl acrylate dissolved in 3 g D_2O in 10 mm NMR tubes under argon atmosphere. To each of the samples, 5 mg of the catalyst system of interest was added. All samples were treated in the same way as described before in the experiments with the water-insoluble catalyst systems. The only difference in this case was, that in order to determine the conversion rates of the hydrogenation reactions, only one sample at the end of the experiment was taken. The hereby obtained hydrogenation rates of the four reaction samples together with the calculated signal enhancements are summarized in Table 3.7.

Investigated system	catalyst 8	catalyst 9	catalyst 10	catalyst 11
Conversion rate	56%	40%	1%	28%
Signal enhancement	0	H_c=9 H_e=11	0	H_c=1510 H_e=1770

Table 3.7: Conversion rates during the hydrogenation reaction of 2-hydroxethyl acrylate with different water-soluble catalyst systems after shaking the NMR tube twice.

With regard to the displayed conversion rates the catalyst systems 8, 9 and 11 fulfill the basic requirement to generate hyperpolarized signals. As catalyst 10 does not show any conversion, no sufficient hyperpolarization is generated which could be detected. This result is really interesting because the estimated activation of this catalyst system due to the introduced methoxy groups did not work. A reason for this can be the high sterical hindrance of the catalyst system because of the high and dense number of functional groups in the aromatic ring. Also catalyst 8 did not generate any typical hyperpolarized signal, although it showed the highest conversion rate in comparison to the other catalysts. Thus, the underlying transfer mechanism of the para-H_2 atoms must have been disturbed in some way, i.e. it does not support the pairwise transfer of the protons to the substrate. In comparison to this result, catalyst 9 not only showed high conversion rates, but also small antiphase signals with a signal enhancement of around 10. In

this case, at least a small part of the protons is transferred in a pairwise manner which happens fast enough to detect the hyperpolarized substrate. The hereby detected PHIP spectrum is shown in Figure 3.9. The two hyperpolarized peaks labeled with H_c and H_e result from the hyperpolarized single bond meanwhile the other signals between 3 and 8 ppm belong to thermal 2-hydroxyethyl acrylate.

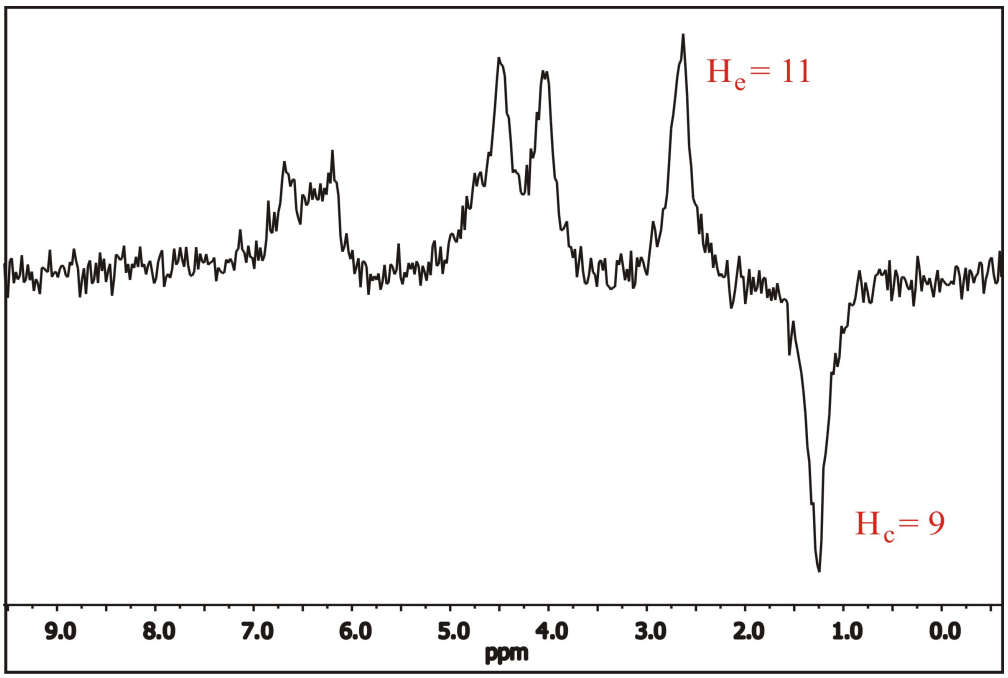

Figure 3.9: Parahydrogenation of 2-hydroxyethyl acrylate with catalyst system 9 and 98% enriched p-H_2.

In spite of the much smaller conversion rate obtained with catalyst system 11 in comparison to catalyst 8 and 9, catalyst 11 yielded considerable higher signal enhancements of up to 1770 (compare Figure 3.10). This allows the conclusion that the underlying transfer mechanism of this system supports the pairwise transfer of the protons. A possible explanation for this possitive effect on the parahydrogenation is the overall small sterical hindrance of the catalytic system. This circumstances in combination with the long sulfonated carbon chains to ensure the water-solubility seems to offer a solution for the implementation of the PHIP technique under physiological conditions. As catalyst system 11 is the most promising catalyst species in this work in order to implement the parahydrogenation in water, this catalyst was chosen for the following experiments under aqueous conditions.

Of high importance for the conversion rate of the hydrogenation reaction and therefore of the achieved signal enhancement seems to be the reaction temperature. In order to investigate the influence of the temperature on the overall hydrogenation process, the sample containing catalyst 11 was shaken once again at room temperature. In addition, an experiment was implemented where the sample was heated up in a water bath to 60 °C and 78 °C and shaken before recording a spectrum. The so obtained PHIP spectra at 25 °C, 60 °C and 78 °C are depicted in Figure 3.10.

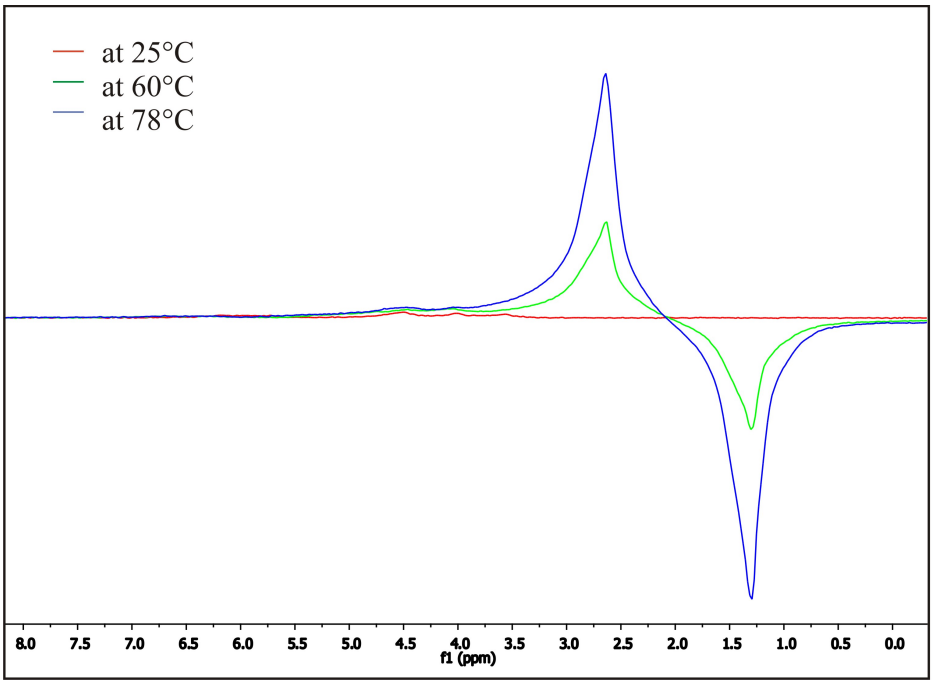

Figure 3.10: ^{1}H PHIP spectra of 2-hydroxyethyl acrylate and catalyst system 11 with 98% enriched p-H_2; parahydrogenations were carried out at different temperatures.

As already seen for catalyst 9, the two hyperpolarized peaks in the high field range of the spectra stemming from hydrogenation respectively, at 60 °C and 78 °C display the generated hyperpolarized single bond. Due to the occurence of foam and bubbles during the shaking process a considerable line broadening is observed. To get an idea of the extremely high signal enhancements, one should have a closer look at the barely visible thermal peaks between 3 and 8 ppm. In conclusion, the high temperature of 78 °C speeds up the overall reaction. It seems that the contrary effect of poor solubility

of hydrogen in solutions at higher temperature does not have an important influence in this case. Hence, the highest signal enhancement of 3930 for H_c and 4130 for H_e could be observed for the reaction at 78 °C. In comparison, the spectra recorded at room temperature does not show the typical hyperpolarized signals besides the thermal peaks in the spectrum.

3.4 Hydrogenation Conditions and Different Ways to Apply Parahydrogen

In order to achieve the highest possible sensitivity gain with the PHIP method it is of great importance to optimize the reaction and measurement conditions of the underlying chemical reaction, namely the homogeneous hydrogenation reaction. As already examined in the last chapter, the achieved conversion rate and signal enhancements are strongly dependent on the applied temperature during the hydrogenation. Also, the implementation of elevated pressure to the reaction sample increases the conversion rate of the reaction. Another important aspect in this context is the manner in which the parahydrogen gas is dissolved in the reaction solution. In order to investigate the dependencies of these aspects on the parahydrogenation technique, different setups were implemented and their experimental outcomes were analyzed with regard to the conversion rate of the homogeneous hydrogenation reaction and the generated signal enhancement.

3.4.1 The Standard PASADENA Experiment

The standard PASADENA experiment as described in literature is carried out by applying a constant flow of enriched parahydrogen through a thin capillary to the reaction mixture inside an NMR tube which is located in the spectrometer [10]. The thin capillary inside the sample tube is extending to the bottom of the tube and was previously attached to the cap of the tube as depicted in Figure 3.11.

Figure 3.11: NMR tube used for the standard PASADENA experiment.

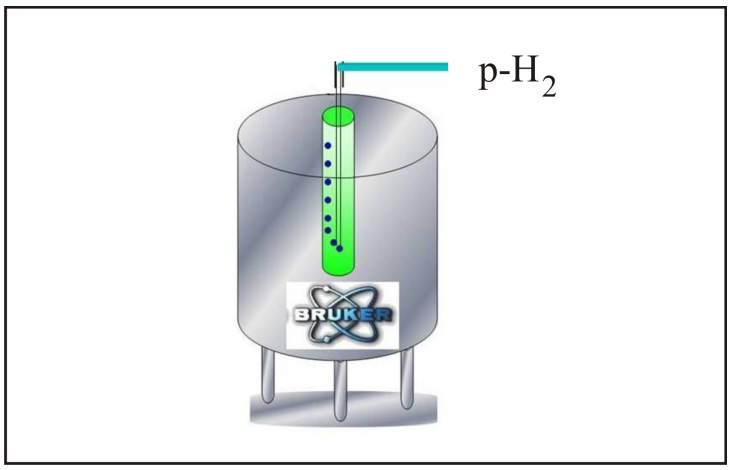

Figure 3.12: Setup for the standard PASADENA experiment.

In order to record a spectrum, it is necessary to stop the para-H_2 gas flow and wait a certain time to let the solution smoothen. This implicates a loss of polarization during the waiting time as a result of spin-lattice relaxation and therefore, smaller observed signal enhancements. Another drawback of this method is the little amount of dissolved hydrogen in the solution due to the small gas-liquid interface of the generated bubbles, which in some cases results in small or even no hydrogenation of the model compound. Moreover, the use of water as a solvent is not possible in this case because under such mild reaction conditions (ambient temperature and pressure) no hydrogenation in aqueous surrounding takes place. The PASADENA setup is displayed in Figure 3.12.

Two experiments carried out with 1-hexyne under standard PASADENA conditions were already discussed in Chapter 3.2 for the examination of different enrichment contents of para-H_2. Both spectra shown in Figure 3.5 were recorded after 8 minutes of bubbling parahydrogen through the reaction mixture. The conversion rate after 8 minutes was determined to a value of 10%. However, it should be mentioned that neither the reaction tube nor the spectrometer itself were heated up in order to increase the hydrogenation reaction. So, there are at least three limiting factors of this procedure: 1) the low temperature, 2) no applied pressure and 3) the small amount of dissolved parahydrogen in the solvent. These three points cause the small conversion rate of 10% after applying a constant flow of parahydrogen through the reaction mixture for 8 minutes.

3.4.2 ALTADENA and PASADENA under Pressure

The standard ALTADENA experiment has to be carried out at low magentic field. Therefore, 10 mm NMR tubes were filled with the reaction mixture under argon atmosphere and sealed with a septum cap (Figure 3.13).

Figure 3.13: NMR tube for the setup of ALTADENA and PASADENA under pressure.

The reaction is carried out at elevated temperature and pressure in order to increase the conversion of the parahydrogenation. Thus, the sample tube is gently heated to $60 - 100\,^{\circ}C$ in a water bath, depending on the boiling point of the chosen solvent and then pressurized with 3.5 bar of para-enriched H_2. Due to the harsher reaction conditions, higher conversion rates are generated and therefore, this method also allows for hydrogenation in aqueous solvents. To achieve ALTADENA conditions, the tube is shaken at low magnetic field with a distance of a few meters to the magnet and inserted afterwards.

Regarding the low conversion rates of the standard PASADENA experiment, the possibility to work under pressure should result in an improvement of the hydrogenation rate also for the PASADENA experiment. In order to use the setup of the ALTADENA experiment and shift the reaction conditions towards PASADENA conditions, the pressurized tube is shaken above the bore of the magnet to start the hydrogenation and immediately inserted into the spectrometer. Depending on the stray field of the magnet, the proceeding of the reaction leads to a certain mixture of PASADENA and ALTADENA spin states at the beginning of the NMR experiment. However, after insertion into the magnet, the ongoing reaction at high magnetic field evokes only PASADENA spin states. This type of PASADENA experiment was already applied to the hydrogenation of barbituric acid derivatives [68]. In this study it is shown, that the hydrogenation reaction of barbiturates under standard PASADENA conditions did not result in any conversion. Instead, the implementation of a PASADENA experiment under pressure at elevated temperature led to a long lasting hydrogenation reaction and hyperpolarized signals.

All experiments implemented for the examination of different catalyst systems in this work were carried out under ALTADENA conditions at elevated temperature and pressure (Chapter 3.3). The resulting conversion rates of the model compound 1-hexyne with the standard catalyst system 1 are approximately 4 – 5% for each shake. As one shake only needs around 5 – 10 seconds, the achieved conversion rate compared to the standard PASADENA experiment is higher. However, one disadvantage of this reaction method is the broadening of the peaks due to foams and bubbles after shaking the sample. Especially the implementation of a parahydrogenation reaction in water using catalyst system 11 with its sulfonate groups results in an undesirable strong foam formation. Thereby, a certain amount of otherwise detectable polarization is lost due to cancellation of the broad signals of the antiphase peaks. Another drawback is the decreasing conversion rate over time during the pressurized and shaken tube is inside the spectrometer.

3.4.3 PASADENA with Membranes

In recent years, major findings were enabled by exploiting the large signal enhancements, which are e.g. of particular importance for the monitoring of dynamic processes in real time in biological [69], chemical [70] and medical [71] investigations. However, one significant drawback remains in all hyperpolarization techniques: the lifetime of the hyperpolarized state is restricted by relaxation processes (in liquids on the order of seconds to minutes) demanding fast applications. Moreover, even the substantial pulses during the NMR measurement destroy parts of the hyperpolarized signal depending on the applied flip angle being particularly problematic for multi-dimensional experiments which are nowadays common practice in NMR and MRI. Contrary to the fast decay of the hyperpolarization, the polarization build up can be time consuming and tedious depending on its physical or chemical origin. Therefore, most techniques are realized in batch processes [3, 67], i.e. one hyperpolarized sample is produced at a time and has to be measured in a limited time frame with carefully designed NMR pulse sequences. Substantial effort has been made to overcome these problems e.g. relying on the stepwise use of the generated hyperpolarization by the application of small flip angles [72] or using specially designed sampling strategies [73, 74] and most importantly prolonging the lifetime of the hyperpolarization utilizing polarization storage in singlet states [51, 54]. Here, a different approach to cope with these difficulties is presented; the PHIP method was implemented with a continuous delivery of parahydrogen through hollow fiber membranes to generate a significant high polarization of ^{1}H which constantly renews for several minutes.

The standard PASADENA experiment is carried out by bubbling hydrogen through a thin capillary into the reaction mixture inside a NMR tube. To acquire a spectrum it is necessary to stop the parahydrogen gas flow and wait a certain time to let the solution smoothen. Of course this implies an interruption of the reaction and furthermore a loss of polarization during the waiting time as a result of spin-lattice relaxation. Another drawback of the standard PASADENA method is the diminutive amount of dissolved hydrogen in the solution due to the small gas-liquid interface of the generated bubbles. To overcome this problem we combined a membrane technique which was previously developed to optimize the dissolution of hyperpolarized Xe in liquids [75] with the PHIP technique in this work. The use of such membranes, which exhibit a very large gas-liquid interface, provides the opportunity to bring a gas molecularly into solution without the problem of foaming and bubbles. Thus, this combination ensures the implementation of a continuous dissolution of parahydrogen in the reaction mixture giving rise to high conversion rates while maintaining a high spectral resolution during the NMR acquisition. In contrast to batch techniques where acquisition is only possible during the T_1 time of the once generated hyperpolarization, the continuous delivery of parahydrogen and the ongoing hydrogenation reaction generate a significant high polarization of ^1H or after application of a polarization transfer sequence of ^{13}C which is stable for several minutes. It is demonstrated here that the constant polarization allows the implementation of more complicated NMR experiments as e.g. recording of 2D NMR spectra requiring multiple acquisitions with equal initial polarization. The parahydrogenation of the well-known model compound 2-hydroxyethyl acrylate was carried out by continuously dissolving p-H_2 with the use of hollow fiber membranes into the aqueous solution (Figure 3.14).

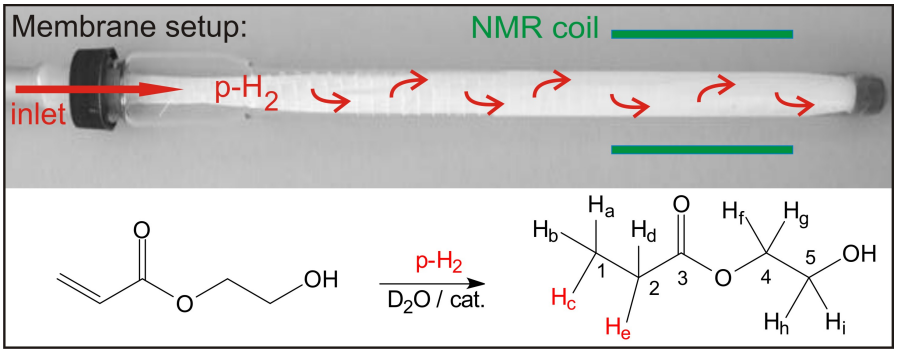

Figure 3.14: Implementation of the hollow fiber membrane setup for parahydrogenation of 2-hydroxyethyl acrylate in D_2O leading to the hyperpolarized product 2-hydroxyethyl propionate.

The hereby generated hyperpolarized product 2-hydroxyethyl propionate led to enhanced ^{1}H antiphase signals in the recorded spectra during the following minutes as displayed in Figure 3.15. The top trace of Figure 3.15 shows a reference spectrum of the thermally polarized product acquired after full conversion after 60 minutes. In the beginning of the parahydrogenation reaction a buildup of hyperpolarized signal can be observed, which is caused by the increasing conversion of the hydrogenation once the p-H_2 flow is switched on and the sample tube is heated up after insertion in the to 80 °C heated spectrometer. At the end of the reaction the intensity of the hyperpolarized signals decreases due to the decreasing amount of starting material in the reaction mixture. However, during a time frame of six minutes being much longer than the T_1 time of the protons the achieved signal enhancements are rather constant between values of 1500 and 2000.

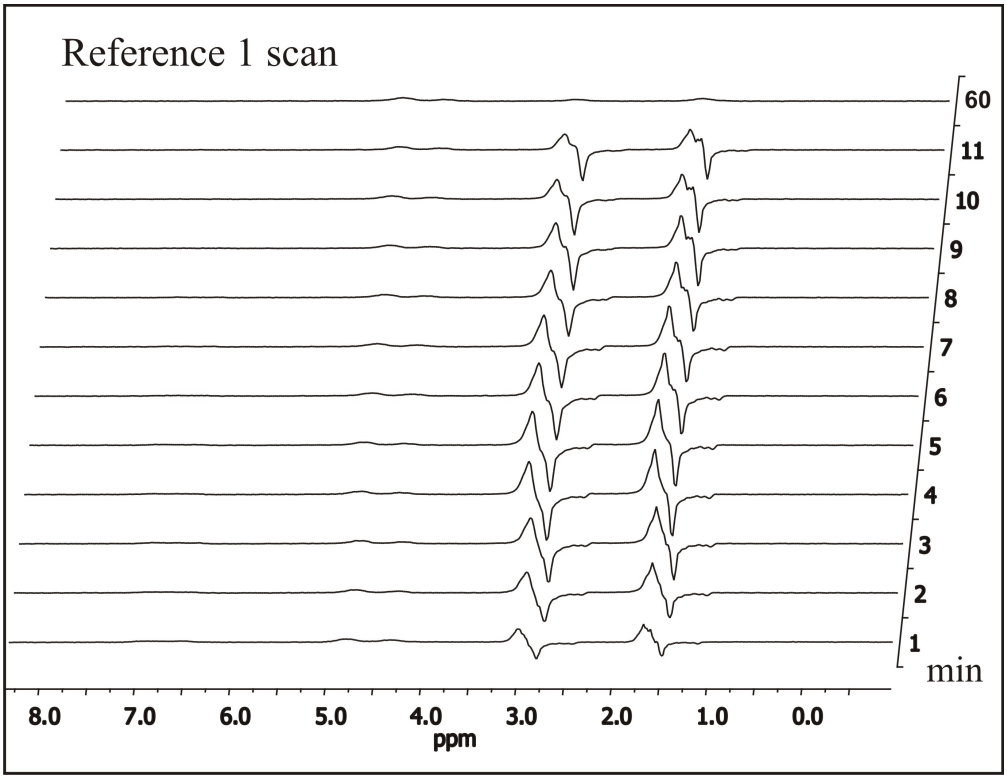

Figure 3.15: ^{1}H NMR spectra during a time period of 11 minutes after starting the hydrogenation reaction.

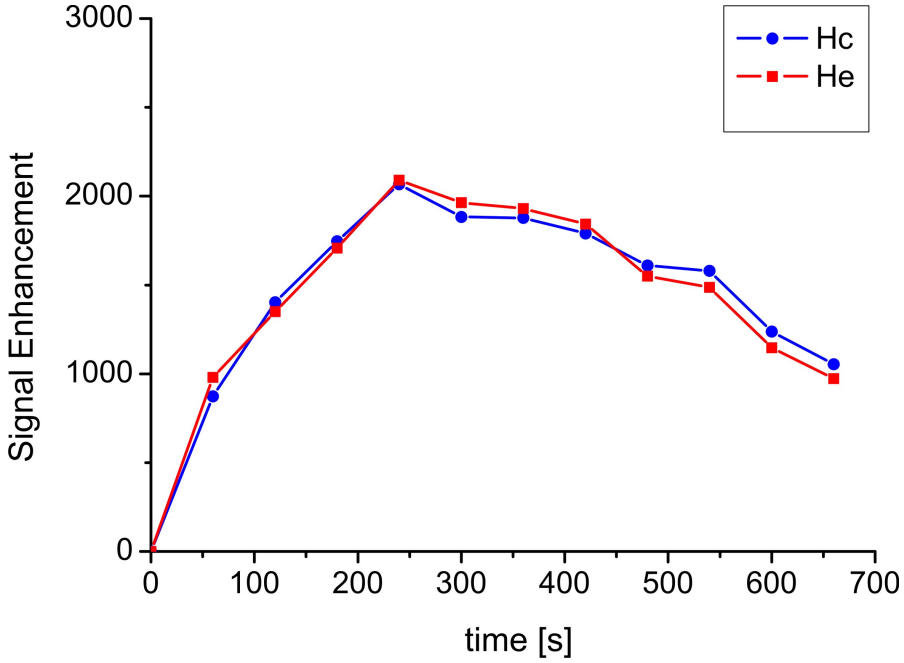

Figure 3.16: Time evolution of the ^{1}H NMR signal enhancements during the parahydrogenation of 2-hydroxyethyl acrylate.

For better comparison the time dependence of the measured signal enhancements of the hyperpolarized protons is plotted in Figure 3.16. As is clearly seen, the observed signal enhancements of the former p-H_2 protons H_c and H_e were similar in height over the observed time period and rather constant between minute 3 and 9 of the parahydrogenation reaction. A ^{1}H-^{1}H COSY experiment was performed during the parahydrogenation of 2-hydroxyethyl acrylate using the membrane setup. To ensure an optimal excitation of the PASADENA spin state the first 90° pulse in the COSY sequence was exchanged by a 45° pulse [76]. Due to the prior observation that the generated proton polarization was nearly constant for approximately 7 minutes, the ^{1}H-^{1}H COSY experiment was implemented by applying only one scan in order to stay in the time frame of constant hyperpolarization. As a reference, a thermal ^{1}H-^{1}H COSY was recorded with 8 scans after total conversion of the hydrogenation reaction was observed. Both 2D NMR spectra are displayed in Figure 3.17.

In the PHIP ^{1}H-^{1}H COSY spectrum only the cross peaks of the hyperpolarized protons at around 1.5 ppm and 3.0 ppm are visible due to the enhanced signal of the corre-

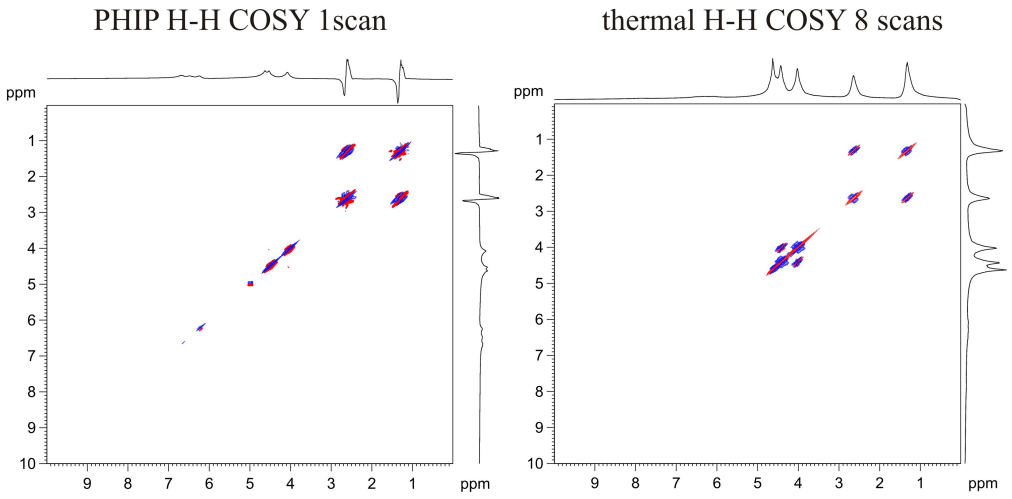

Figure 3.17: ^{1}H-^{1}H COSY NMR spectrum acquired during parahydrogenation of 2-hydroxyethyl acrylate in D_2O, single scan (left), ^{1}H-^{1}H COSY reference spectrum of thermally polarized 2-hydroxyethyl propionate, 8 scans.

sponding protons and the special excitation of the PHIP spin state. Furthermore, the acquisition of the 2D spectrum during the ongoing reaction led to observation of small signals between 6 and 7 ppm stemming from the double bond of the starting material. These peaks cannot be observed in the reference ^{1}H-^{1}H COSY because it was acquired with the fully converted sample. As a consequence of the acquisition of the PHIP ^{1}H-^{1}H COSY without phase cycling, a small artifact can be recognized in the middle of the spectrum at 5 ppm which is not present in the reference COSY experiment where full phase cycling was applied.

PHIP 2D NMR spectroscopy was previously applied by Duckett et al. to obtain structural information of metal dihydride complexes [76]. In comparison to the experiments presented in this work they were able to perform much faster 2D experiments with full phase cycling (e.g. ^{1}H-^{1}H PHIP COSY in 2.6 min). In their method, hyperpolarization is achieved without a chemical reaction. This allows short recycle delays (typically 20-100 ms) enabled by the fast refreshment of hyperpolarized signal due to the fast exchange of gaseous and bound p-H_2 in metal dihydride complexes. The 2D experiment demonstrated here acquired during an ongoing chemical reaction had to be performed by applying a recycle time of 2 s which is a trade-off of the time of constant proton polarization, signal enhancement due to conversion of the parahydrogenation, and the T_1 relaxation time of the PHIP protons. However, it was demonstrated here that by

using the membrane technique it was possible to obtain a reliable 2D spectrum with chemical selectivity in much shorter time than by measuring a sample with thermal polarization. Other 2D experiments could be used for exploring the structure of reaction products resulting in a significant time saving compared to the usage of thermally polarized samples. In addition, the presented setup opens up the possibility to investigate otherwise elusive reaction intermediates due to the possibility of accumulating several scans during the ongoing reaction.

Different Investigated Membrane Systems

With regard to the encouraging results obtained for parahydrogenation reactions using hollow fibre membranes, smaller module systems were built of different membrane systems (different wall thickness, inner diameter and pore size) in order to investigate the efficiency of these types of hollow fibre membranes. Overall seven membranes were examined with regard to the achieved conversion rate of the reaction and the generated signal enhancement. All implemented membrane systems are shown in Figure 3.18. The varying diameters of the membranes evoked different amounts of capillarys inserted into the reaction chamber resulting in different amounts of membrane surface. To simplify matters, they were labeled with the letters A – F and the previously investigated membrane system on the left maintained its name Celgard.

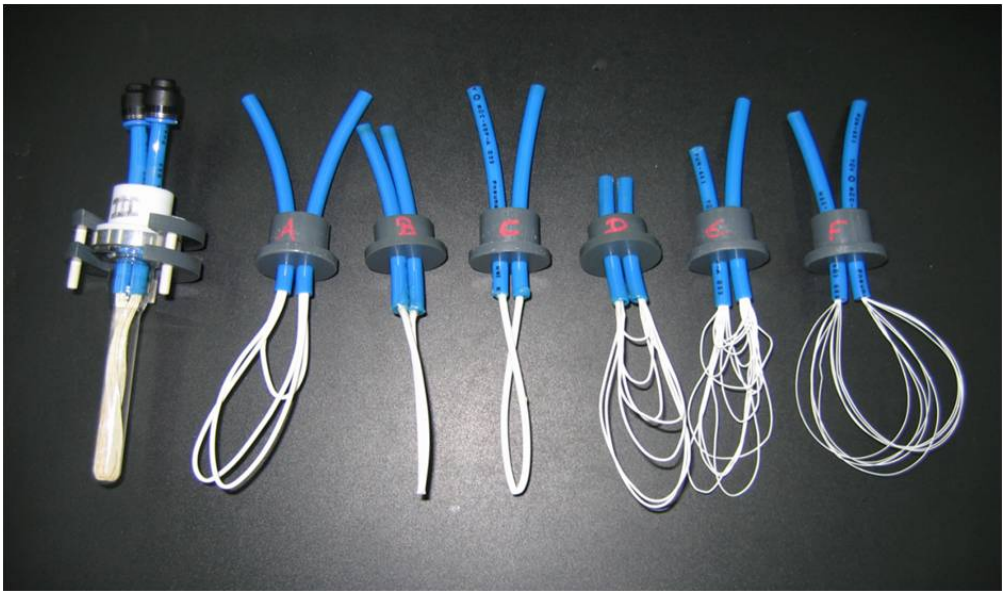

Figure 3.18: Different investigated membrane systems for the parahydrogenation technique.

All depicted membranes were received from Membrana and contain the polymer polypropylene. Their commercial names are displayed in table 3.8, together with their inner diameter and the utilized letters in this study.

Commercial name of the membrane system	inner diameter	Abbreviation
Celgard X 50	$<$ 1mm	Celga.
Accurel 300/1200	$>$ 1mm	A
Accurel S 6/4	$>$ 1mm	B
Accurel S 6/2	$>$ 1mm	C
Accurel Q 3/2	$<$ 1mm	D
Plasmaphan P1 LX	$<$ 1mm	E
Accurel 50/280	$<$ 1mm	F

Table 3.8: Different tested membrane systems from Membrana.

The seven membrane systems were all utilized for a parahydrogenation reaction under PASADENA conditions at 80 °C and 3.5 bar. Therefore, each membrane module was filled with 75 mg of 2-hydroxyethyl acrylate, 5 mg of catalyst 11 and 2.5 g D_2O. The achieved conversion rates after carrying out the reaction for 8 minutes are summarized in table 3.9.

Membrane	Celga.	A	B	C	D	E	F
Conversion rate	95%	4%	6%	6%	92%	12%	72%

Table 3.9: Achieved conversion rates of membrane system A – F and Celgard, recorded after carrying out the hydrogenation reaction for 8 minutes.

Concerning these data, the Celgard membranes showed the best results with a total hydrogenation rate of 95%. Nearly the same performance showed the module system with membrane D, achieving a conversion rate of 92%. With a further exception of membrane F which implemented a converison rate of 72%, the other membrane systems achieved small hydrogenation rates of less than 12%. For all membrane systems, hyperpolarized signals were observed in the recorded proton NMR spectra after 30 seconds and 5 minutes as depicted in Figure 3.19.

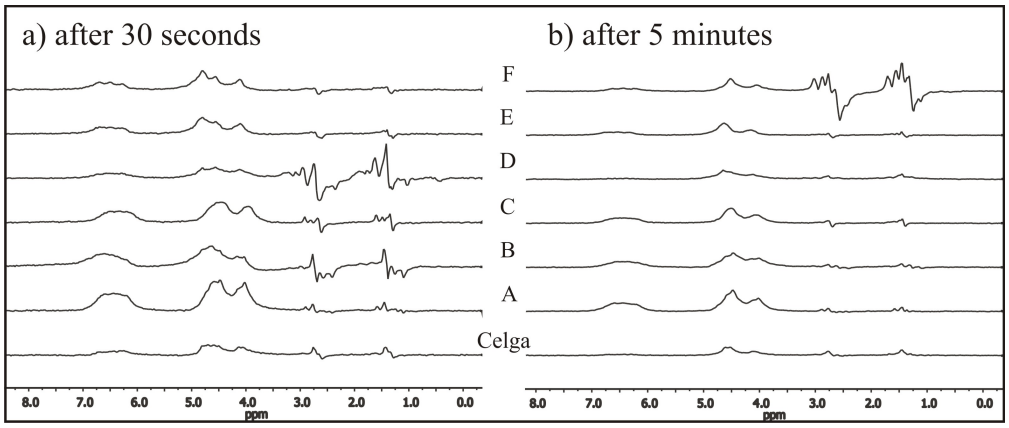

Figure 3.19: Recorded NMR spectra of the parahydrogenation with different membrane systems after a) 30 seconds and b) 5 minutes after starting the reaction.

The signal enhancements calculated relatively to the amount of produced hyperpolarized product are summarized in Table 3.10. Caused by the small conversion rates of membranes A, B, C and E, the calculated signal enhancements relative to these small amounts of produced hyperpolarized product yielded amounts between 205 and 35 for the spectra recorded after 30 seconds and after 5 minutes reaction time. However, the obtained antiphase signals in the spectra were comparitively small. Due to these small hyperpolarized signals and the slow reaction proceeding, membrane systems A, B, C and E are not suitable for utilization in the PHIP technique.

Membrane	Celga.	A	B	C	D	E	F
Signal Enh. after 30 sec.	H_c=25 H_e=25	H_c=75 H_e=65	H_c=205 H_e=210	H_c=110 H_e=90	H_c=85 H_e=110	H_c=40 H_e=35	H_c=15 H_e= 10
Signal Enh. after 5 min	totally reacted	H_c=60 H_e=55	H_c=60 H_e=50	H_c=70 H_e=75	totally reacted	H_c=45 H_e=40	H_c=275 H_e=265

Table 3.10: Calculated signal enhancements for the parahydrogenation with membrane system A – F and Celgard, once recorded 30 seconds after starting the reaction and once after 5 minutes.

With regard to the implemented conversion rates, the two most promising membrane systems Celgard and D only showed hyperpolarized peaks in the recorded spectra at

the beginning of the reaction. The spectra recorded after 2 minutes of membrane Celgard already did not feature any hyperpolarized signal due to the finished hydrogenation reaction. For membrane D, this was the case after 5 minutes. Relative to this reaction proceeding, the highest achieved signal enhancement for the membrane system Celgard amounted to 25 and for membrane system D to 110. In contrast to all other membranes, membrane system F displayed higher signal enhancements after 5 minutes than after 30 seconds. Hence, for this membrane system the reaction seems to start slower and is speeding up after a certain time. In the recorded spectrum of membrane F after 5 minutes, the highest signal enhancement of the whole experiment was observed amounting to 275 for H_c and 265 for H_e of the product 2-hydroxyethyl propionate.

In conclusion, the implemented membrane systems with diameters larger than 1 mm (membranes A–C) showed the smallest conversion rates. A reason for this can be found in the smaller amount of implemented cappilarys into the reaction chamber resulting in a smaller surface area. Membrane systems exhibiting smaller diameters labeled with D and Celgard implemented the highest conversion rates for the parahydrogenation reaction of 2-hydroxyethyl acrylate using catalyst system 11. However, with regard to all investigated membrane systems exhibiting diameters smaller than 1 mm, no direct dependency of the diameter and the conversion rate was distinct. Concerning the signal enhancements, system F achieved the best results. Hence, in future further systematic studies with these three types of membranes should be done in order to investigate their praticability for the PHIP method in more detail.

3.5 Polarization Transfer to Heteronuclei

The implementation of polarization transfer from the hyperpolarized protons to heteronuclei like ^{13}C and ^{15}N is beneficial because these nuclei exhibit an even smaller gyromagnetic ratio and therefore less sensitivity in the NMR experiment. Additionally ^{13}C and ^{15}N exhibit long T_1 times and can be used to prolong the lifetime of the hyperpolarization. Thus, optimization of polarization transfer to e.g. ^{13}C is crucial for applications like metabolic imaging where the highest possible ^{13}C polarization is required to obtain high SNR images. Transfer of polarization to heteronuclei can be implemented randomly in weak magnetic fields or selectively via special pulse sequences as discussed in the next sections.

3.5.1 Spontaneous Polarization Transfer at low Field

When performing a hydrogenation with p-H_2, two different cases of initial proton magnetization occur, namely the proton magnetization of the PASADENA technique and the one of the ALTADENA technique. Characterized by strongly and weakly coupled systems, these two techniques show entirely different behavior with regard to polarization transfer during the parahydrogenation itself. With respect to a definition in literature [77], two spins are considered weakly coupled if the nuclear spin-spin interaction is much smaller than the difference in their Zeeman interaction with the external field, otherwise they are strongly coupled. Performing an ALTADENA experiment at low field, any nuclear spins are strongly coupled. Thus, these strong couplings enable polarization transfer from protons to heteronuclei without any further spin manipulations being necessary. In this case, it is sufficient to apply a simple $\pi/2$ pulse on the heteronuclei to observe a heteronuclei spectra with hyperpolarized signals.

In order to investigate the efficiency of spontaneous polarization transfer at low magnetic field, a standard ALTADENA experiment of 1-hexyne in acetone-d_6 was performed with the use of catalyst system 1. For further optimization of the reaction conditions in this work presented here, the sample was heated up in a water bath at 60 °C and a content of 98% of enriched p-H_2 was utilized. To allow for a better understanding of the efficiency of the implemented polarization transfer, a one scan proton spectrum was measured immediately before the ^{13}C spectrum to facilitate the comparison of different polarization transfer techniques. Afterwards, the hyperpolarized ^{13}C spectrum of 1-hexene was recorded with one 90° pulse. The reference spectrum was recorded immediately afterwards under the same measurement conditions as the ^{13}C PHIP spectrum but, instead of one scan, 174 scans were accumulated.

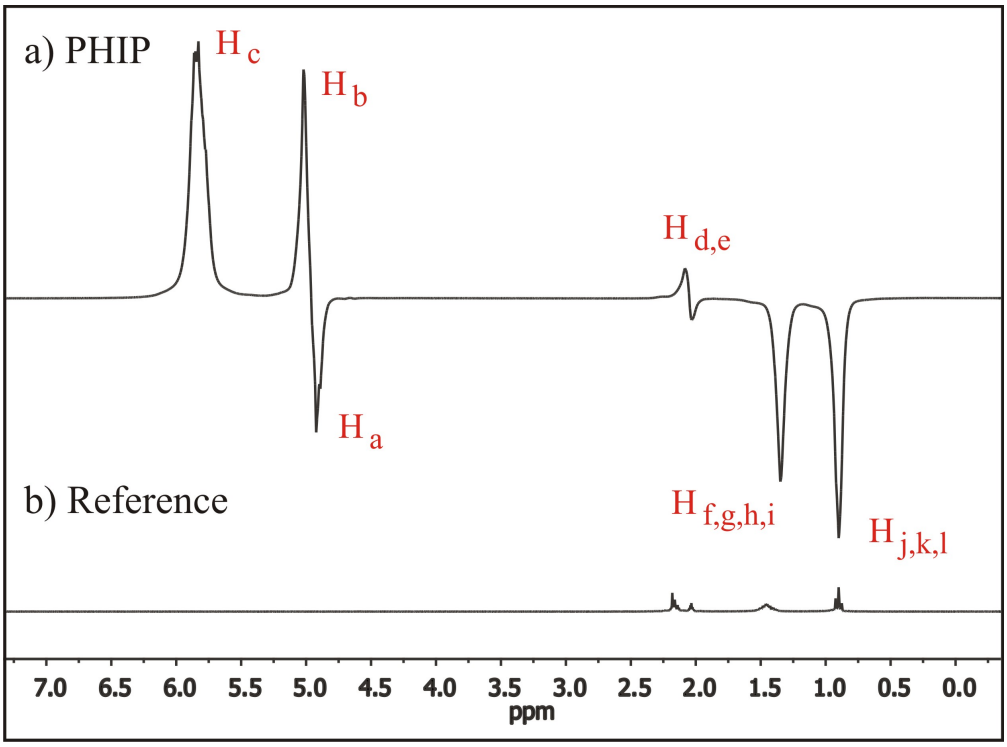

Figure 3.20: ALTADENA ^{1}H spectrum of the parahydrogenation of 1-hexyne.

The recorded ALTADENA PHIP spectrum is shown in Figure 3.20. In comparison to the PASADENA spectra shown in Chapter 3.2 in Figure 3.5, the obtained ALTADENA spectrum shows hyperpolarization of all protons in the hydrogenation product 1-hexene. Thus, the calculated signal enhancements observed in this spectrum are calculated according to the procedure for ALTADENA experiments. Hereby, all hyperpolarized signals are divided by the amount of protons they stem from. This is done because under ALTADENA conditions not only the two introduced protons are hyperpolarized, but a "flow" of the introduced polarization to other protons in the molecule occurs due to the strong couplings at low magnetic field which is clearly visible in Figure 3.20. Therefore, a partial cancelation of observable hyperpolarization is noticeable for H_a and H_b which exhibit different phases but are located closely. Hence, the calculated signal enhancements (summarized in Table 3.11) represent a spreading of the introduced hyperpolarization over the whole molecule. More details of the calculations of the signal enhancements are described in the experimental Chapter 6.

In the obtained ^{13}C PHIP spectrum (Figure 3.21), hyperpolarized signals of the entire carbon skeleton of the hydrogenation product 1-hexene are present likewise for a similar experiment presented 2002 in literature [78]. Also depicted in Figure 3.21 is the

	$H_{a,b}$	H_c	$H_{d,e}$	$H_{f,g,h,i}$	$H_{j,k,l}$	C_1	C_2	C_3	C_4	C_5	C_6
T_1 [s]	25.3	33.4	16.4	14.4	12.8	14.8	23.1	19.0	19.0	19.2	14.4
SE	1445	4810	165	510	845	365	2060	5740	4035	685	2450

Table 3.11: Summary of the T_1 times of the protons and carbons and their observed signal enhancements for the model compound 1-hexene.

recorded reference spectrum. The highest signal enhancements were not observed for the two carbons directly bound to the polarized protons but for the two atoms in the middle of the carbon chain. The highest calculated signal enhancement in this experiment was achieved for C_3 with an amount of 5740. Hence, the region of the molecule which showed the lowest signal enhancement for the protons, namely H_d and H_e afterwards showed the highest signal enhancement of the directly bound carbon, namely C_3. This leads to the assumption, that during the transfer of polarization over the whole molecule at low magnetic field, nearly all the hyperpolarization from H_d and H_e was transferred to the carbon molecule in direct neighborhood. The calculated signal enhancements of every carbon in the chain of 1-hexene are summarized in Table 3.8, together with the measured T_1 times of the carbon atoms. With regard to the T_1 times of the carbons of the hydrogenation product, carbon 2, exhibiting the longest spin-lattice relaxation time of 23 seconds was expected to give the highest signal enhancement in the spectrum. As this is not the case, another effect during the "flow" of polarization over the molecule at low magnetic field has to be responsible for the resulting peak pattern as observed in the hyperpolarized ^{13}C spectrum in Figure 3.21.

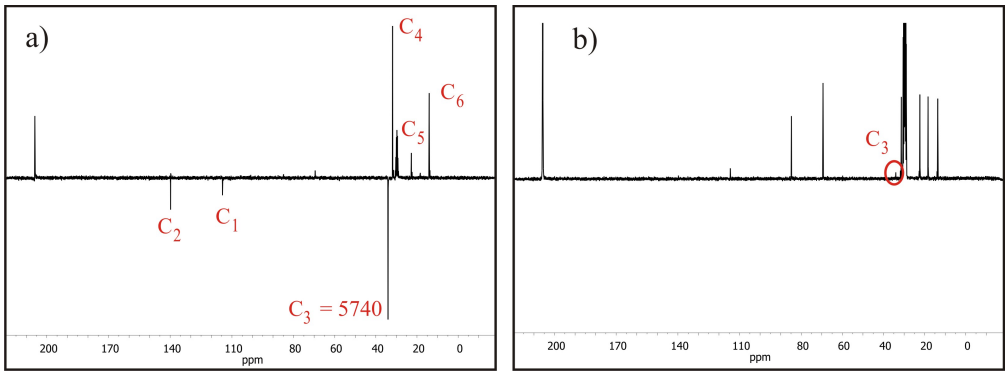

Figure 3.21: Recorded ^{13}C spectra when performing a parahydrogenation with 1-hexyne a) of the spontaneous polarization transfer under ALTADENA conditions of the parahydrogenation product 1-hexene and b) the reference spectrum recorded immediately afterwards with 174 scans.

In conclusion, this type of polarization transfer experiment with the ALTADENA spin system at low field offers a simple way to achieve hyperpolarized peaks of ^{13}C with signal enhancements of more than 5000. Additionally, for the hydrogenation product 1-hexene, the underlying mechanism under these conditions prefers the transfer of polarization to carbon molecules located in the middle of the molecule and not at its end.

3.5.2 Polarization transfer via INEPT(+π/4) and PH-INEPT+ Sequences

When performing PASADENA with weakly coupled spin systems as it is in general the case at high magnetic field an appropriate pulse sequence is needed in oder to transfer the polarization from the PASADENA spin system to heteronuclei. Therefore, two pulse sequences already known in literature were investigated in this study with regard to our model compound 1-hexyne, namely the INEPT(+π/4) sequence and the PH-INEPT+ sequence [61] shown in Figure 3.22 and 3.23.

In order to achieve polarization transfer from the two former p-H_2 nuclei to heteronuclei under PASADENA conditions, a PASADENA under pressure experiment was implemented for model compound 1-hexyne with catalyst system 1. The used temperature and pressure conditions, as well as the sample composition of this experiment was chosen according to the already described ALTADENA setup in the previous chapter.

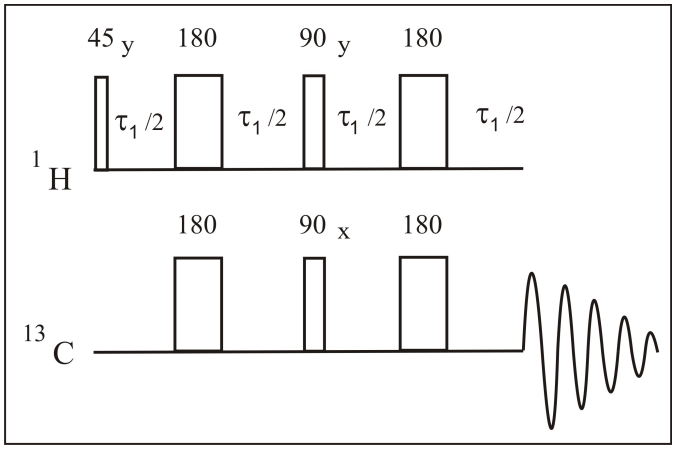

Figure 3.22: NMR pulse sequence PH-INEPT+ applied to a PHIP spin system for polarization transfer from ^{1}H to ^{13}C.

One significant difference of the entire experiment was shaking of the sample tube directly above the bore of the magnet in order to obtain a PASADENA spin system. For a better investigation of the transfer efficiency of the hyperpolarization, a proton PHIP spectrum was recorded additionally with a 2.5° pulse immediately before the polarization transfer sequence was applied.

In order to build the PH-INEPT+ sequence, the initial $\pi/2_x$ pulse was substituted in the standard INEPT sequence by $\pi/4_y$, the first and the last pulse in the ^{1}H-channel then having the same phase (Figure 3.22). Applying the sequence on the initial density matrix for PASADENA experiments should yield refocussed signals on the heteronuclei. For further signal enhancement, these resulting inphase signals were recorded ^{1}H-decoupled. For the PH-INEPT+ sequence, the occurrence of a signal on the heteronuclei crucially depends on the size of the ^{1}H – ^{1}H coupling of the PHIP protons J^{12}, as a result of the present density matrix. For cases where J^{12} is small or absent, this feature makes signal detection on the heteronuclei with the PH-INEPT+ sequence difficult or impossible. This problem can be solved by utilizing the INEPT(+π/4) sequence which does not depend on the ^{1}H – ^{1}H coupling of the PHIP protons. The conventional INEPT sequence leads to trilinear terms which are not detectable on the hetero nucleus when applied on the p-H_2 density matrix. However, they can be transferred into detectable terms simply by applying an additional $\pi/4$ pulse on the protons at the end of the conventional INEPT sequence as shown in Figure 3.23.

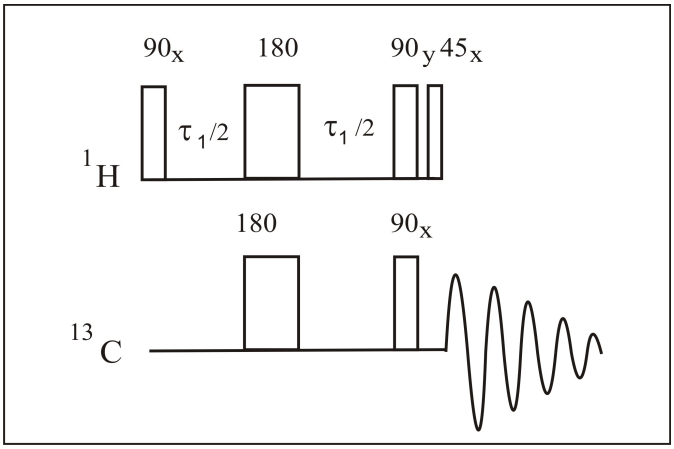

Figure 3.23: NMR pulse sequence INEPT(+π/4) applied to a PHIP spin system for polarization transfer from ^{1}H to ^{13}C.

The ^{1}H PHIP spectrum recorded immediately after shaking the tube above the bore of the magnet did not show the expected PASADENA peak pattern but instead, the same peak pattern as received for the ALTADENA experiment. Thus, the stray field of the magnet is not high enough to generate PASADENA conditions but gives rise to ALTADENA polarization in the beginning of the parahydrogenation. The continued reaction inside the NMR magnet then results in the build-up of PASADENA polarization prior to the NMR experiment. Regarding 1-hexene with spin-lattice relaxation times between 15 and 33 seconds, most of the significant high ALTADENA polarization is still present after the insertion in the spectrometer (around 20 seconds) and at the moment of acquisition. Hence, freshly generated PASADENA polarization after shaking the tube is negligible with regard to the huge amount of generated ALTADENA hyperpolarization at the beginning of the experiment. In order to obtain a major part of PASADENA spin system for the hydrogenation product 1-hexene, it would be essential to wait a longer time after the insertion of the tube. However, this delay would also implicate a loss of polarization during the waiting time. Hence, the following experiments were focused on the outcome of implementing the INEPT(+π /4) and PH-INEPT+ sequence (created for PASADENA spin systems) to an ALTADENA spin system.

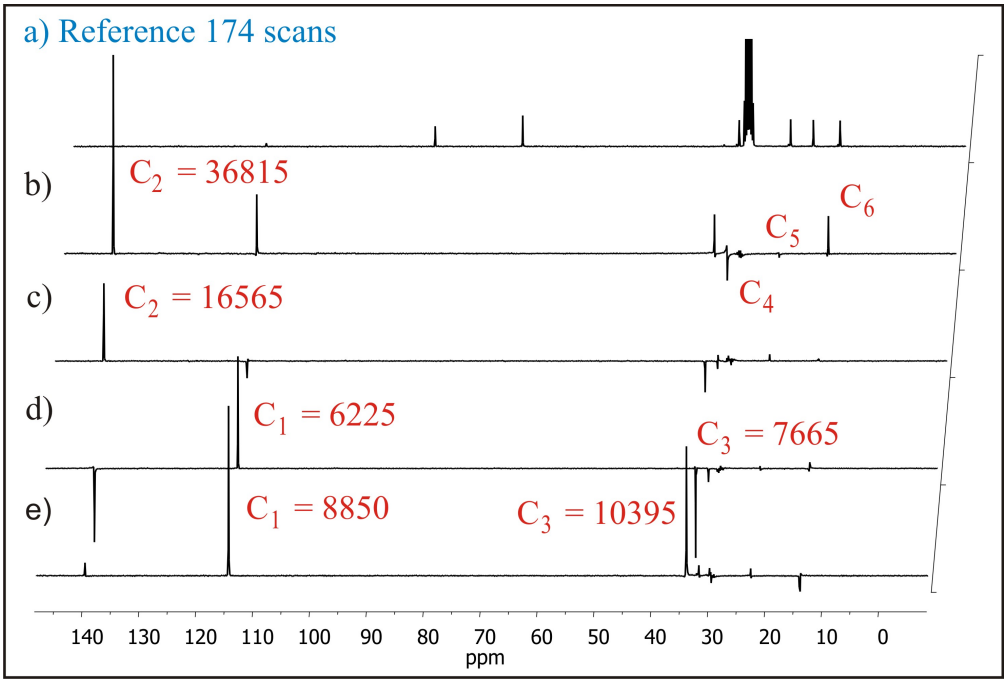

Figure 3.24: ^{13}C NMR spectra of the parahydrogenation of 1-hexyne recorded with a) 174 scans for the reference spectrum and after applying the PH-INEPT+ sequence with delays of b) 5 ms, c) 10 ms, d) 15 ms and e) 20 ms.

In order to examine the dependence of the PH-INEPT+ sequence on the ^{1}H – ^{13}C couplings in the molecule, it was applied with different delays $t_1/2$ between 5 and 20 ms. The hereby recorded ^{13}C spectra are displayed in Figure 3.24. Also shown in this figure is the reference spectrum recorded with 174 scans immediately after shaking the reaction sample for the first time. This spectrum was chosen as a reference for every hyperpolarized ^{13}C spectrum, representing the amount of thermally polarized peaks assumed for a conversion rate of 5% of the hydrogenation product 1-hexene after each shake of the tube. The calculated signal enhancements of the carbons, as well as the calculated signal enhancements of the proton spectra recorded each time before applying the pulse sequence are summarized in Table 3.12.

$H_{a,b}$	H_c	$H_{d,e}$	$H_{f,g,h,i}$	$H_{j,k,l}$		C_1	C_2	C_3	C_4	C_5	C_6
					$t_1/2$						
2315	7595	245	725	1340	5 ms	3535	36815	3610	2120	330	3105
2345	8070	290	870	1480	10 ms	1180	16565	3320	470	615	210
2665	8475	280	905	1470	15 ms	6225	12710	7665	1000	180	485
1305	6165	200	530	1220	20 ms	8850	905	10395	495	510	1140

Table 3.12: Summary of the observed signal enhancements of 1-hexene in the ^{1}H spectra recorded before applying the PH-INEPT+ sequence and afterwards in the ^{13}C spectra.

All signal enhancements of the proton spectra were in the same regime. The only exception in this case was the proton spectra recorded before applying the PH-INEPT+ sequence with a delay of 20 ms, where the former polarization of all the protons in the molecule was not as a high as for the experiments implementing the other delays. Comparing the peak pattern of the ^{13}C spectra obtained for different delays $t_1/2$, it is obvious that the outcome of it strongly depends on the chosen delay time. Applying a delay of 5 ms led to the highest observed signal enhancement of the whole experiment amounting to 36815 for carbon 2. In comparison to the delay of 10 ms, all signal enhancements of the carbons were higher. The implemented delays of 15 ms and 20 ms led to highest signal enhancements obeserved for carbon 1 and carbon 3. Comparing these cases, the calculated signal enhancements for the delay of 20 ms were even higher, amounting to 8850 for carbon 1 and 10395 for carbon 3, meanwhile the former proton polarization for this delay was less than for all the others.

An important result of these experiments is, that the application of the PH-INEPT+ sequence to an ALTADENA experiment leads to significant higher hyperpolarization on the carbon nuclei as observed in the recorded standard ALTADENA spectrum without applying a pulse sequence. Furthermore, the strength of the signal enhancement of the different carbon atoms strongly depends on the implemented delays $t_1/2$ of the PH-INEPT+ sequence.

The achieved carbon spectra after applying the INEPT($+\pi$ /4) sequence to the parahydrogenation of 1-hexyne also with different delays $t_1/2$ ranging between 5 – 20 ms are shown in Figure 3.25. From these spectra it is obvious, that the peak pattern is independent of the implemented delay $t_1/2$. The only difference between the recorded carbon spectra are the different total intensities of the achieved signal enhancements. For better comparison, all calculated signal enhancements of the protons measured immediately before the polarization transfer experiment and also the ones of the carbons measured with differnt delays of $t_1/2$ are summarized in Table 3.13.

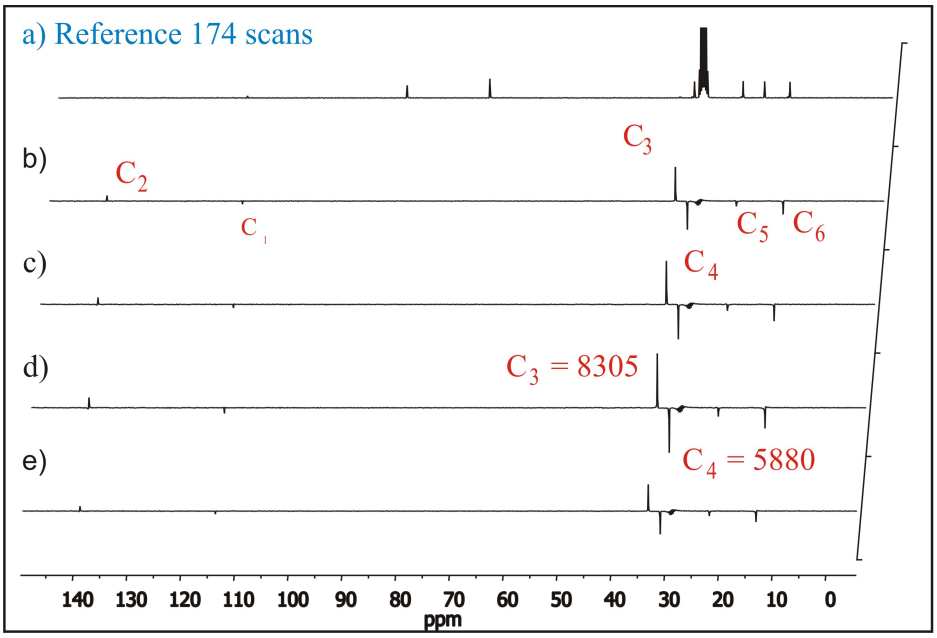

Figure 3.25: ^{13}C NMR spectra of the parahydrogenation of 1-hexyne recorded with a) 174 scans for the reference spectrum and after applying the INEPT($+\pi$ /4) sequence with delays of b) 5 ms, c) 10 ms, d) 15 ms and e) 20 ms.

$H_{a,b}$	H_c	$H_{d,e}$	$H_{f,g,h,i}$	$H_{j,k,l}$		C_1	C_2	C_3	C_4	C_5	C_6
					$t_1/2$						
1720	5855	335	595	1040	5 ms	345	1865	5600	4000	760	1975
2090	7540	270	785	1345	10 ms	355	2160	6695	4494	865	2335
2380	8530	315	885	1535	15 ms	565	3155	8305	5880	1165	2850
1475	4605	265	445	905	20 ms	340	1670	4390	3260	700	1610

Table 3.13: Summary of the observed signal enhancements of 1-hexene in the ^{1}H spectra recorded before applying the INEPT(+π /4) sequence and afterwards in the ^{13}C spectra.

With regard to the previous recorded proton spectra, the polarization transfer efficiency linearly depends on the achieved signal enhancement for the protons. For example, the ^{1}H spectrum recorded immediately before applying the INEPT(+π/4) sequence with a delay of 15 ms showed the highest signal enhancement, the same as the afterwards recorded ^{13}C spectrum which resulted in the highest signal enhancements achieved for the carbons amounting to 8305 for carbon 3 and to 5880 for carbon 4. Another interesting fact is, that like for the spontaneous transfer, the region of the molecule which showed the lowest signal enhancement for the protons (H_d and H_e) afterwards obtained the highest signal enhancement of the directly bound carbon (C_3). However, this phenomenon did not appear for every region of the molecule, as for example H_c showed the highest signal enhancement for the protons, but the directly bound carbon did not show the smallest signal enhancement for the carbons. Thus, an additional effect seems to be responsible for the observation of the highest signal enhancements of the carbons in the middle of the chain as already observed for the spontaneous polarization transfer.

Having a closer look to these two types of experiments, the peak pattern of the spontaneous polarization transfer under ALTADENA conditions of the ^{13}C spectrum is similar to the ones obtained by applying the INEPT(+π/4) sequence with any delay. The only difference is, that by phasing the acetone peak at 210 ppm to an absorption peak in every spetrum, all peaks of 1-hexene change their direction when switching between the spontaneous polarization transfer and the one with the INEPT(+π /4) sequence. Only exception is the signal of carbon 1 which in both cases stays in emission. Furthermore, regarding the achieved signal enhancements of the carbons in both experiments, the additional implementation of this pulse sequence did not lead to a significant gain of sensitivity.

All polarization transfer experiments performed in the last chapters resulted in significant high signal enhancements for all carbons in the molecule. Spontaneous polarization transfer under ALTADENA condtions generated the highest signal enhancements for carbon 3 and carbon 4 in the middle of the chain of up to nearly 6000. Additional implementation of the INEPT($+\pi$ /4) sequence with different delays to such an ALTADENA experiment did not result in more efficient polarization transfers. Furthermore, as this sequence is independent of the ^{1}H – ^{1}H coupling [61], different chosen delays always showed the same peak pattern which moreover were rather similar to the one obtained for spontaneous polarization transfer. In difference, applying the PH-INEPT+ sequence to an ALTADENA experiment led to much higher signal enhancements of up to 37000. In addition, implementation of this sequence with different delays offers the opportunity to transfer the major part of hyperpolarization to one desired carbon molecule. Hence, implementation of the PH-INEPT+ sequence to an ALTADENA experiment results in a huge sensitivity gain of the carbon molecules which for 1-hexene was calculated to be around six times higher than for applying spontaneous polarization transfer.

However, under the chosen reaction and measurement conditions, no investigation of the implementation of such polarization transfer sequences to a pure PASADENA spin state was feasible. However, there are different possibilities to overcome this problem. One would be the embedding of a further delay after the insertion of the reaction tube inside the spectrometer, which would lead to a loss of observable ALTADENA polarization. Alternatively, one could use this kind of experiment for substances possessing shorter T_1 times of the protons resulting in a faster decay of the ALTADENA spin system. Hence, the pulse sequences would be applied to a major part of PASADENA spin system. The most interesting method to apply such pulse sequences to real and pure PASADENA spin states exhibits the combination of the recently investigated membrane setup with the introduced polarization transfer experiments. Thus, the next part will focus on this kind of experiment.

3.5.3 Combination with the Membrane Setup

As described before in Chapter 3.4.2, the PHIP method was implemented with a continuous delivery of parahydrogen through hollow fiber membranes to generate a significant high polarization of ^{1}H which constantly renews itself on a time scale of several minutes. In contrast to batch techniques where acquisition is only possible during the T_1 time of the once generated hyperpolarization, the continuous delivery of parahydro-

gen and the ongoing hydrogenation reaction generate a significant high polarization on the protons which is stable for several minutes. This constant proton polarization can be used for the application of a polarization transfer sequence on ^{13}C which leads to also stable polarization of the carbons for several minutes.

Polarization transfer from the PHIP protons to the carbons in 2-hydroxyethyl propionate was investigated by carrying out an ALTADENA experiment at elevated temperature and pressure with regard to different implemented delays in the PH-INEPT+ sequence as shown in Figure 3.26. Therefore, 10 mm NMR tubes were filled with 5 mg catalyst, 0.86 mmol of 2-hydroxyethyl acrylate and 3 ml D_2O under argon atmosphere. The tubes were heated in a water bath at 80 °C and pressurized with 3 bar of p-H_2. A delay of 10 ms transferred the proton polarization only to C_3 and C_2 with the highest achieved signal enhancement of 1945 for the CH_2 group of C_2. Implementing delays of 15, 20 and 25 ms yielded in polarization of C_1, C_2 and C_3.

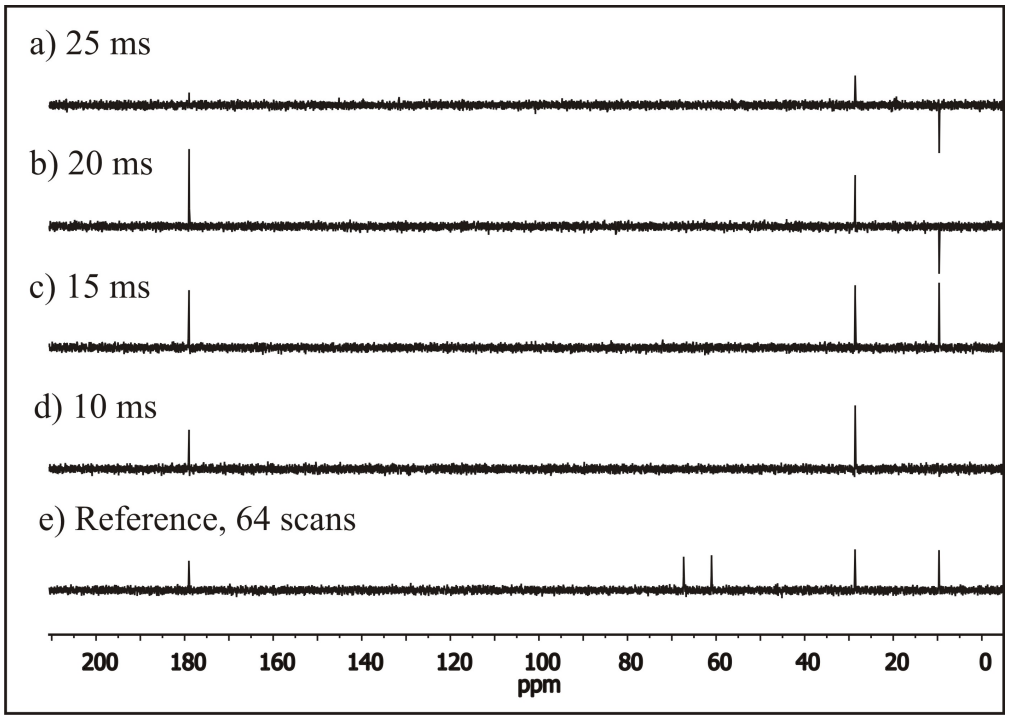

Figure 3.26: ^{13}C NMR spectra of the parahydrogenation of 2-hydroxyethyl acrylate recorded after applying the PH-INEPT+ sequence with delays of a) 25 ms b) 20 ms, c) 15 ms and d) 10 ms. e) Reference spectrum of the thermally polarized product acquired using 64 scans.

Meanwhile the delay of 15 ms nearly equally transferred the polarization to this three nuclei (a bit higher for C_3), the delay of 20 ms resulted in the highest achieved signal enhancement for the carbonyl group (C_3) amounting to 3405. Applying a delay of 25 ms transferred most of the polarization to the CH_3 group C_1 yielding a signal enhancement of 1515.

In order to achieve constant ^{13}C polarization by transferring the high proton polarization to the carbon nuclei in the molecule the experiment using the membrane setup as described in Chapter 3.4.2 was repeated. Therefore, a PH-INEPT+ sequence with a delay of 15 ms was applied to the parahydrogenation reaction every minute. The spectra featuring hyperpolarized ^{13}C signals recorded during a time frame of eleven minutes are depicted in Figure 3.27. In addition, a reference spectrum was measured of the fully converted sample after 1 hour with 64 scans and is displayed in the top trace.

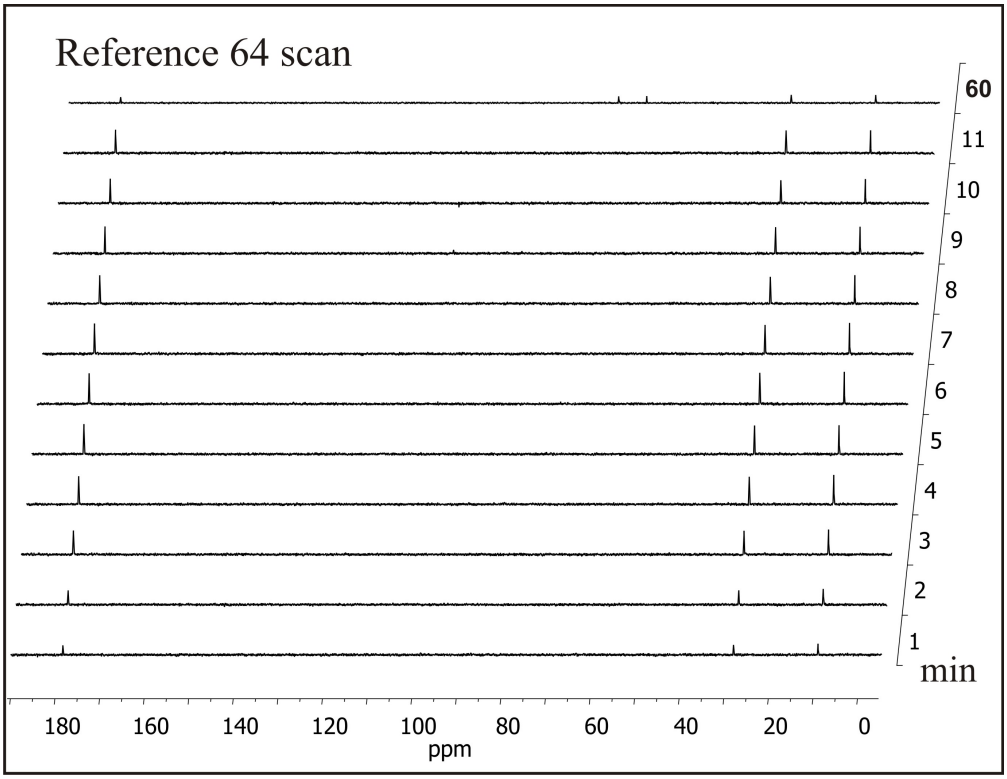

Figure 3.27: ^{13}C NMR spectra during a time period of 11 minutes after starting the hydrogenation reaction.

As can be seen in Figure 3.27 the implementation of the PH-INEPT+ sequence resulted in polarization transfer from the two introduced protons H_c and H_e to the carbons C_1, C_2 and most efficiently to C_3 of the hydrogenation product. The time evolution of the ^{13}C spectra is following the one of the ^{1}H spectra (described in Chapter 3.4.2) featuring almost constant ^{13}C polarization for several minutes. For better comparison the time dependence of the measured signal enhancements of the hyperpolarized carbons is plotted in Figure 3.28. The signal enhancements of the carbons belonging to the generated single bond C_1 and C_2 are similar to one another ranging from 3000 to 4000. They show the same time evolution like the proton signal and are constant for six minutes. Specifically the carbonyl group in the product molecule C_3 showed significant signal enhancements between 4000 and 5500 after the conversion rate of reaction stabilized around minute 3. The reason of the higher signal enhancement of the carbonyl group might be that the 15 ms time delay chosen for the PH-INEPT+ sequence might be more effective for the J-couplings between the hyperpolarized protons and C_3 resulting in more efficient polarization transfer than to C_1 and C_2.

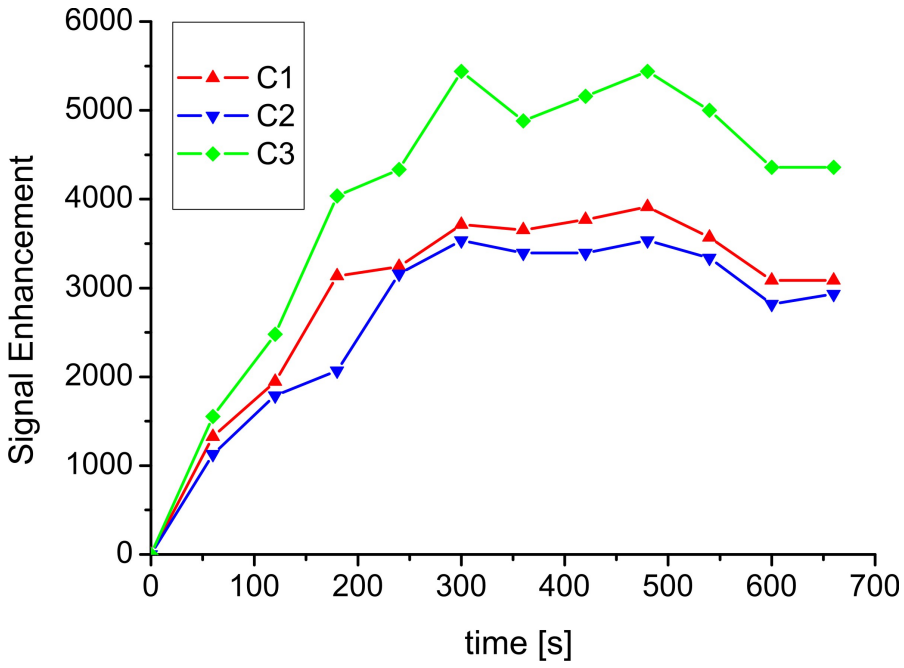

Figure 3.28: Time evolution of the ^{13}C NMR signal enhancements during the parahydrogenation of 2-hydroxyethyl acrylate.

In conclusion, combination of the membrane setup with polarization transfer experiments allowed to investigate the efficiency of the polarization transfer using pure PASADENA spin states. The investigations led to significant high ^{13}C polarization of C_1, C_2 and C_3 with varying amounts depending on the implemented delay for the PH-INEPT+ sequence. The investigated parahydrogenation of 2-hydroxyethyl acrylate using the membrane setup for dissolving parahydrogen into the aqueous solution combined with the PH-INEPT+ sequence led to a stable ^{13}C polarization for several minutes. These results open up the possibility to investigate the ongoing reaction with regard to elusive reaction intermediates and furthermore allows for more complicated NMR experiments like e.g. a two-dimensional ^{1}H-^{13}C COSY experiment.

4 Physiologically Relevant Substances for PHIP

In comparison to other methods, magnetic resonance imaging is a rather insensitive technique; especially ^{13}C magnetic resonance imaging is tedious due to the small magnetogyric ratio of the ^{13}C nucleus and its low natural abundance. Therefore, the application of ^{13}C MRI for clinical diagnosis has been limited so far due to the extremely long acquisition times that are required to obtain high signal-to-noise ratios (SNR) under physiological conditions. However, it was recently demonstrated, that this obstacle can be overcome by in vitro hyperpolarization of a molecule with long ^{13}C spin lattice relaxation time and subsequent injection into the animal or patient of investigation [19,20,58,71,79–81].

Hyperpolarization techniques like DNP, CIDNP and PHIP offer the unique possibility to use active MRI contrast agents, which are the direct signal source and do not rely on T_1 and/or T_2 changes of surrounding water molecules like classical passive (Gd or Fe based) contrast agents [19]. Therefore, interesting "active" contrast agents have to be identified and their ability of being hyperpolarized have to be investigated. Realising this, the role of certain target compounds and their use in clinical diagnosis could be investigated by a combination of a suitable hyperpolarization and magnetic resonance imaging technique.

Especially for the application of the PHIP method in medicine, suitable precursors of physiological relevant substances are essential which have to contain an unsaturated group to introduce the hyperpolarization in the molecule. A matter of particular interest is the identification of unsaturated precursors which after implementation of the parahydrogenation directly lead to the desired biological active compound. However, the realization of utilizing such a precursor is not always possible due to its malfunctioning or its non-existence. Hence, in some cases model compounds similar but not equal to the physiological relevant substances have to be utilized for the parahydrogenation. In order to identify different types of potential hyperpolarization agents for MRI the following chapters deal with the examination of different physiological relevant substances with regard to their applicability in the formerly optimized parahydrogen induced polarization method.

4.1 Metabolites and Neurotransmitters

4.1.1 Towards Metabolites of the Citric Acid Cycle

The citric acid cycle is a metabolic pathway which is of central importance in all living cells. In eukaryotic cells, the citric acid cycle occurs in the matrix of the mitochondrion and consists of a series of enzyme-catalyzed chemical reactions. In recent years, intensive work was focused on hyperpolarization of reactants out of this pathway via different techniques [82]. With regard to parahydrogen induced polarization, acetylene dicarboxylic acid is an interesting precursor substance as it contains an unsaturated group which can be used to introduce the hyperpolarization. Hydrogenation of its triple bond leads to two different isomers, namely the trans isomer fumaric acid and the cis isomer maleic acid. Fumaric acid is an intermediate in the citric acid cycle which is generated by oxidation of succinate via the enzyme succinate dehydrogenase and is afterwards converted to malate by the enzyme fumarase. In contrast, the cis isomer maleic acid does not play any role in this metabolic pathway. Due to their different constitutions, maleic acid is soluble in water, whereas fumaric acid is not. The melting point of maleic acid ($139 - 140\,^{\circ}\mathrm{C}$ [83]) is also much lower than that of fumaric acid ($287\,^{\circ}\mathrm{C}$ [84]). These properties of maleic acid can be explained on account of the intramolecular hydrogen bonding [85] that takes place at the expense of intermolecular interactions. One drawback of carrying out the parahydrogenation reaction of acetylene dicarboxylic acid with rhodium catalyst systems is that in general the cis isomer is formed. This drawback can be overcome by using a special ruthenium catalyst system that trans-hydrogenates internal alkynes directly and stereoselectively [86]. However, as this catalyst system is not commercially available and in order to get a first insight into the utility of the model compound, this disadvantage was disregarded for the experiments in this work. Taking these difficulties into account, there are also several studies concerning the parahydrogenation of fumaric acid to succinic acid which is another intermediate of the citric acid cycle and does not show the formation of different active or non-active isomers [82, 87, 88].

As already explained at the beginning of Chapter 3, there are different interacting aspects to optimize the PHIP procedure. One important point in this context concerns the relaxation of the hyperpolarized state to the ground state. This limiting factor can be reduced in some special cases: In studies of two-spin systems [52,54] it was demonstrated that singlet states in isolated spin pairs are long-lived under suitable conditions. Such lifetime prolongations require magnetic equivalence between the two spins which can be achieved by keeping the samples in low magnetic field. Here, quantum mechanical symmetry considerations in the isolated spin pair imply that the singlet state is

immune to the dipole-dipole relaxation mechanism. Combination of such long-lived states with hyperpolarization techniques may provide the basic opportunity to extend applications of hyperpolarized NMR and MRI to timescales that are inaccessible at the moment. Therefore, this phenomenon will be discussed in this section dealing with an appropriate substance, namely acetylene dicarboxylic acid and its ester acetylene dicarboxylic acid dimethylester. The latter was already investigated with regard to lifetime prolongation of the ^{13}C nucleus [89] which however did not result in a significant increase for ^{13}C relaxation times.

Another interesting feature of the substances acetylene dicarboxylic acid, acetylene dicarboxylic acid dimethylester and their resulting hydrogenation products are their symmetric structures. Due to this symmetry, the two inserted parahydrogen protons are magnetically equivalent in the molecule. Thus, they should not result in any hyperpolarized signal because their emission and absorption part of the antiphase signals exhibit the same chemical shift and therefore should cancel out. However, it was recently shown that this is not always the case and that hyperpolarized signals from symmetric molecules can be observed [90], which is still not fully understood. In any case, even if the proton polarization is not detectable, it should be present and could be transferred to observable ^{13}C polarization as already presented in the literature [57] for acetylene dicarboxylic acid dimethylester.

In order to investigate the applicability of acetylene dicarboxylic acid for PHIP, first experiments were implemented together with catalyst system 11 in D_2O. Unfortunately, nearly no hydrogenation took place and only minimal antiphase signals were observable under our reaction conditions. Implementation of harsher reaction conditions would lead to hydrogenation of acetylene dicarboxylic acid as demonstrated in the literature [81]. However, for the following experiments its ester acetylene dicarboxylic acid dimethylester was chosen which is less soluble in water but in acetone-d_6. The scheme of its parahydrogenation is shown in Figure 4.1.

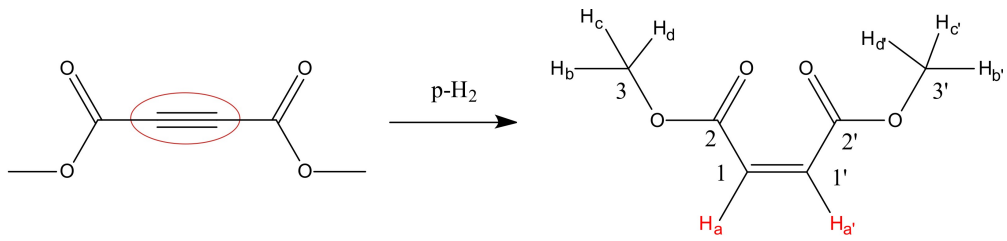

acetylene dicarboxlic acid dimethylester maleic acid dimethylester

Figure 4.1: Parahydrogenation of acetylene dicarboxylic acid dimethylester.

This bears the opportunity to investigate a model compound similar to the desired acetylene dicarboxylic acid by using one of the water insoluble catalyst systems. Taking this into account, the first point of interest was whether the parahydrogenation of acetylene dicarboxylic acid dimethylester leads to hyperpolarized signals in the product even if it is symmetric. Thus, an ALTADENA experiment was implemented with a sample tube containing 150 mg of acetylene dicarboxylic acid dimethylester, 10 mg catalyst 1 and 2.5 g acetone-d_6. Before starting the hydrogenation, the sample tube was heated in a water bath at 60 °C and pressurized with 3 bar of 98% p-H_2. After shaking the reaction tube for 5 seconds it was inserted in the spectrometer and a ^{1}H spectrum was recorded immediately. The achieved PHIP spectra is depicted in Figure 4.2 together with its reference spectrum measured before the experiment of the same sample tube under the same measurement conditions. In order to calculate the ALTADENA signal enhancements, the conversion rate at the time point of aquisition (TPA) was estimated to amount to 20%.

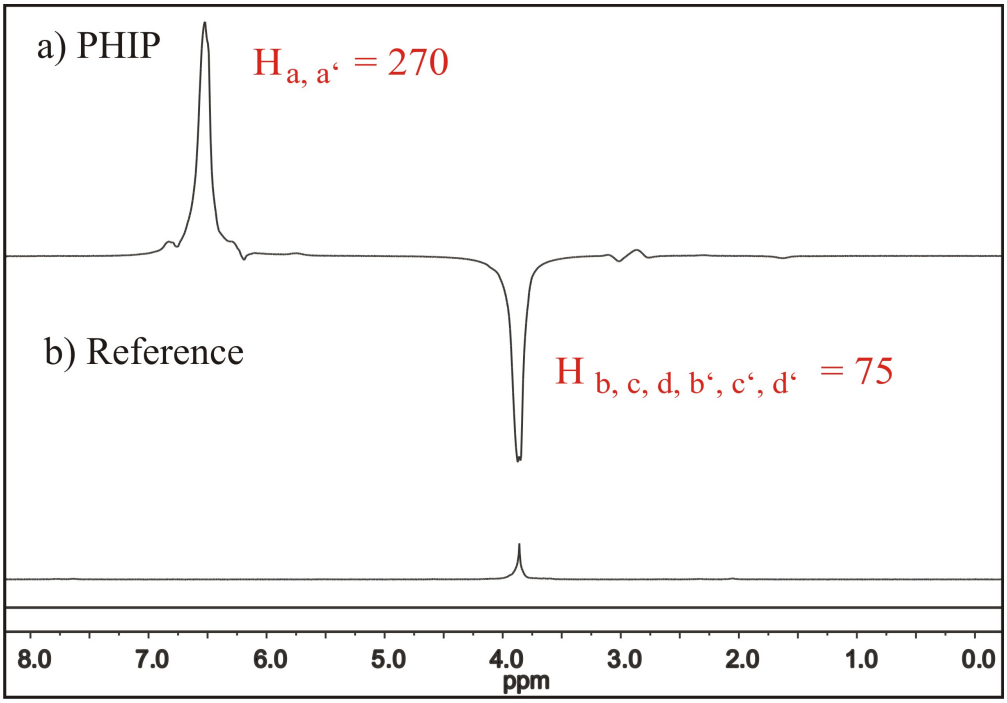

Figure 4.2: ^{1}H NMR spectra acquired using one pulse a) upon parahydrogenation of acetylene dicarboxylic acid dimethylester at 60 °C with 3 bar of 98% enriched para-H_2 and b) the reference spectrum of the same reaction mixture acquired before the reaction under the same conditions.

The calculated signal enhancements of the PHIP spectrum amount to 270 for each proton H_a and $H_{a'}$ and 75 for the six protons $H_{b,\,c,\,d,\,b',\,c',\,d'}$. In order to get a better understanding of the achieved signal enhancements, the corresponding T_1 times of the protons and the carbons in the product molecule maleic acid dimethylester are summarized in Table 4.1.

maleic acid dimethylester				
T_1 times of the protons [s]		T_1 times of the carbons [s]		
$H_{a,a'}$	$H_{b,\,c,\,d,\,b',\,c',\,d'}$	$C_{1,\,1'}$	$C_{2,\,2'}$	$C_{3,\,3'}$
15.2	7.7	7.7	75.9	11.4

Table 4.1: T_1 relaxation times of maleic acid dimethylester dissolved in acetone-d_6.

The fact that for the equal protons in the molecule H_a and $H_{a'}$ a hyperpolarized peak in absorption was observed together with small peaks on each side of it is in good agreement with the results presented in literature [90]. Also the hyperpolarized signal of the methyl group in Figure 4.2 was investigated in this article to always occur in emission. In addition, small hyperpolarized signals of the catalyst system occur in the recorded spetrum between 1.0 and 3.0 ppm. One could conclude that the observed hyperpolarized peaks of H_a and $H_{a'}$ arise from the small amount of molecules containing a ^{13}C nucleus in the molecule which breaks the symmetry. Contrary to this assumption, the authors of the article calculated that this hyperpolarized signal stems from symmetric molecules not containig ^{13}C nuclei which, however, is not fully understood. Also postulated is that when performing a parahydrogenation with weakly coupled systems (PASADENA) the resulting peak at 6.8 ppm of the protons H_a and $H_{a'}$ occur in emission and not as usual as an antiphase peak. For evaluation of this prediction, the same ALTADENA experiment as described before was carried out again but this time, more spectra were recorded of the ongoing reaction inside the spectrometer in order to investigate the evolution of the PHIP signal at high magnetic field. The evolution of the signal is clearly visible in the recorded spectra which are displayed in Figure 4.3. The first spectrum a) was divided by 10 in order to enhance the resolution of the other spectra b) – e). In the spectra a) and b) of Figure 4.3 a decrease of the hyperpolarized absorption peak at 6.8 ppm is observable. In spectra c) recorded 2 minutes after shaking the tube it already evolved into an intense PASADENA emission peak which, however, is not as high as the ALTADENA signal of the first spectrum. In the last two spectra d)

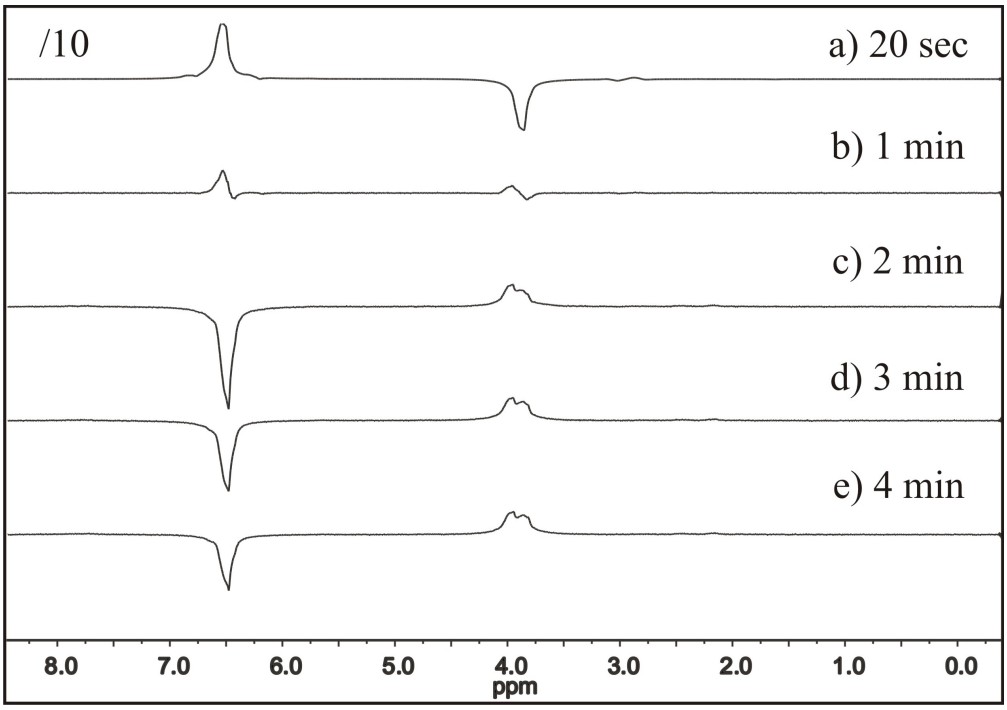

Figure 4.3: ^{1}H NMR spectra upon parahydrogenation of acetylene dicarboxylic acid dimethylester at 60 °C with 3 bar of 98% enriched p-H_2 recorded at different times after starting the reaction by shaking the sample tube. To enhance the resolution of spectra b) – e), spectrum a) was divided by 10.

and e) the signal started to decrease again due to the smaller conversion rate of the reaction at this time point. Also visible in these spectra is the evolution of the hyperpolarized peak of the methyl group at 3.8 ppm from emission into a thermal peak in absorption. Furthermore, the signal of the methyl group stemming from educt molecules is observable in spectra b) – e), shlightly shifted to the lowfield regime.

Four minutes after shaking the sample tube it was transferred outside the spectrometer to the low earthfield and cooled in an ice bath to stop the reaction. After seven minutes of starting the hydrogenation the same tube was inserted again in the spetrometer to measure the conversion rate of the reaction. Thereby, the ALTADENA peak in absorption was observed again at 6.8 ppm. In order to get a better idea of this not expected hyperpolarized signal at this moment further spectra were recorded at different time points after the start of the reaction. The recorded spectra are depicted in Figure 4.4.

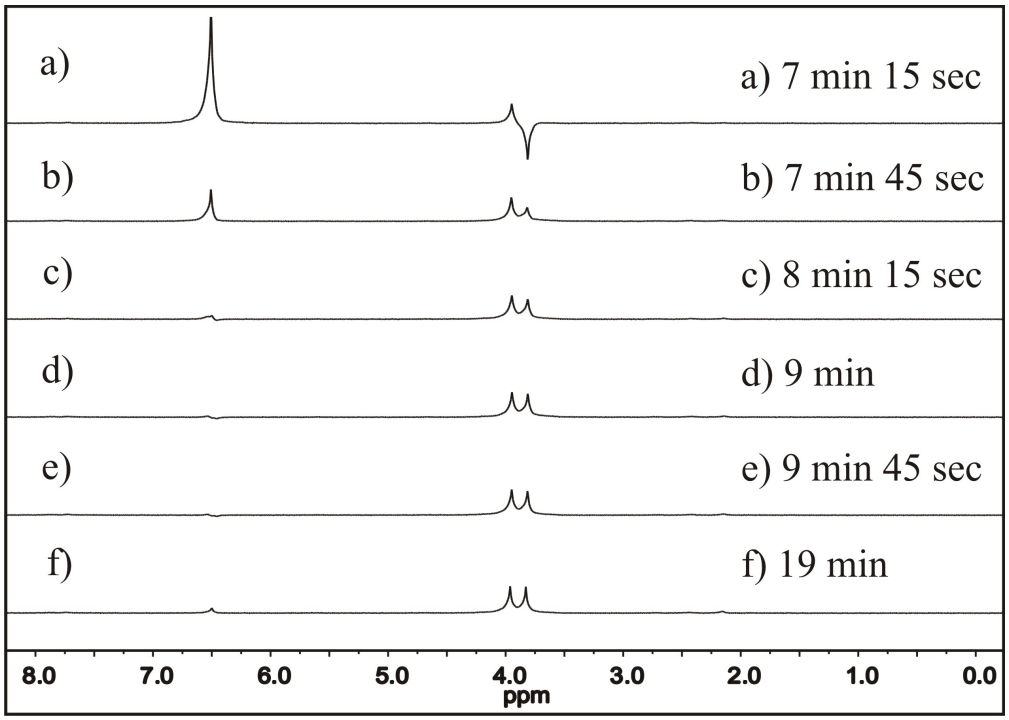

Figure 4.4: ^{1}H NMR spectra acquired using only one pulse upon the hyperpolarized product maleic acid dimethylester after storing the reaction sample for a few minutes in an ice bath outside the spectrometer and subsequent insertion in the spectrometer.

The first important point regarding the recorded spectra after storing the reaction tube for 3 minutes in an ice bath (Figure 4.4a) is, that the first spectrum shows a higher hyperpolarization level than the last spectrum recorded before transferring the sample tube outside the magnet. This seems unusual as the conversion rate after such a time in an ice bath should be really small and therefore should also lead to smaller or at least no higher hyperpolarized signals. This result supports the assumption of lifetime prolongation of the isolated spin system in the singlet state of the introduced parahydrogen atoms at low magnetic field. Thus, the generated hyperpolarization outisde the spectrometer was stored in the singlet state and could be accumulated due to the ongoing reaction. After inserting the sample again in the spectrometer, a spectrum of all stored hyperpolarization was recorded showing a higher signal enhancement. An additional hint for this theory is that the observed hyperpolarization in the spectrometer decays faster without even evolving in a PASADENA signal in emission (spectra a) – e)). This fast decay of the observed hyperpolarization reflects the minimal conversion rate of the

reaction at this moment. In the last recorded spectra f) 19 minutes after starting the reaction the thermal peak of the product becomes already visible at 6.8 ppm.

Based on these results, further experiments were implemented with regard to lifetime prolongation in the singlet state of the present isolated two spin system. Similar investigations were already done by E. Vinogradov and A. K. Grant concerning ethylpropiolate yielding relaxation twice as long as the longest T_1 observed in the high field [55]. However, as the product molecule upon parahydrogenation of acetylene dicarboxylic acid dimethylester not only exhibits an isolated two spin system but furthermore a symmetric conformation, two different effects are present during the parahydrogenation. Therefore, the investigation of one of these effects could be more distinct by avoiding the other effect. Thus, acetylene dicarboxylic acid dimethylester was ^{13}C labeled on one side at the C_2 position in order to break the symmetry of the molecule. The synthesis was carried out according to a procedure in literature [91, 92] described in detail in Chapter 6. This approach bears the possibility to compare the PHIP pattern of the symmetric molecule with the labeled and unsymmetric one and furthermore offers a way to examine the lifetime prolongation of the singlet state without any disturbing overlap with another effect. Hence, two times 50 mg of the ^{13}C labeled acetylene dicarboxylic acid dimethylester were used for ALTADENA experiments under equal conditions as the ones explained before for the symmetric acetylene dicarboxylic acid dimethylester. In order to investigate the lifetime prolongation of the hyperpolarized state, different time frames were chosen for shaking the tubes, leaving them at the earthfield without further moving, inserting them in the spectrometer and immediately measuring a spectrum. Therefore, each sample tube was used for three experiments dealing with different time frames. The hereby obtained six spectra are shown in Figure 4.5. As a result of the non-symmetric molecule, the hyperpolarized peaks occur as two inphase peaks with different phase, one for H_a and the second one a bit shifted for $H_{a'}$.

Shaking each sample for three times led to a total conversion rate of around 57% for each sample tube, measured approximately one hour after starting the experiments. The estimated conversion rates at the TPA are based on the total conversion rate measured at the end of the experiment by taking the ongoing reaction into account. For each shaking of the reaction sample for 5 seconds (first four experiments) a conversion rate of approximately 13% was estimated. The conversion rate for shaking the sample for 50 seconds was assumed to amount to 20%. Shaking the sample for even longer times will only give little higher conversion rates because no additional fresh parahydrogen is transferred to the sample. Therefore, the conversion rate after shaking the sample

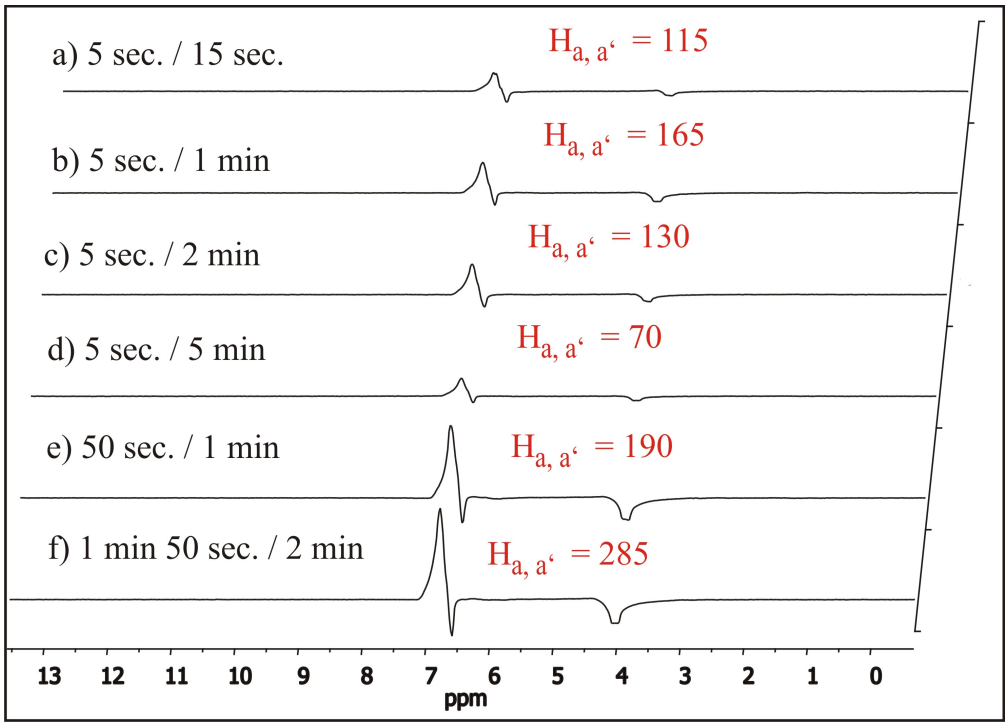

Figure 4.5: Examination of the lifetime prolongation due to the singlet state of hyperpolarized labeled maleic acid dimethyl ester under different timing conditions. The first noted time describes the duration of shaking the sample and the second depicted time is the time point of acquisition. Before this second time point, the sample was kept at earthfield without further moving. The calculated signal enhancements are highlighted in red.

for 1 minute and 50 seconds was estimated to amount to 22%. In order to get a better overview over the six implemented experiments the different chosen time frames are summarized in Table 4.2. Also depicted in Table 4.2 are the assumed conversion rates at the TPA and the achieved signal enhancements (SE).

The achieved signal enhancement for shaking the sample for 5 seconds and directly inserting it in the spectrometer amounted to 115. In comparison to the signal enhancement of the symmetric molecule achieved under similar measurement conditions the signal enhancement is smaller. A possible reason for this is the cancellation of the enclosed peaks of H_a and $H_{a'}$ exhibiting a different phase. Shaking the reaction sample for the same time but keeping it a longer time at low magnetic field before inserting

time of shaking	TPA	conversion rate	SE of $H_{a,\,a'}$
5 seconds	15 seconds	13%	115
5 seconds	1 minute	13%	165
5 seconds	2 minutes	13%	130
5 seconds	5 minutes	13%	70
50 seconds	1 minute	20%	190
1 min 50 seconds	2 minutes	22%	285

Table 4.2: Summary of the results of lifetime prolongation experiments.

it to record a spectrum yielded higher signal enhancements of 165 for a waiting time of 1 minute and 130 for a waiting time of 2 minutes, respectively. This gain of signal enhancement in both cases is due to the ongoing reaction and storage of the hereby generated hyperpolarization in the singlet state for a certain time. The smaller amount of SE after a waiting time of 2 minutes is based on the fact that the amount of new generated hyperpolarization at the end of the waiting time is smaller than the amount of lost hyperpolarization due to relaxation at this time. This is even more obvious after a waiting time of 5 minutes, where the part of lost hyperpolarization during the total time frame is bigger than the freshly generated one. Hence, a signal enhancement of only 70 was observed in the spectrum which nevertheless is considerably high after such a time. These results lead to the conclusion that there are two independent processes present during the waiting time frame (Figure 4.6).

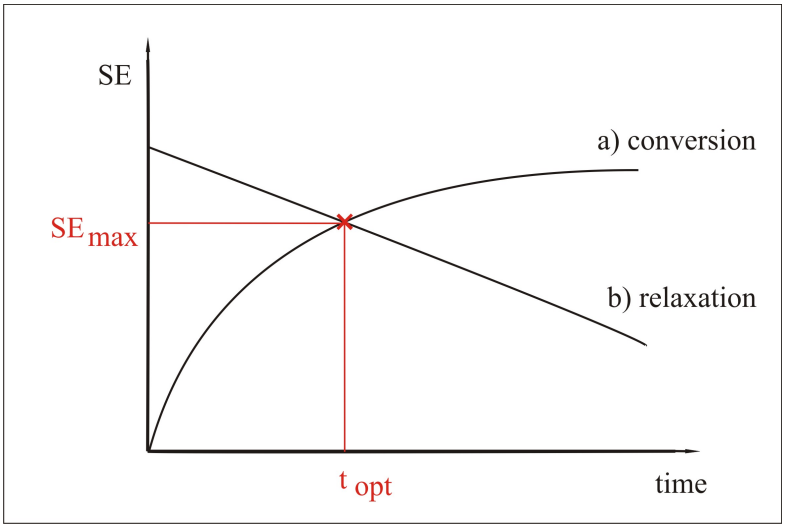

Figure 4.6: Scheme of the two present processes during parahydrogenation.

One process is the generation of freshly hyperpolarized product which corresponds to a gain of SE which can be thought of as function a) with a positive gradient. The other one is the indeed reduced, but anyhow present relaxation process which yields a loss of hyperpolarization represented as function b) with a negative gradient. The highest possible amount of signal enhancement SE_{max} for such an experiment can be achieved at the time point t_{opt} where both graphs intersect. This effect in general is not such important, as without lifetime prolongation of the singlet state the process of spin-lattice relaxation is always the dominating one which always determines to do the measurement as fast as possible.

In order to yield even higher values of SE, the amount of generated hyperpolarized product can be increased by shaking the sample tube for a longer time in order to ensure a better dissolution of parahydrogen into the reaction solution during the waiting time at low magnetic field depending on the total amount of present p-H_2. This was done in the last two experiments once shaking the sample for 50 seconds and directly inserting it and once shaking it for 1 minute and 50 seconds and directly inserting it to record a spectrum. In both cases, higher signal enhancements were observed due to higher amounts of generated hyperpolarized product. The signal enhancement for shaking the tube nearly 2 minutes resulted in the highest observed signal enhancement of the experiment with a value of 285.

The presented experiments of the hyperpolarized product maleic acid dimethylester at low magnetic field prooved the estimated lifetime prolongation due to the singlet state of this isolated two spin system. Thus, storage of hyperpolarization was possible at the generated double bond in the earthfield and it was still observable after a waiting time of 5 minutes. However, the effect was hard to quantify because of the ongoing chemical reaction of the pressurized sample. This results bear the opportunity to use this time frame in order to e.g. seperate the catalyst system from the reaction mixture.

Last point of interest with regard to the parahydrogenation of acetylene dicarboxylic acid dimethylester is the possibility to transfer the proton polarization to ^{13}C nuclei which exhibit long T_1 times. By taking the measured T_1 times of the carbons in Table 4.1 into account, the most promising carbon nuclei are C_2 and $C_{2'}$ both belonging to the carbonyl group in the molecule exhibiting a T_1 time of 76 seconds. In addition, C_2 and $C_{2'}$ are located near the introduced hyperpolarized protons which should result in a high ^{13}C polarization. To investigate the efficiency of polarization transfer to ^{13}C nuclei in the molecule, 70 mg acetylene dicarboxylic acid dimethylester was dissolved together with 2 mg of catalyst system 1 in 2.5 g acetone-d_6. Before applying 3.5 bar 98%

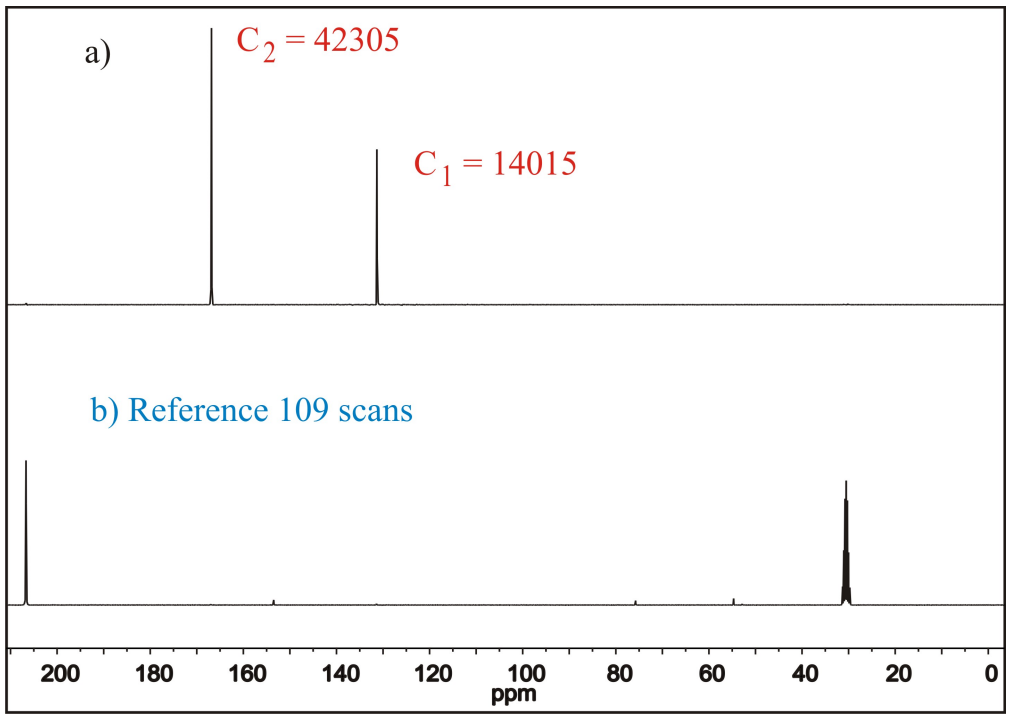

Figure 4.7: a) ^{13}C PHIP NMR spectrum of hyperpolarized maleic acid dimethylester recorded upon one pulse using a delay $t_1/2$ for the PH-INEPT+ sequence of 10 ms. b) Reference spectrum of the thermally polarized product acquired using 109 scans. The highlighted numbers correspond to the observed signal enhancements of the carbons $C_{1,1'}$ and $C_{2,2'}$.

para-enriched hydrogen to the sample tube, it was heated in a water bath to 60 °C. In order to get not only a high amount of ALTADENA polarization but additionally PASADENA polarization after inserting the sample tube, the spectrometer was also heated to 50 °C to allow the chemical reaction to continue. This proceeding insured the highest possible amount of generated hyperpolarized spin systems (either ALTADENA or PASADENA) which in the next step could be transferred from the protons to the carbons. Thus, the sample tube was shaken for 10 seconds above the bore of the magnet before inserting it in the spectrometer and applying the PH-INEPT+ sequence with a delay of 10 ms. The obtained single scan ^{13}C spectrum is shown in Figure 4.7 together with the reference spectrum measured immediately after applying the PH-INEPT+ sequence. As the total conversion rate after one shake amounted to 9%, 109 scans were

necessary in order to make the small amount of product signal visible in the reference spectrum. The calculated signal enhancements of the observed hyperpolarized peaks showed values of 42305 for $C_{2,2'}$ and 14015 for $C_{1,1'}$.

In order to investigate how long the generated ^{13}C hyperpolarization is observable in the NMR spectrum, a similar experiment was implemented again with the aim to detect simple ^{13}C spectra of the reaction sample after transfering the polarization once. The recorded spectra of different time points after polarization transfer are shown in Figure 4.8. The first spectrum a) was aquired by the read out of the PH-INEPT+ sequence 20 seconds after shaking the sample tube. This spectrum showed the highest hyperpolarization and therefore was divided by 25 in order to reach better resolution of the other spectra b) – f). Figure 4.8 shows that the once generated significant high hyperpolariza-

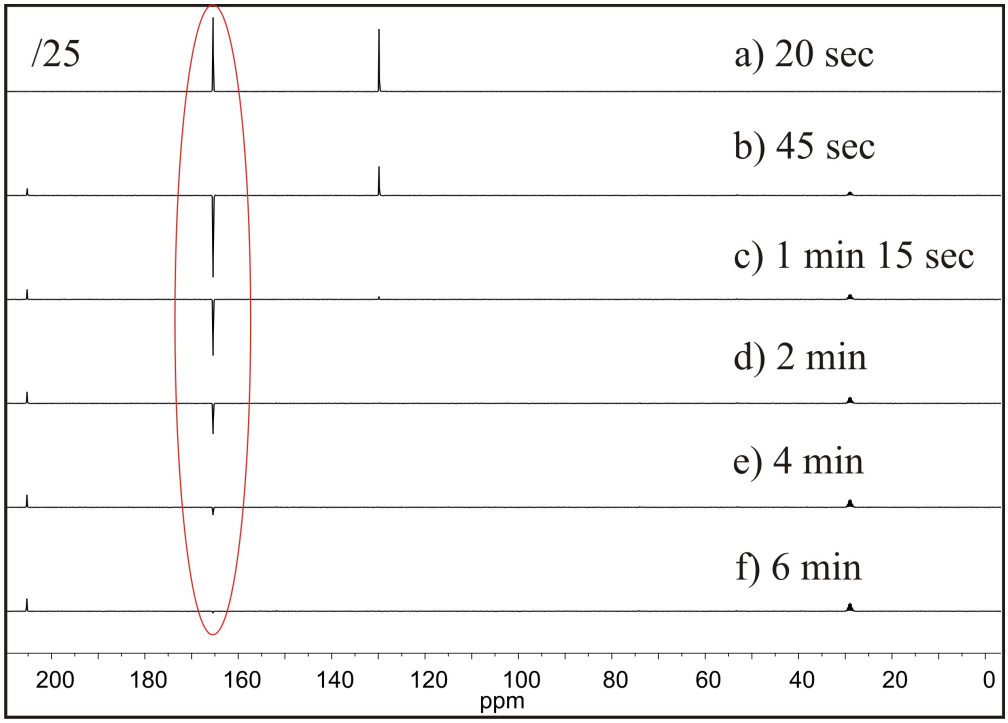

Figure 4.8: Investigation of the decaying hyperpolarization during a time of 6 minutes via the recorded ^{13}C spectra of hyperpolarized maleic acid dimethyl ester. a) read out of the PH-INEPT+ sequence with a delay of 10 ms and b) – f) single scan ^{13}C spectra. To obtain higher resolution of spectra b) – f), spectrum a) was divided by 25.

tion of $C_{1,1'}$ and $C_{2,2'}$ were still observable in the third recorded sectrum after 1 minute and 15 seconds; despite the fact that the applied rf pulses (45°) of the formerly two recorded spectra destroyed a huge part of observable hyperpolarization. Especially $C_{2,2'}$ with its long T_1 time of 76 seconds was still observable after 6 minutes as a small peak at 166 ppm even with five previously applied rf pulses. Thus, the achieved large hyperpolarization of 42305 for $C_{2,2'}$ together with its long relaxation time offers the possibility to store the generated hyperpolarization for at least six minutes on this nucleus. Taking the applied rf pulses into account which always destroy a huge part of the generated hyperpolarization, even higher signal enhancements should be observable by only recording one spectrum after 6 minutes.

In conclusion, the symmetric product molecule maleic acid dimethylester showed the peak pattern predicted in literature [90]. Furthermore, by examining the signal enhancements of the ongoing reaction of acetylene dicarboxylic acid dimethylester under different conditions (ALTADENA and PASADENA) first hints were found for lifetime prolongation of the generated isolated two spin system. Experiments concerning this effect were focussed on using the labeled prescursor acetylene dicarboxylic acid dimethylester. Labeling of one side of the molecule broke its symmetry and therefore created the assumed peak pattern in the ^{1}H PHIP spectrum. The investigations of lifetime prolongation of singlet states kept at the low magnetic field fulfilled the estimations. Thus, due to supressing spin-lattice relaxation of the hyperpolarized molecules, higher signal enhancements could be achieved by implementing longer delay times between shaking the sample and inserting it to measure. Even after a waiting time of 5 minutes at low magnetic field, hyperpolarization of H_a and $H_{a'}$ was still observable which opens up the possibility to use this time to implement e.g. a further reaction step or to seperate the toxic catalyst system from the reaction mixture. Polarization transfer from the protons to the carbons yielded in significant large hyperpolarizations of $C_{1,1'}$ and $C_{2,2'}$ by implementing the PH-INEPT+ sequence with a delay of 10 ms. Especially $C_{2,2'}$ showed a signal enhancement of more than 42300. Due to the long T_1 time of 76 seconds of the corresponding $C_{2,2'}$ this hyperpolarization was even visible 6 minutes after applying the polarization transfer sequence. In ongoing ^{13}C experiments upon parahydrogenation of acetylene dicarboxylic acid dimethylester an additional gain of hyperpolarization can be achieved by taking the knowledge of the singlet state experiments into account and searching the optimal time frame for shaking and measuring the sample tube. This would provide larger hyperpolarization of the protons which then can be transferred to ^{13}C nuclei. A further signal gain can be achieved by ^{13}C enrichment.

4.1.2 GABA and its Derivatives

The chief inhibitory neurotransmitter in the mammalian central nervous system is γ-aminobutyric acid (GABA). Although chemically it is an amino acid, GABA is rarely referred to this group because the term "amino acid" is commenly used for the alpha amino acids. GABA plays a role in regulating neuronal excitability throughout the nervous system. In humans, GABA is also directly responsible for the regulation of muscle tone [93]. In vertebrates, GABA acts at inhibitory synapses in the brain by binding to specific transmembrane receptors in the plasma membrane, namely $GABA_A$ in which the receptor is part of a ligand-gated ion channel complex, and $GABA_B$ metabotropic receptors, which are G protein-coupled receptors. This binding causes the opening of ion channels to allow the flow of either chloride ions into the cell or potassium ions out of the cell. GABA is mostly found as a zwitterion, i.e., with the carboxyl group deprotonated and the amino group protonated. Its conformation depends on its environment. In solution five different conformations some folded and some extended are found as a result of solvation effects. The conformational flexibility of GABA is important for its biological function, as it has been found to bind to different receptors with different conformations [94]. After binding to its certain receptors, it either becomes metabolized via GABA-transaminase or absorbed by the pre-synaptic cells. The application of via PHIP hyperpolarized GABA would open up the possibility to investigate this mechanisms at the target area with the help of imaging techniques. Therefore, an adequate unsaturated precursor has to be identified, if necessary synthesized and hydrogenated with parahydrogen. A possible precursor for this purpose is trans-4-amino-crotonic acid (TACA) or cis-4-amino-crotonic acid (CACA). As an example, the parahydrogenation of the stereoisomer TACA is depicted in Figure 4.9.

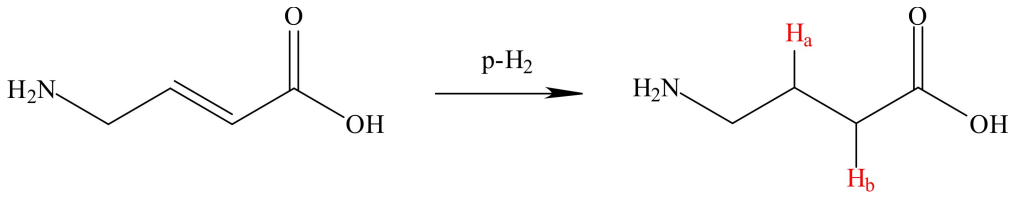

TACA / CACA GABA

Figure 4.9: Parahydrogenation of 4-amino-crotonic acid resulting in hyperpolarized γ-aminobutyric acid.

The synthesise of cis/trans-4-amino-crotonic acid is described in the literature [95]. As this precursor is poorly soluble in organic solvents, the reaction of 50 mg of it was carried out in 2.5 g D_2O by using 5 mg of the previously examined catalyst system 11 of Chapter 3. The parahydrogenation was carried out by using the membrane technique at elevated temperature and pressure. Therefore, the magnet was heated up to 80 °C and the 10 mm NMR tube was pressurized through the hollow fibre membranes with 3 bar of 98% p-H_2 before the reaction was started by inserting the tube in the spectrometer.

In the ^1H spectrum recorded during the parahydrogenation of TACA/CACA no typical antiphase signal was observed. However, 15 minutes after starting the reaction the conversion rate of the hydrogenation already yielded 100%. This indicates that the transfer mechanism of the protons to the substrate either did not follow a pairwise transition or that this transfer was too slow in comparison to the rate of the relaxation process. Hence, another water-soluble catalyst system was investigated with regard to this precursor, namely catalyst system 9 of Chapter 3. The parahydrogenation was implemented under the same conditions as described before for the other catalyst. This time, neither the typical PHIP pattern nor any hydrogenation product were observed. As this precursor did not lead to hyperpolarized GABA, another unsaturated precursor was required possessing better properties in order to generate hyperpolarized hydrogenation products. Thus, the second examined precursor contained a triple bond instead of a double bond for the hydrogenation in order to create hyperpolarized protons with longer T_1 times. Furthermore, the unsaturated group in this precursor was located at the end of the carbon chain in order to avoid sterical hindrance of the substrate. One drawback of this precursor is that the parahydrogenation will not lead to GABA itself, but to a GABA-derivative (Figure 4.10).

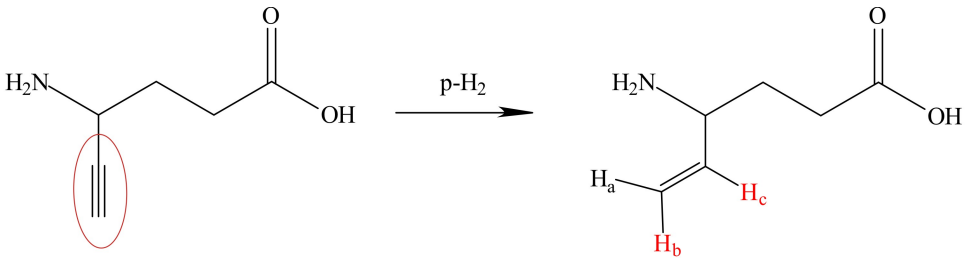

4-amino-5-hexynoic acid 4-amino-5-hexenoic acid

Figure 4.10: Scheme of the parahydrogenation of 4-amino-5-hexynoic acid.

This precursor is commercially available from Sigma Aldrich with a cost of 1475 Euro per 100 mg. Thus, only 40 mg of the GABA-derivative was dissolved in 2.5 g D_2O together with 5 mg of catalyst system 11 under argon atmosphere. The NMR tube was sealed with a screw cap, heated up to 80 °C and afterwards pressurized with 3 bar of 98% p-H_2. In order to start the parahydrogenation, the tube was shaken above the bore of the magnet and immediately inserted to record a spectrum.

Using this precursor for the implementation of the PHIP technique led to the observation of antiphase signals belonging to the generated double bond of the hydrogenation product. The obtained PHIP spectrum of the protons after the first shake is shown in Figure 4.11, together with a reference spectrum recorded after all the hyperpolarization was gone. Calculating the signal enhancement by assuming a conversion rate of 5% at the point of aquisition led to an amount of 375 for proton H_b and 150 for proton H_a.

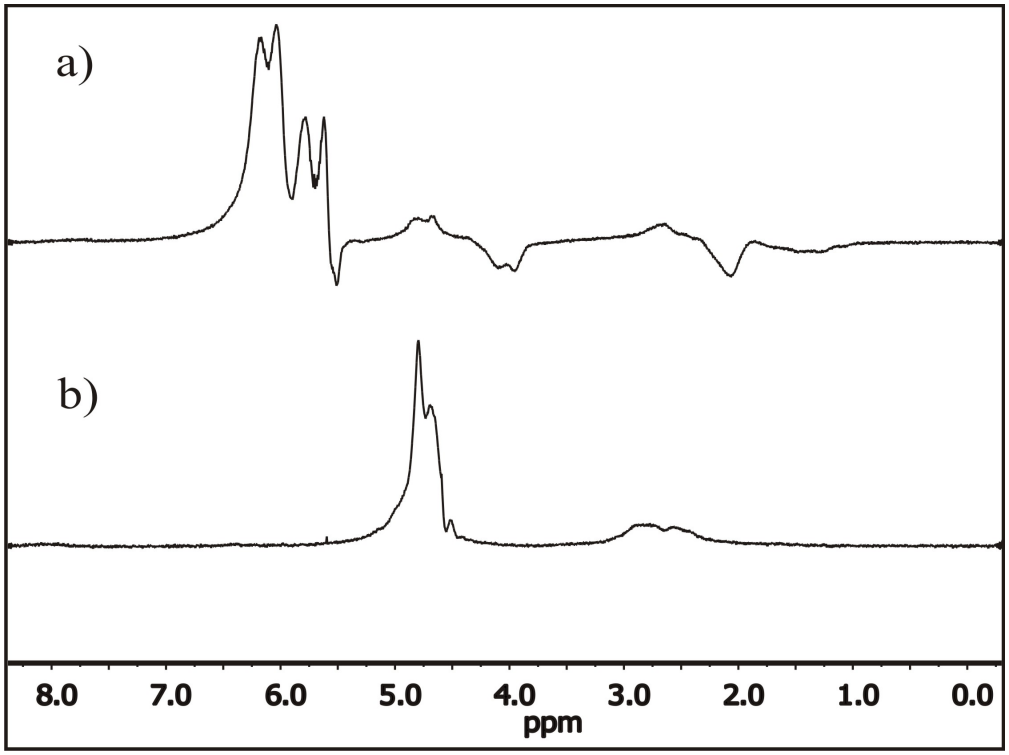

Figure 4.11: Proton spectra recorded during the parahydrogenation of 4-amino-5-hexynoic acid, a) immediately after the first shake and b) a few minutes after the first shake.

In conclusion, the generation of hyperpolarized GABA could not be implemented under the present conditions. One drawback arising for nearly all physiological relevant substances in this work is that as of now only one efficient water soluble catalyst system is available. Whereas this catalyst system works quite well for our model compound 2-hydroxyethyl acrylate under our reaction conditions, its application to biological active compounds seems to be limited. Thus, we observed a high conversion rate for the hydrogenation reaction from TACA/CACA to GABA, but no hyperpolarized signal was obtained due to any disturbance of the transfer mechanism of the catalyst system. At least, hyperpolarization via the PHIP method of a GABA derivative was achieved by utilizing catalyst system 11 at elevated temperature and pressure. The generated signal enhancement for the protons of the double bond amounted to 150 – 375. Thus, further optimization of the basic parahydrogenation experiment would open up the possibility to implement more complicated experiments such as polarization transfer to ^{13}C or 2 dimensional NMR. However, as the substrate is rather expensive no further experiments were realized in this study.

4.2 Drugs and Pharmaceuticals

4.2.1 Hyperpolarization of a Barbituric Acid derivative

Until today, mostly components of the citrate cycle were hyperpolarized and applied for in vivo metabolic imaging [19, 20, 80, 81]. ^{13}C hyperpolarization can also be employed, however, to study pharmaceuticals. Along these lines results on hyperpolarization of a barbituric acid derivative are presented. Barbiturates are clinically applied for the treatment of epilepsy or as injection narcotics [96]. They are well suited for parahydrogen induced polarization because of the straightforward synthesis of their unsaturated precursors. Moreover, long ^{13}C spin-lattice relaxation times make these derivatives of high interest as a potential "active" contrast agent in MRI.

Barbituric acid itself is not particularly suited for application in the human body due to its high acidity which prevents it from crossing the blood-brain barrier [97]. Therefore, only barbituric acid derivatives are clinically relevant. On substitution of the two protons at the C5 position during the synthesis of the barbiturate, it is possible to reduce the acidity of the whole molecule and, additionally insert an unsaturated group for the later incorporation of parahydrogen into the molecule. The barbiturates, which now can pass the blood-brain barrier, bind at the $GABA_A$ - receptor (GABA: Gamma-aminobutyric acid) of neurocytes [97] and increase the GABA-induced chloride influx into the cell. Therefore, they can stimulate different states of central depression depending on the applied dose and can work as anticonvulsants. By a significantly high ^{13}C polarization information on the location and the mechanism of action of the barbituric acid derivatives may be obtained (LD50 of the similar and well known barbiturate Phenobarbital is 835-1003 mg/kg for a rat [98]). Moreover, selective polarization of carbon-positions, which play an important role in the biotransformation of the substrate, offer the possibility to investigate the pharmacokinetic of this pharmaceutically important drug.

Recently, we demonstrated that homogeneous hydrogenation of unsaturated barbituric acid derivatives with 50% enriched parahydrogen resulted in a substantial increase of the ^1H-NMR signals of the reaction products [68]. However, ^{13}C signal enhancement by randomly triggered polarization transfer to ^{13}C in the weak magnetic field was not observed. Hence, the aim of this study was to obtain considerable ^{13}C NMR signal enhancement of barbiturates. This was achieved by applying a closed-cycle cryostat setup for parahydrogen enrichment up to 98% in combination with effective INEPT-derived pulse sequences for polarization transfer to ^{13}C.

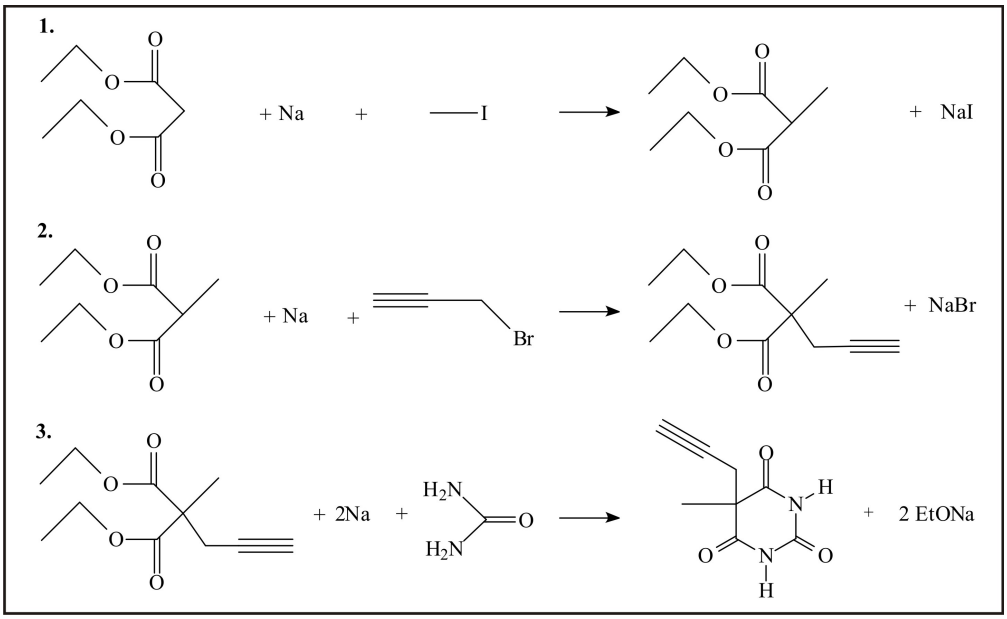

Figure 4.12: Three step synthesize of 5-methyl-5-propargyl-barbituric acid.

Barbituric acid derivatives were synthesized from urea and unsaturated malonic acid derivatives [68]. The synthesis of 5-methyl-5-propargylbarbituric acid is depicted in Figure 4.12. The synthesis of the hydrogenation product 5-methyl-5-propenyl-barbituric acid for T_1 measurement is described more detailed in Chapter 6. For parahydrogenation reactions the commercially available rhodium catalyst system [Rh(COD)(dppb)]BF4 (Catalyst 1) was used. 10 mm NMR tubes were filled with 0,007 mmol (5 mg) catalyst, 0.28 mmol (50 mg) of the unsaturated barbiturate precursor and 3 ml acetone-d_6 under argon atmosphere and sealed with a septum cap. Parahydrogenation was carried out at elevated temperature and pressure in order to increase the conversion of the hydrogenation reaction. Therefore, the reaction tube was gently heated to 60 °C in a water bath and then pressurized with 3.5 bar of para-enriched H_2. Subsequently, the tube was shaken closely above the bore of the magnet to start the hydrogenation and immediately inserted into the spectrometer. Shaking the tube in the stray field of the magnet should create polarization in the PASADENA spin state which is necessary for polarization transfer using the PH-INEPT+ pulse sequence. All experiments were performed on a Bruker AVANCE DRX 300 MHz spectrometer. The high proton polarization was transferred to ^{13}C using the PH-INEPT+ sequence [61] with different delays $t_1/2$ ranging from 5 to 20 ms. All reference spectra of the thermally polarized products were measured using the same NMR parameters as

for the PHIP spectra. Signal enhancements were calculated by comparing the NMR line integrals of the recorded PHIP spectrum with a reference spectrum measured in the same sample after the hydrogenation reaction has stopped (which can take up to 20 minutes) and the polarization relaxed to thermal equilibrium. Therefore, the conversion of the parahydrogenation reaction at the acquisition time point of a PHIP spectrum and the reference spectrum is different, which has to be taken into account for the calculation of the ^{1}H-signal enhancement. The conversion at the time point of acquisition of the hyperpolarized PHIP spectrum was estimated to be 10% by comparison with the total conversion after 20 minutes (30%, calculated from the integrals of the NMR peaks of the thermally polarized product). For the carbon spectra, the signal enhancements were calculated simply by comparing the amplitudes of the NMR lines of the hyperpolarized and thermally polarized compounds. Such a thermal spectrum was recorded with 256 scans immediately after the ^{13}C polarization was destroyed by the read out pulse of the PH-INEPT+ sequence. This served as a reference for all hyperpolarized ^{13}C spectra.

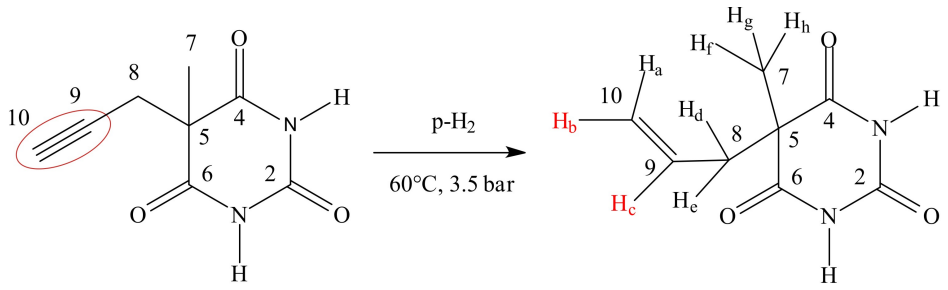

5-methyl-5-propargyl-barbituric acid 5-methyl-5-propenyl-barbituric acid

Figure 4.13: Parahydrogenation of 5-methyl-5-propargyl-barbituric acid at optimized reaction conditions.

The parahydrogenation of 5-methyl-5-propargyl-barbituric acid leads to the hyperpolarized product 5-methyl-5-propenyl-barbituric acid, as shown in Figure 4.13 with the hyperpolarized protons depicted in red. The ^{1}H and ^{13}C T_1 relaxation times of the hydrogenation product 5-methyl-5-propenyl-barbituric acid are presented in Table 4.3. The T_1 times were measured in D_2O because of the much higher solubility of the barbituric acid derivative in D_2O than in acetone resulting in a higher NMR signal and in order to confirm long-lived hyperpolarization in an aqueous environment to allow for in vivo experiments.

5-methyl-5-propenyl-barbituric acid									
T_1 times of the protons [s]				T_1 times of the carbons [s]					
$H_{a,b}$	H_c	$H_{d,e}$	$H_{f,g,h}$	C_4	C_5	C_7	C_8	C_9	C_{10}
1.8	3.8	0.9	0.8	27.7	15.5	1.0	0.7	2.1	1.0

Table 4.3: T_1 relaxation times of 5-methyl-5-propenyl-barbituric acid dissolved in D_2O.

However, so far we did not find a suitable catalyst for the parahydrogenation of 5-methyl-5-propargylbarbituric acid in water.The spin-lattice relaxation times of the protons are in the range between 0.7 and 3.8 seconds, whereas the carbons exhibit T_1 times of about 15 and 27 seconds for the quaternary carbon and the carbonyl group, respectively, which should be sufficient to perform in vivo experiments. The ^{1}H NMR spectrum of the hyperpolarized product 5-methyl-5-propenyl-barbituric acid acquired using a 45 pulse is presented in Figure 4.14. It was acquired 35 s after the parahydrogenation reaction was initiated by shaking the NMR tube containing the reaction mixture charged with 3.5 bar of 98% enriched parahydrogen in the stray field of the NMR magnet. The reference spectrum (which is also depicted in Fig 4.14) was obtained from the very same reaction using the identical sample tube 20 minutes after the start of the parahydrogenation reaction. This delay is necessary to ensure both the termination of the reaction inside the pressurized tube and a complete decay of the hyperpolarization.

The ^{1}H signal enhancements of H_b and H_c at the resulting double bond are 640 and 1025, respectively, and therewith much larger than the ^{1}H signal enhancement of 40 which we had achieved in our first attempt to hyperpolarize barbiturates [68]. This improvement in signal enhancement was achieved by optimizing the reaction conditions (elevated temperature and pressure) of the parahydrogenation reaction in combination with the application of 98% enriched para-H_2. Further improvement of the reaction conditions as were realized e.g. in a recently built PASADENA polarizer [67, 87]. could maximize the conversion of the parahydrogenation reaction and would result in even higher NMR signal enhancements. A closer look at the ^{1}H PHIP signals of the hyperpolarized spectrum in Figure 4.14 suggests, however, that the spectrum is not the result of pure PASADENA conditions: Instead, the peak pattern suggests that the eventually recorded signals stem from a mixture, i.e. from a superimposition of PASADENA and ALTADENA conditions. This indicates that

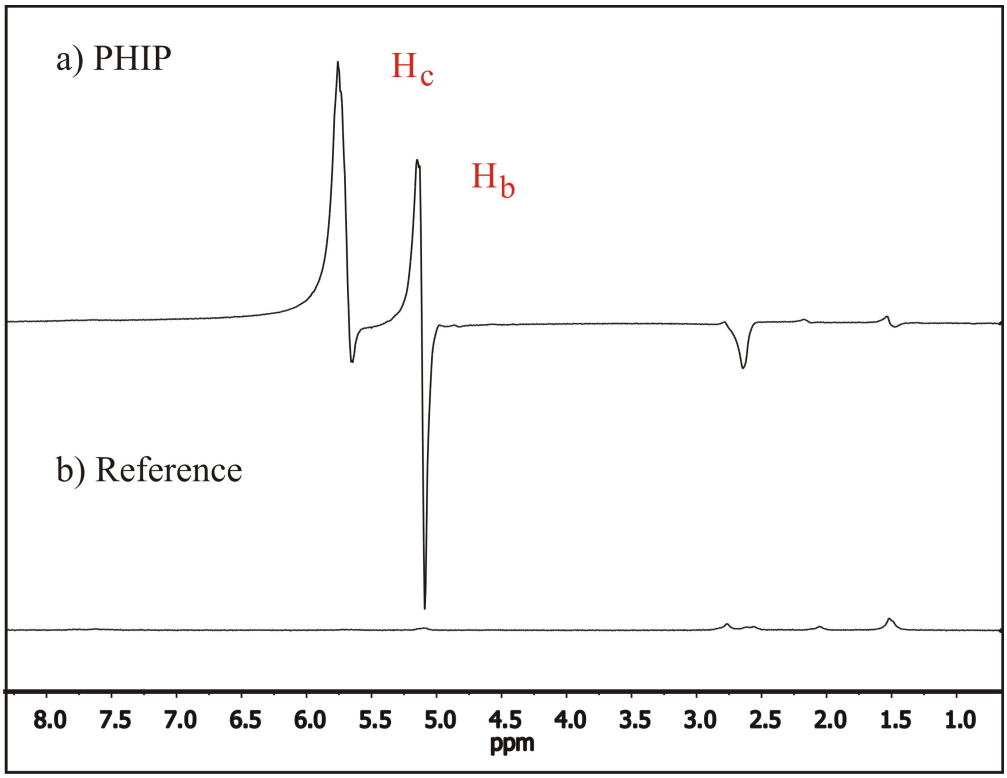

Figure 4.14: ^{1}H NMR spectra acquired using only one pulse a) upon parahydrogenation of 5-methyl-5-propargylbarbituric acid at 60C with 3.5 bar of 98% enriched para-H_2, and b) the reference spectrum of the same reaction mixture acquired 20 minutes afterwards under the same conditions. The signal enhancement of the PHIP spectrum amounts to 640 for H_b and 1025 for H_c.

the stray field of the magnet is not high enough to ensure PASADENA conditions but give rise to ALTADENA polarization in the beginning of the parahydrogenation. However, if the reaction started at ALTADENA conditions and then continued inside the NMR magnet (PASADENA condition) for 20s (time necessary to insert the NMR tube in the coil) most of the ALTADENA polarization should be decayed due to the short T_1 relaxation times of the protons. The proceeding of the reaction inside the magnet should result in the build-up of PASADENA polarization prior to the NMR experiment. The superposition of PASADENA and ALTADENA spin states can be concluded from the antiphase signal of C_{10} (PASADENA peak pattern) and from the spread of the hyperpolarization over the whole molecule (see emission peak at 2.6 ppm), since the latter takes place only under ALTADENA conditions. In view

of the considerable linewidths of the resonances in the hyperpolarized spectrum we expect that a certain amount of the achieved hyperpolarization is not observed due to cancellation of the antiphase signals of the multiplets due to their closely spaced peaks. Thus, better shimming should result in even higher ^{1}H NMR signal enhancements. Since our aim was to polarize ^{13}C positions, however, we did not optimize recording the ^{1}H NMR spectra. The signal enhancements of the ^{13}C PHIP-NMR spectra after polarization transfer from the initially hyperpolarized protons to the carbons via the PH-INEPT+ sequence are presented in Figure 4.15. For a better comparison of the signal enhancements of the various carbons obtained with different $t_1/2$ times in the PH-INEPT+ sequence Table 4.4 provides a summary of these data.

Delay	^{13}C signal enhancement			
[ms]	C_{10} (CH_2)	C_9 (CH)	C_8 (CH_2)	C_4 (C=O)
5	1720	1930	-	-
10	1700	790	605	-
15	2100	450	5200	-
20	3395	765	-	700

Table 4.4: Comparison of the ^{13}C signal enhancements of the product 5-methyl-5-propenyl-barbituric acid for different delays of the PH- INEPT+ sequence.

All spectra depicted in Figure 4.15 were recorded under the same reaction conditions, namely upon one scan but with different $t_1/2$ delays in the PH-INEPT+ sequence. As noted before, the reference spectrum was recorded with 256 scans immediately after the hyperpolarized single scan spectrum and was scaled in order to show the same noise level as the hyperpolarized spectra. The strong signal at 30 ppm in the reference spectrum belongs to the solvent acetone-d_6. For the short pulse delay of 5 ms the polarization is almost equally transferred to both carbons of the resulting double bond yielding a signal enhancement of 1930 for the CH-group. With the somewhat longer delay of 10 ms in the PH-INEPT+ sequence polarization transfer to the carbons of the double bond as well as to the neighbor carbon C8 occurs. Under these conditions the highest signal enhancement is obtained for the CH_2-group C_{10} amounting to 1700. Compared to the high proton polarization of more than 1000 the PH-INEPT+ polarization transfer to ^{13}C does not seem to be very efficient for these delays.

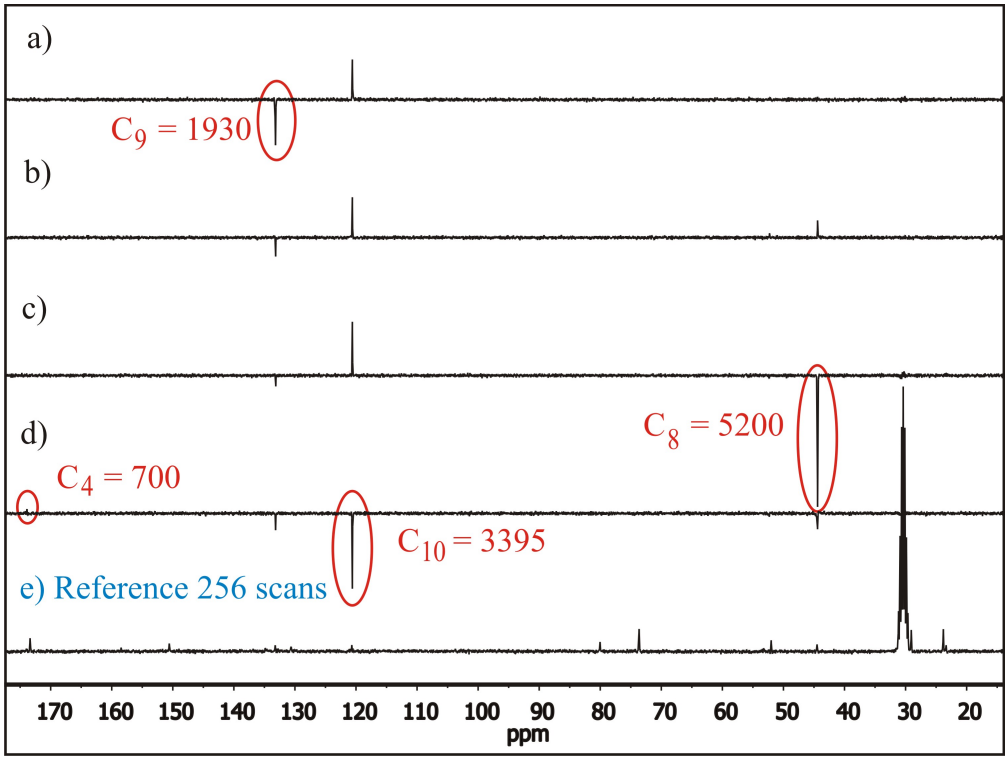

Figure 4.15: a) - d) ^{13}C PHIP NMR spectra of hyperpolarized 5-methyl-5-propargyl-barbituric, all recorded upon one pulse but using different delays $t_1/2$ for the PH-INEPT+ sequence a) $t_1/2 = 5$ms, b) $t_1/2 = 10$ ms, c) $t_1/2 = 15$ ms, and d) $t_1/2 = 20$ ms. e) Reference spectrum of the thermally polarized product acquired using 256 scans. The highlighted peaks correspond to the highest observed signal enhancements of the carbons C_4, C_8, C_9, and C_{10}.

However, implementing a longer delay of 15 ms most of the polarization is transferred to the vicinal CH_2 group C_8 of the product featuring the dramatic enhancement factor of 5200. Indeed, this represents the highest signal gain achieved for the barbituric acid derivative in our study and proves the effectiveness of the PH INEPT+ sequence for polarization transfer to ^{13}C when using an appropriate timing. This result demonstrates that the investigation of the target location and the mechanism of action of this molecule by MRI should be feasible with ^{13}C enriched barbiturates. Finally, the even longer delay of 20 ms resulted in a large signal enhancement of the C_{10} of approx. 3400 and even more interestingly polarization is also transferred to the carbonyl group of

the molecule which takes part in the biotransformation of the molecule. This provides an opportunity to store the polarization on this nucleus with its long T_1 time in order to investigate the substrate's metabolic pathway subsequently.

Haake et al. pointed out that the transfer efficiency of the PH-INEPT+ sequence critically depends on the ^{1}H-^{1}H coupling strength of the initially polarized protons [61]. However, the transfer efficiencies to the various carbon positions in the molecule also depend on the J couplings between the carbons and the polarized protons. This is clearly reflected in our data, since longer delays in the PH-INEPT+ sequence allow polarization transfer through weaker couplings and hence polarization of more distant carbons (compare Table 2). More advanced polarization transfer sequences derived by optimal control theory could optimize the polarization transfer efficiency and selectivity from the initially created ^{1}H polarization to the carbon position of choice [99,100].

In my diploma thesis, I demonstrated that homogeneous hydrogenation of an unsaturated barbituric acid derivative with 50% parahydrogen resulted in a signal enhancement of around 40 for the ^{1}H-NMR signals of the reaction product [68]. However, no signal enhancement by randomly triggered polarization transfer to ^{13}C in the weak magnetic field could be achieved. In our present study we demonstrated significantly larger signal enhancements of up to 1000 of ^{1}H in barbiturates by using 98% enriched para-H_2 in combination with optimized reaction conditions (elevated temperature and pressure). Moreover, this optimization together with the application of an INEPT-derived pulse sequence for effective polarization transfer allowed for dramatic ^{13}C NMR signal enhancements up to 5200 of the different sites of the product 5-methyl-5-propenyl-barbituric acid. The implementation of different delays in the PH-INEPT+ sequence showed that the polarization can be selectively transferred to different carbons in the barbituric acid derivative. Notably, even polarization of the carbonyl group featuring a long T_1 time was achieved, which is of high importance for storing the polarization within this molecule. Optimized polarization transfer sequences based on optimal control theory could be beneficial in order to improve the efficiency and selectivity of polarization transfer [99, 100]. The presented results [101] open up the opportunity to use barbituric acid derivatives as ”active” contrast agents in MRI and enable investigations of the function of an important pharmaceutical substrate in vivo.

4.2.2 Citalopram

Heteronuclei MRI investigations of the roles and metabolisms of biologically active compounds (BACs) require huge signal enhancements as can be provided by hyperpolarization via parahydrogen induced polarization. Thus, antidepressant drugs can likewise be ^{13}C- or ^{19}F-hyperpolarized and investigated. Citalopram belongs to a class of drugs known as selective serotonin reuptake inhibitors (SSRIs). These drugs are essential for sufferers of clinical depression. This wide-spread mood disorder affects about 7-18% of the population, and currently ranks as the leading cause of disability in North America.

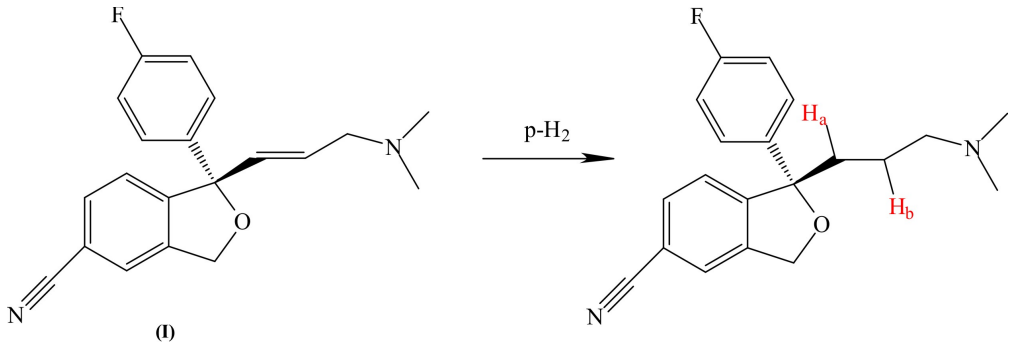

Figure 4.16: Possible precursor for carrying out a parahydrogenation generating S-(+)-citalopram as the hyperpolarized product.

Citalopram is a P-glycoprotein (permeability glycoprotein, abbreviated as Pgp) substrate and is actively transported by that protein from the brain. P-glycoprotein is a well-characterized ABC-transporter of the MDR/TAP subfamily [102]. Citalopram is sold as a racemic mixture, consisting of 50% R-(-)-citalopram and 50% S-(+)-citalopram. Only the S-(+) enantiomer has the desired antidepressant effect. In Figure 4.16 S-(+)-citalopram is depicted together with a possible precursor for the implementation of the PHIP technique to this BAC.

The synthesis of the citalopram-precursor (I) as described in the literature [103] is depicted in Figure 4.17 a). The herefore needed educt is not commercially available and has to be synthesized via a complicated route. Thus, a previous investigation of a similar, but easier to synthesize model compound was advisable. Therefore, 1-allyl-1-(4-fluorophenyl)-1,3-dihydroisobenzofuran-5-carbonitrile (IIb) was synthesized in order to investigate the applicability of the PHIP technique to this type of molecule (Figure 4.17 b). The synthesis is described in the appendix. The terminal double

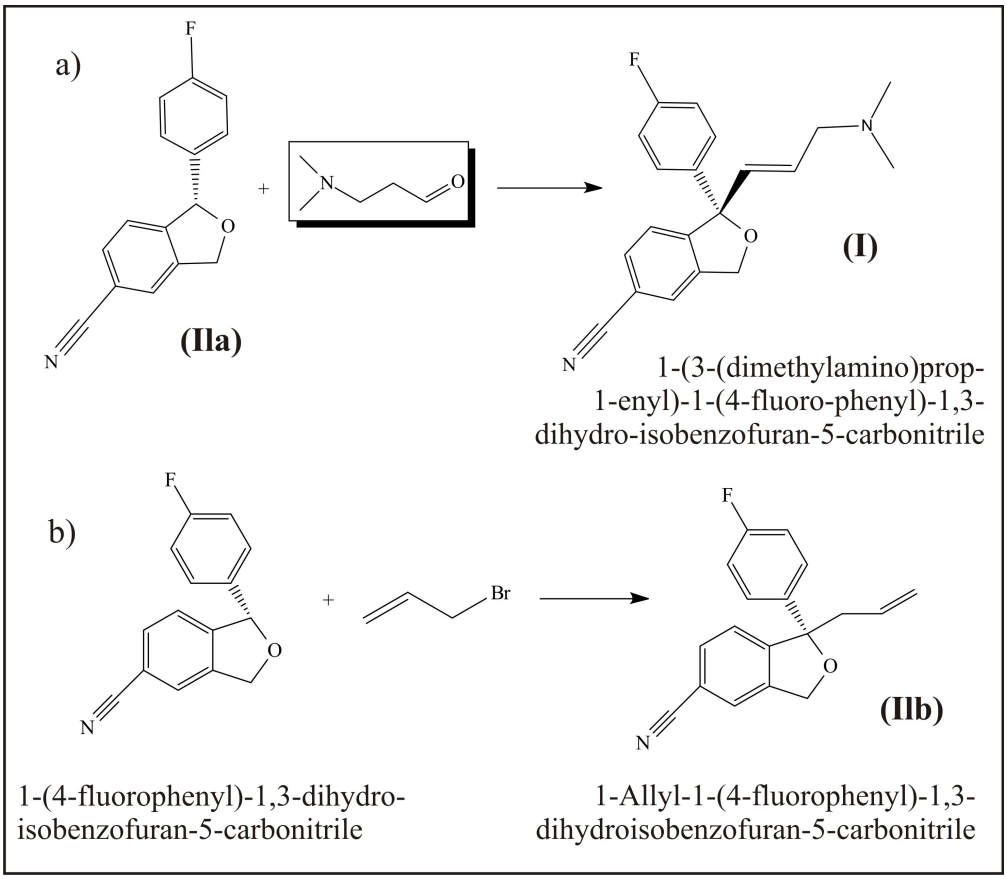

Figure 4.17: Synthesis of a) the direct citalopram precursor (I) and b) a similar model compound (II).

bond serves as the unsaturated group to introduce the hyperpolarization into the molecule. The parahydrogenation of 100 mg of substance IIb was carried out as an ALTADENA experiment at elevated temperature and pressure in 3 g acetone-d_6. 5 mg of the rhodium complex [Rh(COD)(dppb)]BF_4 (catalyst 1) served as the homogeneous cationic catalyst system.

Although a significant hydrogenation reaction was observed under these conditions, no typical PHIP pattern was apparent in the recorded spectrum. After the reaction, the conversion rate was calculated to amount to 90% after shaking the reaction mixture three times with p-H_2. This result leads to the assumption that either the transfer mechanism does not follow a pairwise procedure or that the relaxation rate is much faster than the conversion proceeding. Due to this unsatisfying results,

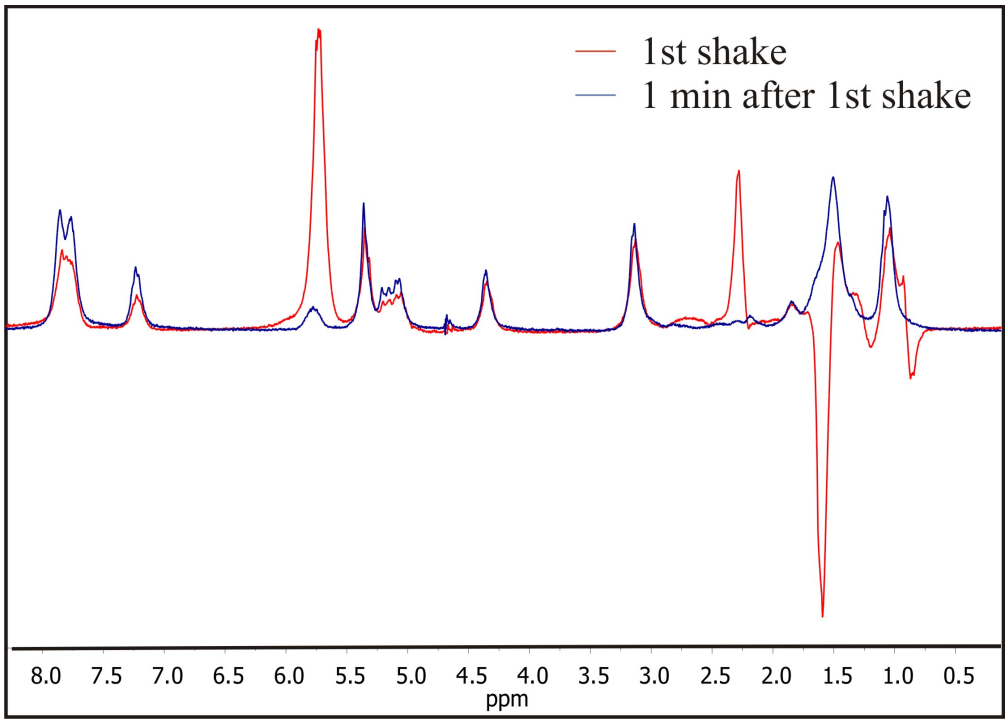

Figure 4.18: Parahydrogenation of the citalopram model compound with catalyst system 4 recorded immediately after insertion and additionally 1 minute after shaking the tube.

further examinations with other catalyst systems were performed. The investigation with the catalyst [Rh(COD)($C_{22}H_{36}P_2$)]CF_3SO_3 (catalyst system 7) also resulted in no typical PHIP pattern and, furthermore, this catalyst did not generate any observable conversion rate at all. On the contrary, catalyst [Rh(COD)($C_{16}H_{24}O_3P_2$)]BF_4 (catalyst system 4) not only showed a conversion rate of 5% after shaking the reaction mixture twice, but also small antiphase signals in the recorded spectrum depicted in Figure 4.18 in red. For better comparison, a second spectrum was recorded 1 min after shaking the sample displayed in blue. Suprisingly, the antiphase signals at 5.73 ppm, 2.28 ppm and 1.60 ppm could not be assigned to the generated single bond of the product or any other proton in the substance. Thus, a side reaction or fragmentation was expected at this time. In order to investigate and allocate this antiphase peaks to the corresponding protons, polarization transfer experiments were implemented applying the PH-INEPT+ sequence with different delays but none led to any hyperpolarized ^{13}C nuclei in the reaction mixture. A possible reason for this could be the already small signal enhancements of the protons.

Since the investigation of the catalyst systems 2, 3 and 5 did not show satisfying results in Chapter 3, these catalysts were not used for this substance. However, catalyst [Rh(nor)(tdmpp)]PF_6 (catalyst system 6) was also examined with regard to this parahydrogenation reaction. In contrast to the other catalysts, it did not only implement a high conversion rate of 65% after the first shake, but also significant high hyperpolarized peaks in the recorded spectrum. Once more, the hyperpolarized antiphase peaks in the PHIP spectrum did not belong to the protons of the hydrogenation product. Therefore, it was not possible to calculate or even estimate a more or less correct signal enhancement. Thus, for a better understanding of the achieved signal enhancement, a reference spectrum recorded before the experiment under the same measurement conditions is displayed together with the proton PHIP spectrum in Figure 4.19. Unlike for the parahydrogenation with catalyst 4, the hyperpolarized peaks were located at 6.1 ppm, 2.9 ppm, 1.7 ppm and 1.0 ppm in this case.

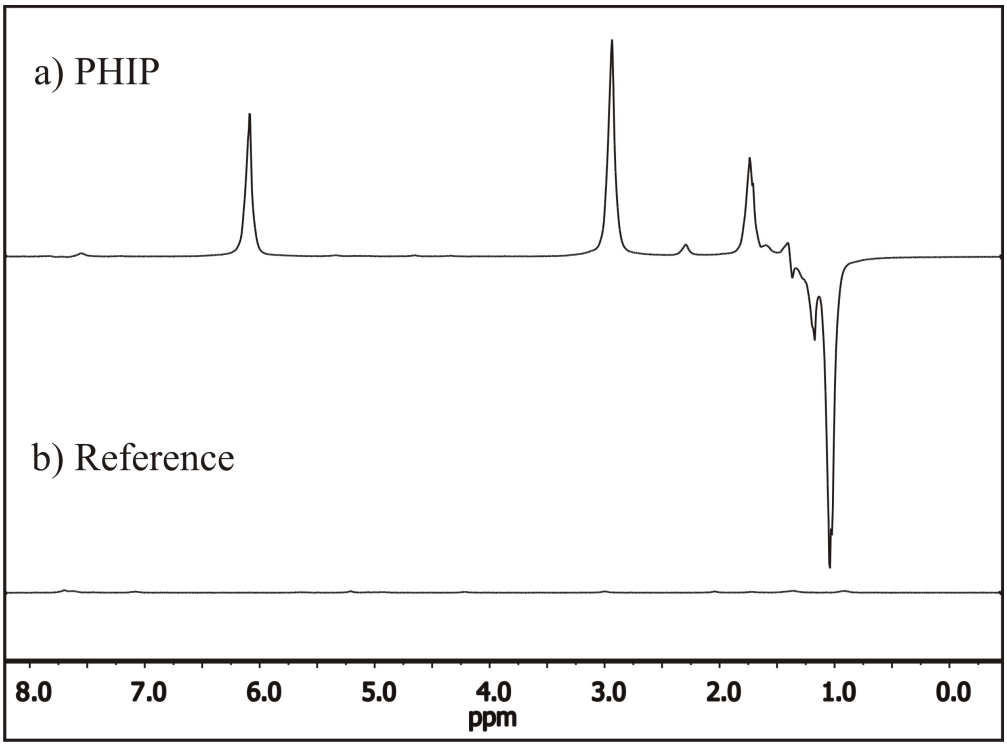

Figure 4.19: Proton spectra of a) the parahydrogenation of the citalopram model compound (I) with catalyst 6 and b) the reference spectrum measured under the same conditions of the same reaction sample.

Furthermore, shaking the reaction mixture for a second time did not lead to this hyperpolarized peaks again but generated signal enhancements for the hyperpolarized protons connected to the Rhodium metal center at -10 ppm and -17 ppm as can be seen in Fig 4.20. In order to prove that the hyperpolarized peaks are not generated by the normal hydrogenation reaction, the component having no allyl group (IIa) was utilized under the same reaction conditions and led to exactly the same results. Once more, only the first shaking of the reaction sample showed the hyperpolarized signals between 6.1 and 1.0 ppm whereas the second shake only resulted in hyperpolarization of the protons at the metal center again. The two recorded spectra of the first and second shake are shown in Figure 4.20. This result proves that the hyperpolarized peaks are not generated via the hydrogenation reaction of the citalopram model compound itself, but could belong to any fragmentation or side reaction going on.

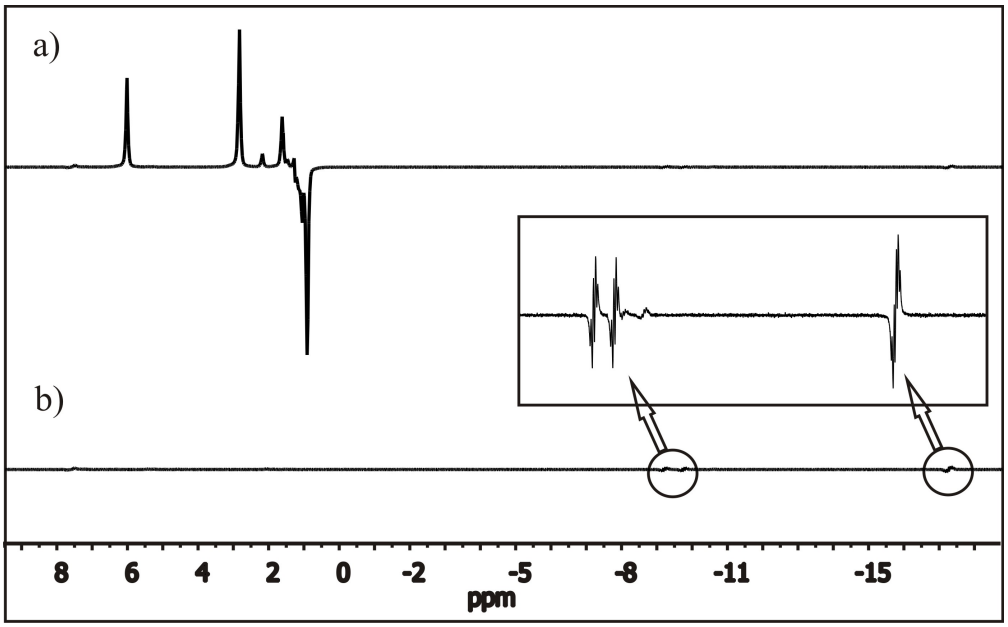

Figure 4.20: Recorded proton spectra of the substance 1-(4-fluorophenyl)-1,3-dihydroisobenzofuran-5-carbonitrile (IIa) immediately after a) the first shake of the sample and b) the second shake of the sample.

In order to investigate the origin of this dramatically enhanced peaks generated by the first shake, the same experiment was carried out again with the aim to transfer polarization from the protons to the carbons. Hence, the PH-INEPT+ sequence was carried out on the model compound IIb and as well on the starting material IIa without

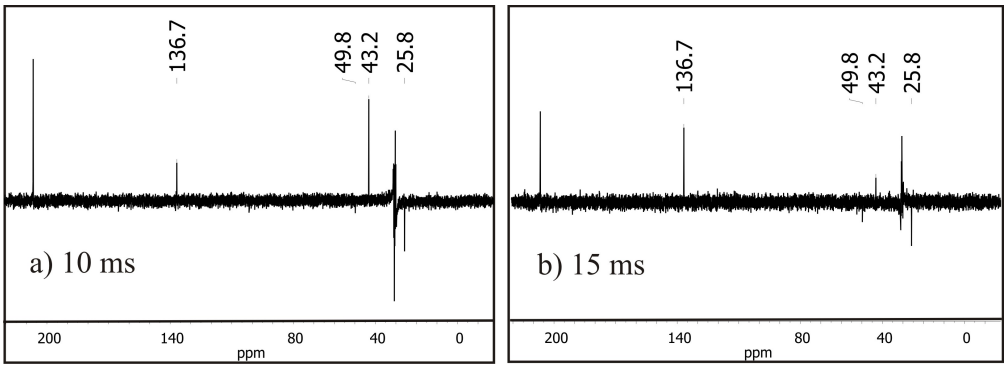

Figure 4.21: ^{13}C spectra of the parahydrogenation of the citalopram model compound 1-allyl-1-(4-fluorophenyl)-1,3-dihydroisobenzo-furan-5-carbonitrile (IIb) using catalyst system 6 and additional implementation of the PH-INEPT+ sequence with delays a) 10 ms and b) 15 ms.

double bond. Again, regardless of the presence of the unsaturated group, both substances led to the same result. The recorded carbon spectra after applying the sequence with delays of 10 ms and 15 ms to substance IIb are depicted in Figure 4.21. In both spectra, the same hyperpolarized peaks at 136.7 ppm, 49.8 ppm, 43.2 ppm and 25.8 ppm were observed but with different intensities due to the different implemented delays. Neither the chemical shifts of the protons, nor the chemical shifts of the carbons can be assigned to the hydrogenation product or any fragmentation product. Thus, the only possible explanation for the occurence of these peaks could be found in the catalyst species, which however never evoke such significant high signals in the spectra before. The first idea was to look at the ligands of this catalyst system. However, no correlation to the observed peaks could be found. The next considered possibility was the protection ligand norbonadiene, which in general reacts in a first step of a hydrogenation reaction to give norbonan. But again, the obtained peaks in the spectra did not correspond to the protons and carbons of norbonadiene or norbonan. In order to investigate the catalyst system more precisely, a parahydrogenation without any substrate but only with catalyst 6 was carried out under the same reaction conditions. In this case, the expected hyperpolarized peaks of the hydrogenation product norbonan were observed in the proton spectrum between 2.2 ppm and 1.2 ppm. Thus, the scaffold of the citalopram model compound seems to interact with the catalyst system 6 in a way which leads to a reaction intermediate responsible for the hyperpolarized peaks.

In the end, the origin of the unexpected peaks was found in the normally elusive reaction intermediate norbonene, which in general reacts further to norbonan in such a fast time regime that it cannot be detected. Norbonene, together with its predicted peaks for the protons and the carbons is shown in Figure 4.22. As this hyperpolarized norbonen was never detected before in any spectrum of any model compound, it suggests itself that this observed phenomenon arises from the chosen substance in this case.

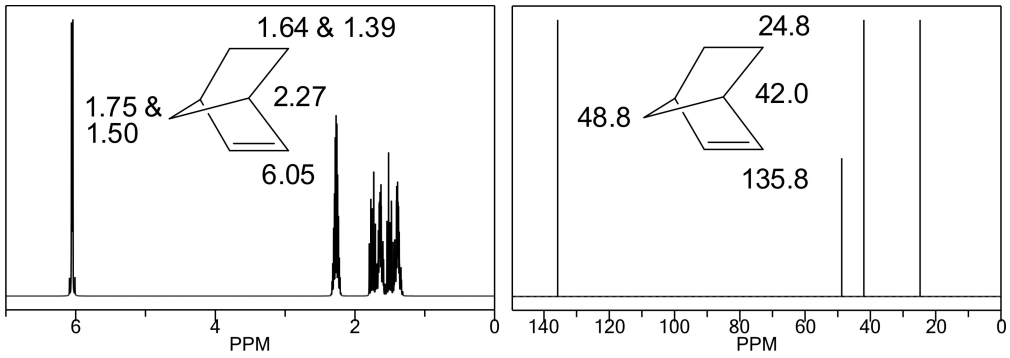

Figure 4.22: On the left the predicted ^{1}H spectrum and on the right the predicted ^{13}C spectrum of the reaction intermediate norbonene.

It is obvious, that something happens to norbonadien in combination with the scaffold of the citalopram model compound during the reaction. This effect inhibits further hydrogenation of the second double bond of norbonadiene in the molecule as it is usual by the case. Reasons for this effect could be blocking of the catalyst system due to binding of a special ligand for example. To get a better idea which part of our model compound is responsible for this interruption of the reaction, the model compound was divided into two parts, namely benzonitrile and fluorobenzene and the parahydrogenation was carried out once again with these two substances. The resulting proton spectra are depicted in Figure 4.23. In the presence of fluorobenzene, the spectrum showed hyperpolarized peaks of the hydrogenation product norbonan, same result as for the spectrum recorded only with catalyst 6. Thus, the subpart fluorobenzene in the scaffold of the citalopram model compound is not responsible for the interruption of the reaction. In contrast, in the spectra recorded in presence of benzonitrile, the typical antiphase peaks of the reaction intermediate norbonene were observed again. Hence, this subpart containing cyanogen is responsible for the break up of the parahydrogenation. A possible reason for this effect could be the

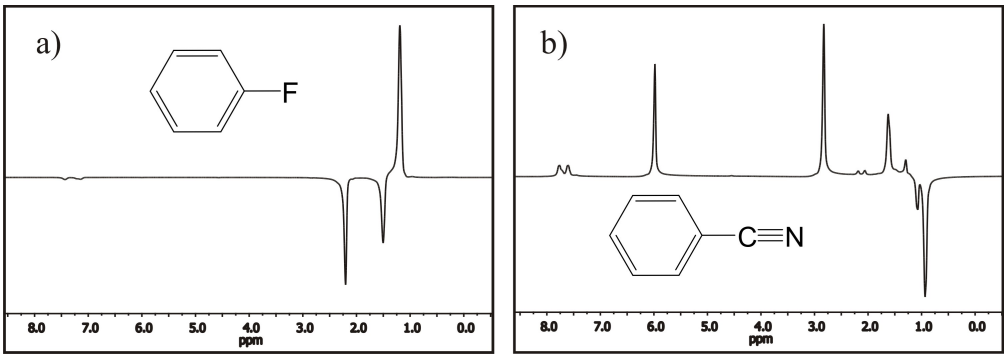

Figure 4.23: Parahydrogenation of catalyst systeme 6 in the presence of a) fluorobenzene and b) benzonitrile.

attachement of this triple bond to the rhodium metal center leading to an inhibition of the whole catalyst species. The same inhibiting effect was also observed for catalyst system 4 together with the citalopram model compound IIb. In this case, the protection ligand cyclooctadiene was only hydrogenated to the intermediate cyclooctene which was observed in the spectrum already shown in Figure 4.18. However, this effect was much less pronounced than observed for catalyst system 6 containing norbonadiene. In addition, none of the other catalysts also containing cyclooctadiene generated hyperpolarized cyclooctene.

In conclusion, the investigation of the citalopram model compound was disturbed by several factors. Meanwhile the hydrogenation could be performed with catalyst system 1, 4 and 6, no signal enhancement of the generated single bond was observed. In contrast, different hyperpolarized signals were generated with catalyst system 4 and 6, both stemming from a reaction intermediate corresponding to the hydrogenation of the protection ligand of the catalyst system. These hyperpolarized peaks were independent from the double bond in the citalopram precursor and also occured in the absence of this group in the substrate. Due to blockage of the catalyst system, the hydrogenation of the protection ligands stopped before hydrogenation of the second double bond took place. This hindrance is caused by the subpart benzonitrile of the scaffold of the citalopram precursor. However, further investigations of the citalopram precursor were not performed due to the fact, that the hydrogenated double bond did not result in observable hyperpolarized peaks of this substrate.

4.3 Polymerizable Monomers

4.3.1 N-Vinyl-2-pyrrolidone

From the polymer chemist's point of view, polymerizable monomers like N-vinyl-2-pyrrolidone (NVP) may also be of interest as substrates for PHIP experiments. Hence, a polymerizable monomer could be hyperpolarized in a first step and afterwards used for a polymerization reaction. It was already shown in literauter that, if the hydrogenation product undergoes a subsequent reaction immediately after its formation, the derived product may also display spin polarization [104].

The NVP monomer is commonly used as a reactive diluent in ultraviolet and electron-beam curable polymers applied as inks, coatings or adhesives [105]. It is also used as precursor to polyvinylpyrrolidone (PVP), an important synthetic material. Moreover, PVP was used as blood plasma expander for trauma victims after the first half of the 20th century. Today, it is used as binder in many pharmaceutical tablets because it simply passes through the body when taken orally [106]. Furthermore, it is used in many technical applications, for example as an adhesive in glue sticks or as a thickening agent in tooth whitening gels. The monomer N-vinyl-2-pyrrolidone is a colorless to yellowish liquid, with a characteristic odor and is soluble in water and organic solvents. As it is commercially available (CAS: 88-12-0), it was chosen for the first parahydrogen experiments itself. As already investigated during my diploma thesis [95], parahydrogenation of NVP (Figure 4.24) with catalyst 1 under standard PASADENA and ALTADENA conditions at room temperature with a content of 50% p-H_2 showed a signal enhancement of 2. Hence, these experiments were repeated in this study at elevated temperature and pressure by using a content of 98% p-H_2.

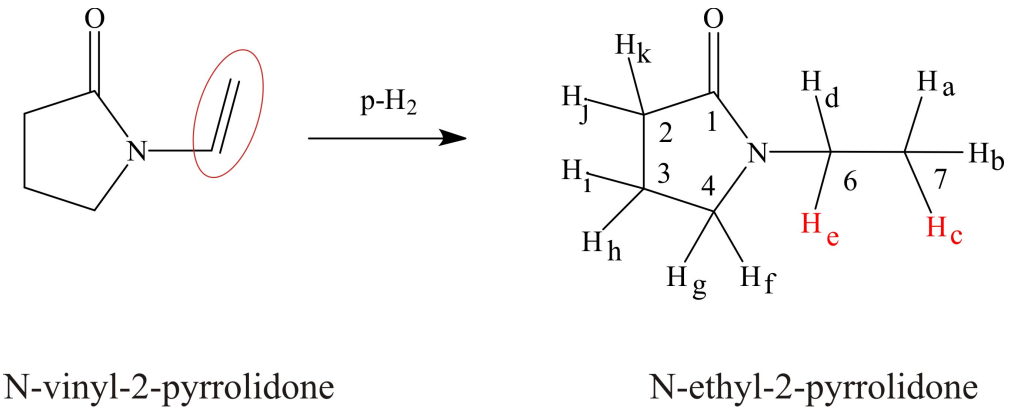

Figure 4.24: Scheme of the parahydrogenation of N-vinyl-2-pyrrolidone.

For the experiment, 150 mg of NVP was dissolved in 2.5 g acetone-d_6 together with 10 mg of catalyst system 1. The hydrogenation was carried out by heating the sample tube in a water bath at 60 °C and pressurizing the tube with 3.5 bar of 98% p-H_2. In order to start the reaction, the tube was shaken a few meters beside the spectrometer before inserting it. The ^{1}H spectrum recorded immediately after the third shake of the sample tube is shown in Figure 4.25, together with the reference spectrum measured after the first shake with 8 scans. The conversion at the time point of aquisition after the third shake was estimated to amount to 15% (total conversion rate after the third shake was calculated to amount to 40%).

In this experiment, the calculated signal enhancements for $H_{a,b,c}$ amounted to 55 meanwhile the calculated signal enhancements for both protons $H_{d,e}$ had a value of 120. Although the achieved signal enhancements were not as high as for our model compound 1-hexyne, they were up to 60 times higher than the corresponding results obtained during my diploma thesis. This improvement is a result of the optimization of the reaction conditions. The measured T_1 times of the protons and the carbons of the hydrogenation product N-ethyl-2-pyrrolidone are summarized in Table 4.5.

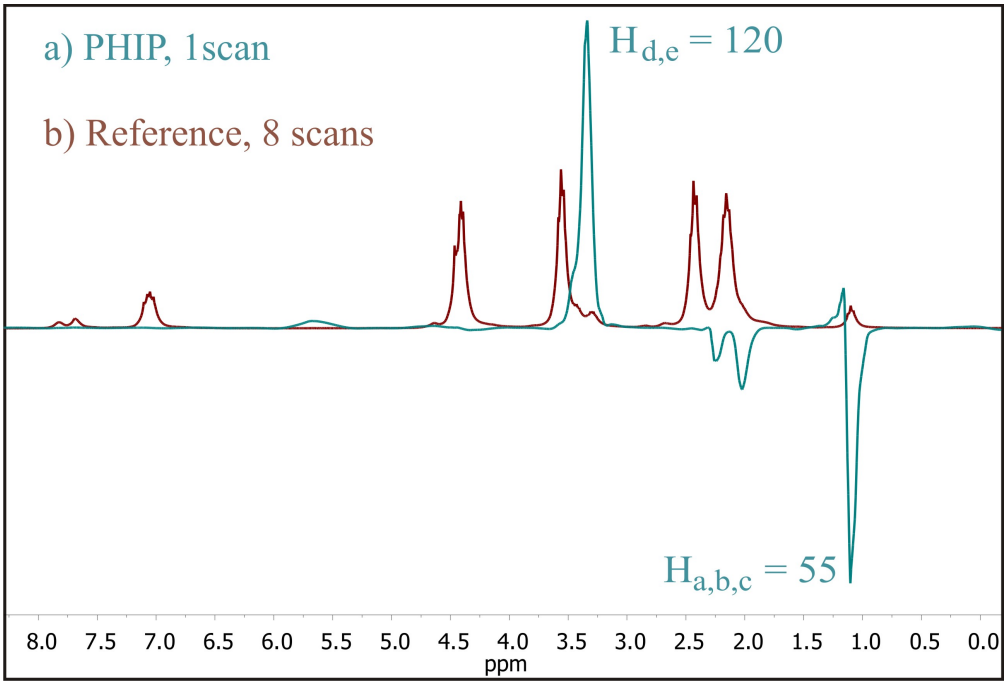

Figure 4.25: PHIP and reference spectra of the parahydrogenation of N-vinyl-2-pyrrolidone resulting in hyperpolarized N-ethyl-pyrrolidone.

N-ethyl-2-pyrrolidone										
T_1 times of the protons [s]					T_1 times of the carbons [s]					
$H_{a,b,c}$	$H_{d,e}$	$H_{f,g}$	$H_{h,i}$	$H_{j,k}$	C_1	C_2	C_3	C_4	C_6	C_7
7.6	10.4	9.1	10.6	11.1	81.4	11.5	12.2	10.4	11.9	8.7

Table 4.5: T_1 relaxation times of N-ethyl-2-pyrrolidone dissolved in acetone-d_6.

Based on the optimized parahydrogenation under ALTADENA conditions, the PH-INEPT+ sequence was applied with delays of 10 and 15 ms to the experiment in order to obtain hyperpolarized carbons in the molecule. The recorded PH-INEPT+ spectra are shown in Figure 4.26.

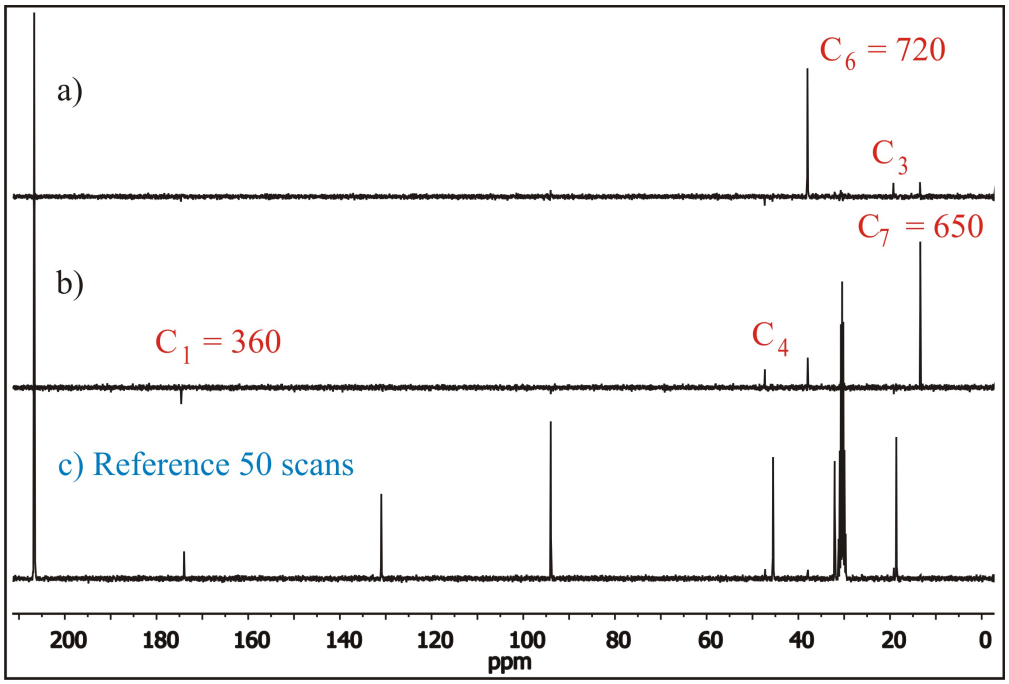

Figure 4.26: a) - b) ^{13}C PHIP NMR spectra of hyperpolarized N-ethyl-2-pyrrolidone, both recorded with a single scan but using different delays $t_1/2$ for the PH-INEPT+ sequence a) $t_1/2$ = 10 ms and b) $t_1/2$ = 15 ms. c) Reference spectrum of the thermally polarized product acquired using 50 scans. The highlighted peaks correspond to the highest observed signal enhancements of the carbons C_1, C_3, C_4, C_6 and C_7.

As a result of my diploma thesis, spontaneous polarization transfer to C_6 and C_7 with a signal enhancement of 10 was observed. Thus, of high interest in the present work was the possibility to transfer polarization, not only to the carbons of the generated single bond but over the nitrogen atom in the molecule to carbon atoms belonging to the ring system. Especially, hyperpolarization of the carbonyl group exhibiting a significant long T_1 time of more than 80 seconds would be desirable in this case.

Implementation of a delay of 10 ms resulted in a significant polarization of carbon 6 amounting to 720. Also polarized was carbon 7 and the ring carbons 3 and 4. The eventually present hyperpolarization of carbon 2 was not observed because its signal is located at the same position as acetone at around 30 ppm. Applying a delay of 15 ms to the ALTADENA experiment led to highest hyperpolarization of carbon 7 amounting to 650. Like for the former delay, carbon 6 of the single bond and the ring carbons 3 and 4 were also hyperpolarized. Remarkably, this delay resulted in additional hyperpolarization of the carbonyl group (C_1) with a value of 360. All calculated signal enhancements observed in the carbon spectra for the delays of 10 and 15 ms are summarized in Table 4.6.

$t_1/2$	^{13}C signal enhancement					
[ms]	C_1 (C=O)	C_2 (CH_2)	C_3 (CH_2)	C_4 (CH_2)	C_6 (CH_2)	C_7 (CH_3)
10			65	50	720	65
15	360		30	95	165	650

Table 4.6: Comparison of the ^{13}C signal enhancements of the product N-ethyl-2-pyrrolidone for different delays of the PH-INEPT+ sequence.

With regard to the application of the hyperpolarized substrate, one should take into account that the hereby generated N-ethyl-2-pyrrolidone is not the desired substrate which can be utilized e.g. for further polymerizaiton reactions. Therefore, it is necessary to start the parahydrogenation with a precursor molecule containing a triple bond instead of a double bond in order to obtain hyperpolarized NVP as shown in Figure 4.27.

However, this molecule named N-acetylene-2-pyrrolidone is neither commercially available (no CAS number) nor known in the literature in any synthesis. Therefore, a synthesis route of N-acetylene-2-pyrrolidone had to be invented and executed

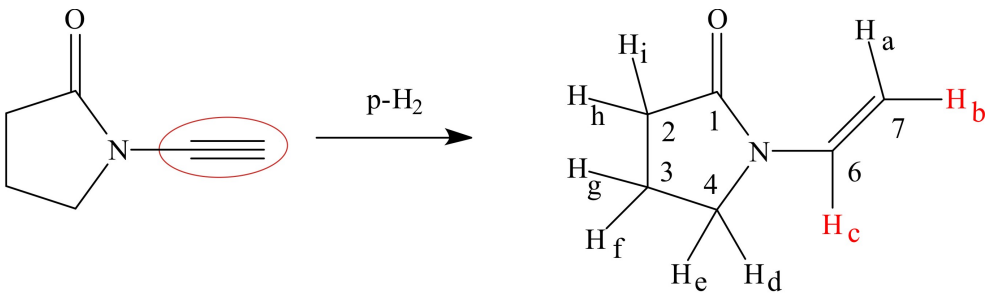

N-acetylen-2-pyrrolidone N-vinyl-2-pyrrolidone

Figure 4.27: Scheme of the parahydrogenation of N-acetylen-2-pyrrolidone.

which was done by M. Kölzer[1]. This precursor molecule should not only offer the opportunity to end up with the desired hyperpolarized and relevant substance after parahydrogenation, but furthermore it should exhibit longer T_1 times for the protons due to the more rigid double bond of the product. The measured T_1 times of the hydrogenation product NVP are displayed in Table 4.7. As estimated, the double bond of N-vinyl-2-pyrrolidone exhibits significant longer T_1 times than the single bond of N-ethyl-2-pyrrolidone. Therefore, the generated hyperpolarization can be stored longer on the introduced protons in the product molecule of the parahydrogenation of N-acetylene-2-pyrrolidone. This should also increase the possible amount of transferred polarization to heteronuclei.

N-vinyl-2-pyrrolidone										
T_1 times of the protons [s]					T_1 times of the carbons [s]					
$H_{a,b}$	H_c	$H_{d,e}$	$H_{f,g}$	$H_{h,i}$	C_1	C_2	C_3	C_4	C_6	C_7
9.0	25.8	7.2	9.0	8.9	75.2	9.2	10.1	8.3	14.0	6.6

Table 4.7: T_1 relaxation times of N-vinyl-2-pyrrolidone dissolved in acetone-d_6.

In order to perform an ALTADENA experiment at elevated temperature and pressure, 50 mg of N-acetylene-2-pyrrolidone were dissolved in 2.5 g acetone-d_6 together with 5 mg of catalyst system 1. The parahydrogenation was carried out under the same conditions as described before for N-vinyl-2-pyrrolidone. After shaking the NMR tube

[1]Michaek Kölzer, AK Opatz, University of Hamburg, PhD thesis

for 5 seconds it was inserted in the spectrometer and a proton spectrum was measured immediately. The obtained ^{1}H spectrum showed a typical ALTADENA peak pattern with signal enhancements of 80 for each proton H_a and H_b and 215 for proton H_c. In addition, a PASADENA spectrum was recorded of an equal sample tube under the same reaction conditions. Therefore, it was necessary to destroy all ALTADENA polarization generated outside the magnetic field at the beginning of the experiment. This was achieved by first implementing a polarization transfer experiment using the PH-INEPT+ sequence with decoupling. Immediately afterwards a 45° pulse was applied in order to record a ^{1}H spectrum exhibiting typical PASADENA antiphase signals. The signal enhancements were calculated to values of 275 for H_b and 205 for H_c. Both the ALTADENA and the PASADENA proton spectra are depicted in Figure 4.28. As they were recorded under the same conditions by shaking the reaction sample for 5 seconds, both showed a total conversion rate after the first shake of around 18%. Thus, the TPA for both reactions was estimated to amount around 11%.

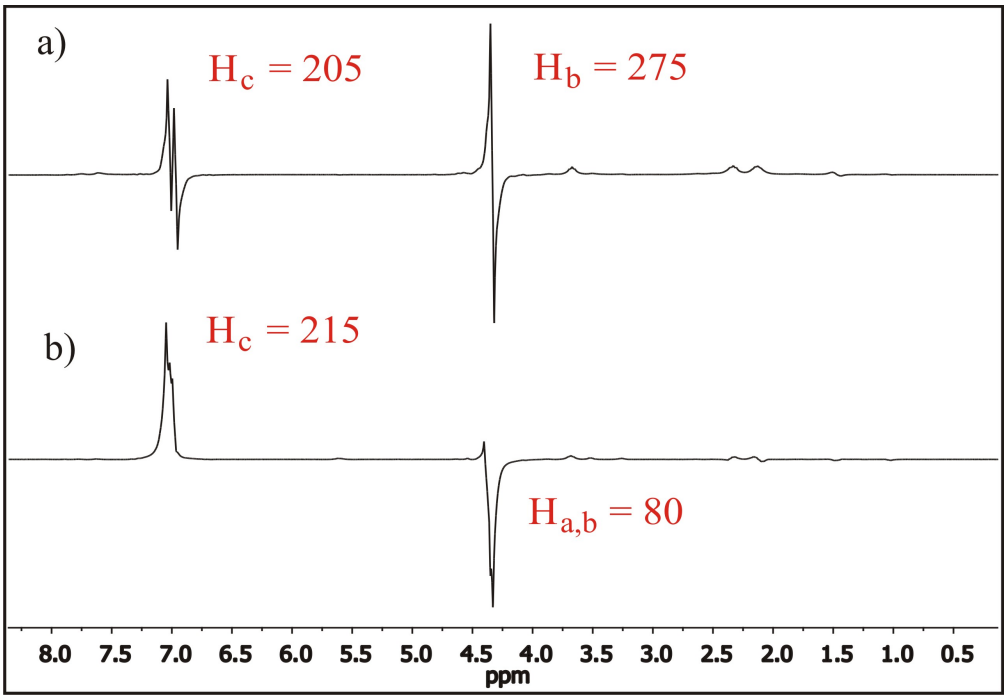

Figure 4.28: ^{1}H spectra of the parahydrogenation of N-acetylen-2-pyrrolidone exciting a) an PASADENA spin system and b) an ALTADENA spin system of the product molecule N-vinyl-2-pyrrolidone.

The PASADENA spectrum showed typical antiphase signals for protons H_b and H_c meanwhile the ALTADENA spectrum showed the typical two inphase peaks, one for H_a and H_b and one for H_c. In the ALTADENA spectrum no further polarization of the ring protons was present due to the nitrogen atom in direct neighborhood to the hyperpolarized group which hinders polarization transfer based on the scalar couplings between the protons. However, the achieved signal enhancements for the parahydrogenation of N-acetylene-2-pyrrolidone were, as expected, higher than the ones obtained for the parahydrogenation of N-vinyl-2-pyrrolidone. One possible reason for this phenomenon are the longer relaxation times of the introduced protons of the generated double bond in the product molecule. Another reason is the higher conversion rate for the hydrogenation reaction of nearly 20% after the first shake. This amount normally was obtained for the hydrogenation of N-vinyl-2-pyrrolidone after shaking the sample twice. As already mentioned above, the significant high proton polarization was used for polarization transfer experiments (Figure 4.29).

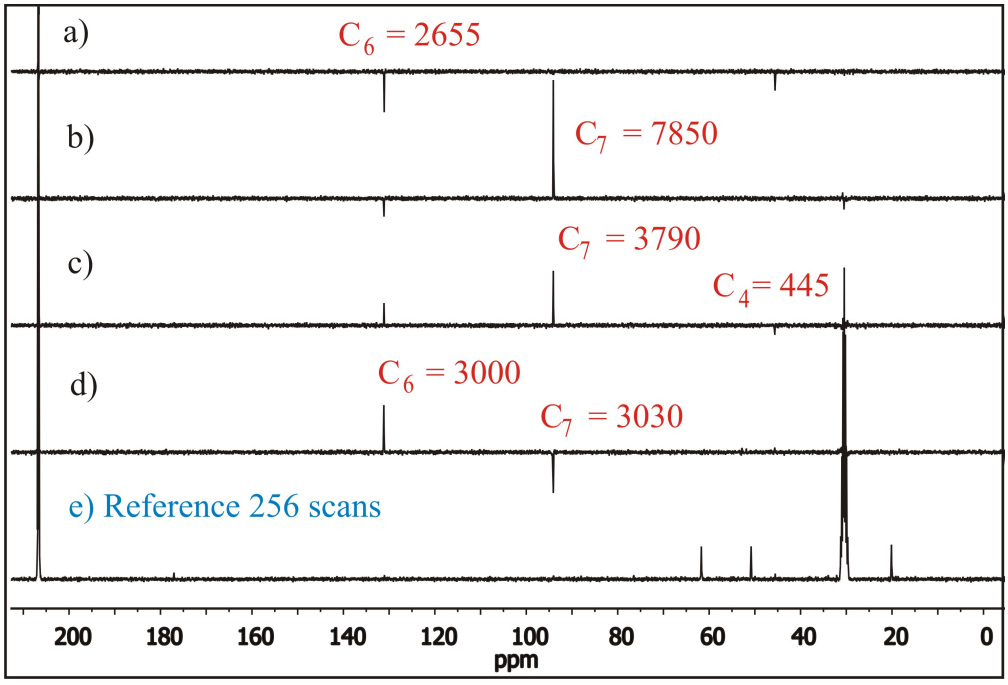

Figure 4.29: a) - d) ^{13}C PHIP NMR spectra of hyperpolarized N-vinyl-2-pyrrolidone, all recorded with a single scan but using different delays $t_1/2$ for the PH-INEPT+ sequence a) $t_1/2$ = 25 ms and b) $t_1/2$ = 20 ms and c) $t_1/2$ = 15 ms and c) $t_1/2$ = 10 ms. e) Reference spectrum of the thermally polarized product acquired using 256 scans. The highlighted peaks correspond to the highest observed signal enhancements of the carbons C_4, C_6 and C_7.

Therefore, the same ALTADENA reaction procedure was chosen and the PH-INEPT+ sequence was applied immediately after inserting the sample tube into the magnet. In order to transfer the hyperpolarization with varying amounts to the carbon molecules, different delays $t_1/2$ were implemented for each experiment ranging between 10 to 25 ms. Implementation of a delay of 25 ms resulted in the polarization of carbon 6 with an amount of 2655; also polarized with this delay was carbon 4 showing the highest amount for all delays of 910. The delay of 20 ms yielded the highest signal enhancement of the entire polarization transfer experiment exhibiting a value of 7850 for carbon 7. Applying the PH-INEPT+ sequence with a delay of 15 ms led to hyperpolarizations reaching a signal enhancement of 1390 for carbon 6 and 3790 for carbon 7. The utilization of a 10 ms delay resulted in a nearly equal polarization of carbon 6 and carbon 7 with amounts of 3000 and 3030. All achieved signal enhancements implementing varying delays are summarized in table 4.8.

$t_1/2$	^{13}C signal enhancement					
[ms]	C_1 (C=O)	C_2 (CH_2)	C_3 (CH_2)	C_4 (CH_2)	C_6 (CH)	C_7 (CH_2)
10	-	-	-	-	3000	3030
15	-	-	-	445	1390	3790
20	-	-	-	-	1065	7850
25	-	-	-	910	2655	

Table 4.8: Comparison of the ^{13}C signal enhancements of the product N-ethyl-2-pyrrolidone for different delays of the PH-INEPT+ sequence.

Interesting in this case is that none of the delays could achieve polarization transfer to other ring carbons than C_4 like for the parahydrogenation of N-vinyl-2-pyrrolidone. A possible explanation for this can be found in the nitrogen atom vicinal to the hyperpolarized protons which hinders the transfer of polarization based on scalar couplings. In addition, polarization transfer based on dipolar couplings seems to be supressed in this molecule due to the rigid conformation of the generated double in comparison to the higher flexibility of the single bond in the product N-ethyl-2-pyrrolidone.

Beside the possibility to transfer the polarization to heteronuclei, the parahydrogenation of N-acetylene-2-pyrrolidone creates a hyperpolarized substrate with a nearly isolated three-spin system. However, lifetime prolongation mechanisms in

multi-spin systems are still under investigation. First experimental observations of a long-lived state in a three-spin system were already presented in the literature yielding a lifetime twice as long as the longest T_1 measured in the system at high field [55]. Thus, an ALTADENA experiment was implemented in order to store the generated hyperpolarization on the isolated protons of the double bond of N-vinyl-2-pyrrolidone. Therefore, the same ALTADENA experiment as described before was carried out by dissolving 30 mg of N-acetylene-2-pyrrolidone in 2.5 g acetone-d_6 together with 5 mg of catalyst system 1. The only difference to the former ALTADENA experiment was an additional waiting time after starting the reaction. Hence, the sample was also shaken for 5 seconds a few meters beside the spectrometer and then kept in the low field for further 40 seconds without shaking it. Most of the generated hyperpolarization should be stored during this delay in the singlet state of the hyperpolarized product. Furthermore, the ongoing reaction during the following 40 seconds outside the field should result in an increase of hyperpolarization stored in the singlet state of the generated product. After the waiting time, the NMR tube was quickly inserted in the spectrometer and a PHIP proton spectrum was recorded exactly 1 minute after starting the reaction (Figure 4.30).

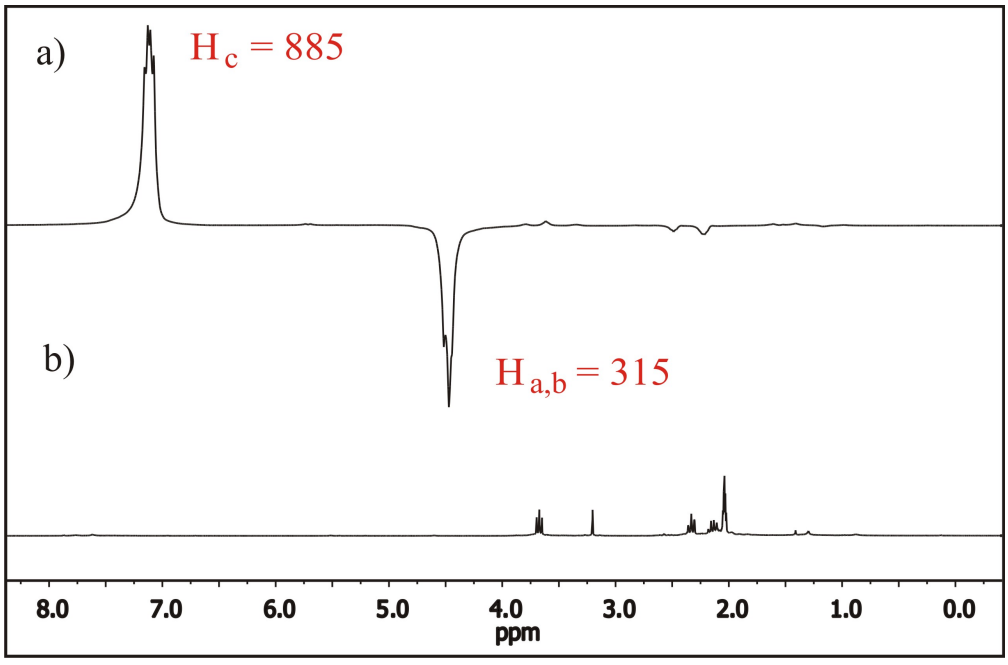

Figure 4.30: Spectra upon the parahydrogenation of N-acetylene-2-pyrrolidone with regard to lifetime prolongation of the generated singlet state.

The achieved signal enhancements in this spectrum were calculated with comparison to the also recorded reference spectrum to amount to 315 for each proton H_a and H_b and to 885 for H_c. Again, the TPA was estimated to amount around 11%, whereas the total hydrogenation rate after 5 minutes was calculated to a value of nearly 20%. This fourfold increased signal enhancement seems to support the thesis of lifetime prolongation of generated hyperpolarization due to isolated spin systems in N-vinyl-2-pyrrolidone.

In conclusion, hyperpolarization of the protons and carbons was achieved for parahydrogenation of both substrates N-vinyl-2-pyrrolidone and N-acetylene-2-pyrrolidone. As expected, the latter showed significant higher signal enhancements for protons and for carbons due to longer relaxation times of the introduced protons in the product molecule and due to the higher conversion rate of the hydrogenation reaction. However, polarization transfer to carbons further away than carbon 4 was only observed for the parahydorgenation of N-vinyl-2-pyrrolidone.

Examination of an ALTADENA experiment with regard to possible storage of hyperpolarization due to an isolated spin system in the the singlet state led to an increase of observable hyperpolarization upon the parahydrogenation of N-acetylen-2-pyrrolidone to N-vinyl-2-pyrrolidone. In future, a combination of this singlet state experiment together with a following polarization transfer experiment would be very interesting and should result in even higher signal enhancements of the carbon molecules. Furthermore, the waiting time after shaking the sample tube could be used for implementing a subsequent polymerization reaction. This bears the possibility to investigate a real time polymerization reaction with the use of magnetic labeling of the educt molecule. In addition, one could implement a polarization transfer experiment in a previous step and thereby examine the polymerization reaction by ^{13}C NMR. Moreover, further signal enhancements could be generated by additional isotope labeling of the interesting carbon atoms in the substrate.

5 Conclusion

In this thesis, different aspects concerning parahydrogen induced polarization were studied with respect to its chemical and spectroscopic background. The first part of this work mainly focused on optimizing the PHIP technique by investigating different catalyst systems and developing new setups for the parahydrogenation. The second part examined the possibility to transfer these results to different biologically active compounds to enable their later applications in medical diagnostics like NMR spectroscopy and MRI.

Optimizing the Parahydrogen Technique on Model Compounds

The investigated catalytic systems in this work were cationic homogeneous catalyst complexes with Rhodium or Iridium as metal centers. Overall, nine commercially available catalyst systems were investigated, only two of them are water-soluble. However, physiologically relevant processes take place in aqueous surroundings which suggests the implementation of a water-soluble catalyst system for the PHIP method. Hence, two additional water-soluble catalysts were synthesized containing sulfonate groups in the ligand system in order to enhance their solubility in water. Examination of these catalysts showed that four of the investigated water-insoluble catalyst systems and only one of the water-soluble catalyst systems implement sufficient high conversion rates and signal enhancements for our model compounds 1-hexyne and 2-hydroxyethyl acrylate. In addition, it was verified that sufficient conversion rate of the hydrogenation reaction represent the basic requirement to obtain hyperpolarized signals. Even more, the height of the intensity gain strongly depends on the underlying mechanism of the hydrogenation reaction which should support the pairwise transfer of the hydrogen atoms and also a fast transfer reaction. Especially the invesitgation of the water-soluble catalysts demonstrated that the underlying transfer mechanism can be disturbed by sterical hindrance of the catalytic species due to a bulky ligand system.

Regarding different setups for carrying out the hydrogenation reaction demonstrated that working at elevated temperature and pressure in general yields higher conversion rates and therefore higher polarization levels. Taking this into account, the setup of the ALTADENA experiment which offers the opportunity to work under pressure (instead of the standard PASADENA setup) was modified to shift the reaction conditions towards PASADENA conditions i.e. to start the parahydrogenation above the bore of the magnet. Depending on the stray field of the magnet, this procedure led to a mixture of PASADENA and ALTADENA spin states at the beginning of the NMR experiment. However, after insertion into the magnet, the ongoing reaction at high magnetic field evokes only PASADENA spin states. Thus, to achieve a major part of PASADENA spin states one could insert a further delay after the insertion of the reaction tube inside the spectrometer, which however would lead to a loss of observable polarization due to T_1 relaxation. For instance, one could use this kind of experiment for substances possessing short T_1 times of the protons resulting in a faster decay of the ALTADENA polarization which was done for the barbituric acid derivatives. In comparison to the advantage of achieving higher conversion rates and higher signal enhancements with this PASADENA method under pressure compared to the standard PASADENA experiment, also disadvantages were noticed in this work. One drawback of this reaction method is the broadening of the peaks due to foams and bubbles after shaking the sample. Especially the implementation of a parahydrogenation reaction in water using catalyst systems with sulfonate groups results in an undesirable strong foam formation. Thereby, a certain amount of otherwise detectable polarization is lost due to cancellation of the broad signals of the antiphase peaks. Another drawback is the decreasing conversion rate over time during the pressurized and shaken tube is inside the spectrometer. To overcome these disadvantages, a method for continuous parahydrogen delivery was designed which allows to perform PASADENA experiments by utilizing hollow fiber membranes. This new way of dissolving parahydrogen more efficiently into water without the occurrence of foam and bubbles offers the opportunity to implement continuous flow measurements under pressure, leading to higher conversion rates and higher polarization levels. Furthermore, this careful control of the parahydrogenation reaction generates a constant hyperpolarization of the protons over a certain time which enables the performance of 2D NMR experiments with very high sensitivity.

The aim to transfer the significant high proton polarization to heteronuclei was investigated with regard to ^{13}C nuclei. Hereby, spontaneous polarization transfer under ALTADENA conditions upon parahydrogenation of 1-hexyne generated the

highest signal enhancements for carbon 3 and carbon 4 in the middle of the chain of up to nearly 6000. Additional implementation of the INEPT($+\pi/4$) sequence with different delays to such an ALTADENA experiment did not result in more efficient polarization transfers. Furthermore, as this sequence is independent of the ^{1}H – ^{1}H coupling, different chosen delays always showed the same peak pattern which moreover were rather similar to the one obtained for spontaneous polarization transfer. On the contrary, applying the PH-INEPT+ sequence to an ALTADENA experiment led to much higher signal enhancements of up to 37000. In addition, implementation of this sequence with different delays offers the opportunity to transfer the major part of the hyperpolarization to one desired carbon site. Hence, implementation of the PH-INEPT+ sequence to an ALTADENA experiment results in a huge sensitivity gain of the carbon molecules which for 1-hexene was found to be around six times higher than for applying spontaneous polarization transfer. However, under the chosen reaction and measurement conditions, no investigation of the implementation of such polarization transfer sequences to a pure PASADENA spin state was feasible. The most interesting method to apply such pulse sequences to real and pure PASADENA spin states exhibits the combination of the recently investigated membrane setup with the introduced polarization transfer experiments. Investigations concerning this combination led to significant high ^{13}C polarization of different carbons in 2-hydroxyethyl propionate with varying amounts depending on the implemented delay for the PH-INEPT+ sequence. The investigated parahydrogenation of 2-hydroxyethyl acrylate using the membrane setup for dissolving parahydrogen into the aqueous solution combined with the PH-INEPT+ sequence led to a stable ^{13}C polarization for several minutes. These results open up the possibility to investigate the ongoing reaction with regard to elusive reaction intermediates and furthermore allows for more complicated NMR experiments like e.g. a two-dimensional ^{1}H-^{13}C COSY experiment.

Physiologically Relevant Substances for PHIP

The studies of metabolites and neurotransmitters for the PHIP technique focused on parahydrogenation of acetylene dicarboxylic acid and its derivatives representing an intermediate of the citric acid cycle and the chief inhibitory neurotransmitter in the mammalian central nervous system γ-aminobutyric acid and its derivatives.

The product molecule upon parahydrogenation of acetylene dicarboxylic acid dimethylester exhibits a symmetric structure causing magnetical equivalence of the two inserted parahydrogen protons in the molecule which in principle should not result in any hyperpolarized signal. Furthermore, it exhibits an isolated two spin system essential for the storage of polarization in the generated singlet state at low magnetic field. However, studies on the symmetric product molecule maleic acid dimethylester showed remarkable high signal enhancements displaying the peak pattern already predicted in literature. Furthermore, by examining the signal enhancements of the ongoing reaction of acetylene dicarboxylic acid dimethylester under different conditions (ALTADENA and PASADENA), first hints were found for lifetime prolongation of the generated isolated two spin system. Experiments concerning this effect were performed using the labeled prescursor acetylene dicarboxylic acid dimethylester which is not symmetric due to the labeling on one side of the molecule. The investigations of lifetime prolongation in singlet states kept at low magnetic field fulfilled the estimations. Based on the suppressed spin-lattice relaxation of the hyperpolarized molecules, higher signal enhancements can be achieved due to the continuing chemical reaction by implementing longer delay times between shaking the sample and inserting it to measure. Even after a waiting time of 5 minutes at low magnetic field, ^{1}H hyperpolarization was still observable which opens up the possibility to use this time to implement e.g. a further reaction step or to seperate the toxic catalyst system from the reaction mixture. Polarization transfer from the protons to the carbons yielded in very large hyperpolarization levels of ^{13}C by implementing the PH-INEPT+ sequence with a delay of 10 ms. Especially the carbonyl group showed a signal enhancement of more than 42300. Due to the long T_1 time of 76 seconds of the carbonyl group this hyperpolarization was visible even 6 minutes after applying the polarization transfer sequence.

Unfortunately, the generation of hyperpolarized GABA could not be implemented under the present conditions. One drawback arising for nearly all physiological relevant substances in this work is, that today only one efficient water soluble catalyst system is available. Whereas this catalyst system functions very well for the model compound 2-hydroxyethyl acrylate, its application to biologically active compounds seems to be limited. Thus, a high conversion rate for the hydrogenation reaction from TACA/CACA to GABA was observed, but no hyperpolarized signal was obtained due to some disturbance of the transfer mechanism of the catalyst system. At least, hyperpolarization via the PHIP method of a GABA derivative was achieved using a water-insoluble catalyst system at elevated temperature and pressure. However, the

generated signal enhancement for the protons of the double bond only amounted to 150 - 375. Thus, before performing more complicated experiments such as polarization transfer to ^{13}C or 2-dimensional NMR, the basic parahydrogenation experiment has to be optimized.

The examination of pharmaceutics and drugs in this work were implemented with regard to a barbituric acid derivative. In my diploma thesis, I demonstrated that homogeneous hydrogenation of an unsaturated barbituric acid derivative with 50% parahydrogen resulted in a signal enhancement of around 40 for the ^{1}H-NMR signals of the reaction product. However, no signal enhancement by randomly triggered polarization transfer to ^{13}C in the weak magnetic field could be achieved. In this work significantly larger signal enhancements of up to 1000 of ^{1}H in barbiturates by using 98% enriched para-H_2 in combination with optimized reaction conditions (elevated temperature and pressure) were demonstrated. Moreover, this optimization in combination with the application of the PH-INEPT+ pulse sequence for effective polarization transfer allowed for dramatic ^{13}C NMR signal enhancements up to 5200 of the different sites of the product 5-methyl-5-propenylbarbituric acid. The implementation of different delays in the PH-INEPT+ sequence showed that the polarization can be selectively transferred to different carbons in the barbituric acid derivative. Notably, even polarization of the carbonyl group featuring a long T_1 time was achieved, which is of high importance for storing the polarization within this molecule. The presented results open up the opportunity to use barbituric acid derivatives as active contrast agents in MRI and enable investigations of the function of an important pharmaceutical substrate in vivo.

With regard to polymerizable substances, parahydrogenation of both substrates N-vinyl-2-pyrrolidone and N-acetylene-2-pyrrolidone resulted in hyperpolarization of the protons and carbons. The latter showed significantly higher signal enhancements for protons and carbons due to longer relaxation times of the introduced protons in the product molecule and due to the higher conversion rate of the hydrogenation reaction. However, polarization transfer to carbons further apart than carbon 4 was only observed for the parahydrogenation of N-vinyl-2-pyrrolidone. Examination of an ALTADENA experiment with regard to possible storage of hyperpolarization in an isolated spin system of the generated singlet state led to an increase of observable hyperpolarization upon the parahydrogenation of N-acetylene-2-pyrrolidone. In future, a combination of this singlet state experiment together with a subsequent polarization transfer experiment would be of high interest and should result in even higher signal enhancements of the carbon molecules. Furthermore, the waiting time after shaking the sample tube could be used for implementing a polymerization

reaction. This bears the possibility to investigate polymerization reaction in real time with the use of magnetic labeling of the educt molecule. In addition, one could implement a polarization transfer experiment in a previous step and thereby examine the polymerization reaction with regard to the carbon atoms present in the molecule. Therefore, further signal enhancements could be generated by additional chemical labeling of the interesting carbon atoms in the substrate.

Hence, the presented work in this thesis covers the optimization of the PHIP technology, hereby combining different fields of research like chemical and spectroscopical aspects, and transfers the results to applications of real biologal acitve compounds.

6 Appendix

6.1 General Experimental Parameters

- All chemicals were purchased from Sigma-Aldrich or Merck and used without further purification. The utilized solvents were purchased from Acros, Fisher Chemicals, Fluka and Riedel-de-Haen with a purity class of ”zur Analyse (p.a.)” or ”Chromasolv”.

- Melting points were examined with the equipment Büchi B-545. The denoted values are uncorrected.

- IR spectra were recorded with a FT-IR spectrometer Perkin Elmer Spectrum BX or a FT-IR spectrometer Nicolet 730.

- Mass spectra were measured with the spectrometer VG ZAB 2-Se-FDP.

- All ^{1}H and ^{13}C NMR spectra for analysis of synthesized substances or for investigation of the hydrogenation rate were performed on a Bruker Spectrospin 250 or a Bruker AMX 300. All ^{1}H PHIP spectra were recorded with the use of the Bruker AMX 300 spectrometer or a 300 MHz widebore magnet with a Tecmag console. Polarization transfer experiments to ^{13}C and ^{15}N (PH-INEPT sequences) and as well the 2D experiments were performed on the Bruker AMX 300 spectrometer. The indicated chemical shifts [δ/ppm] refer to the signal of solvent relative to tetramethylsilane.

- Numbering of the displayed structural formulas in the general and experimental part served for the allocation in NMR spectra and are not necessarily according to the IUPAC nomenclatur.

6.2 Parahydrogen Enrichment

For the enrichment of parahydrogen, two different approaches were employed yielding contents of 50% and 98% parahydrogen. For both setups, normal hydrogen with a purity of 5.0 was used as received from a commercial source (Westfalen AG, Münster, Germany). 50% enriched parahydrogen was generated via utilizaton of a copper u-tube filled with active charcoal as a catalyst for the symmetry forbidden conversoin from ortho- to para-H_2. The active charcoal was fixed inside by closing both ends of the tube with glass wool and valves. After floating the equipment with normal hydrogen and cooling it with liquid nitrogen, a continuous flow of hydrogen was allowed to pass through the tube yielding in a constant delivery of 50% enriched parahydrogen. This setup is depicted in Figure 6.1.

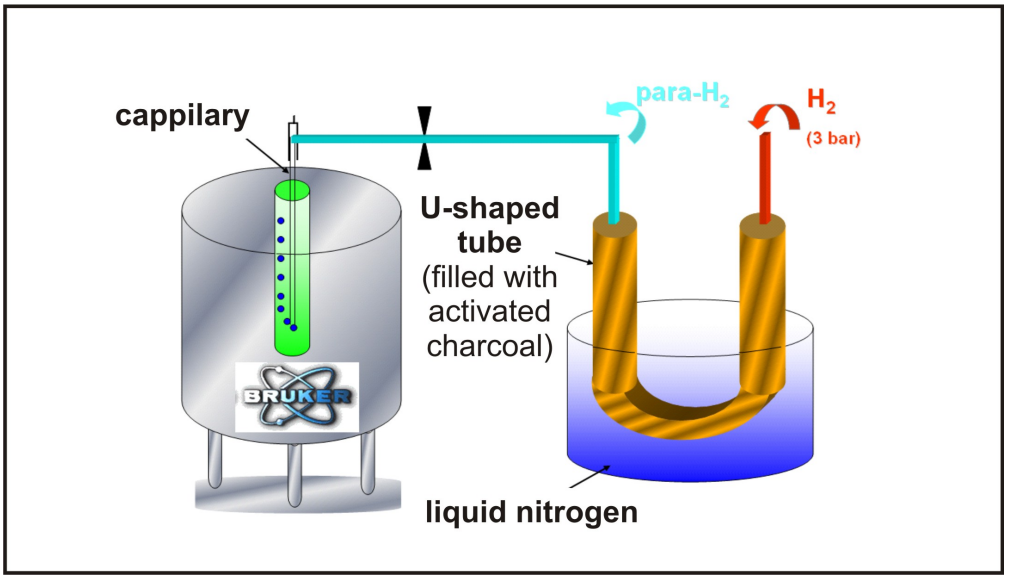

Figure 6.1: Experimental setup for the enrichment content of 50% parahydrogen by cooling with nitrogen

The enrichment factor of 98% parahydrogen was generated by cooling thermal hydrogen to 30 Kelvin. Therefore, a closed-cycle cryostat setup (Advanced Research Systems, Macungie, PA, USA) was used operating with helium as the cooling agent. In a pressure tight chamber of the cooling device, active charcoal was placed as the transition catalyst. This setup is shown in Figure 6.2. The para-H_2 afterwards was stored in transportable aluminium cylinders at 3.5 bar.

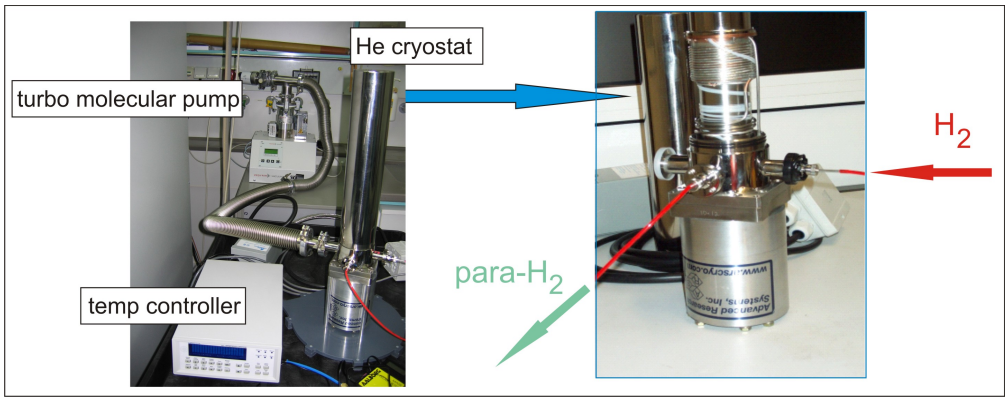

Figure 6.2: Setup operating with a closed cycle cryostat and helium as the cooling agent.

6.3 Sample Preparation

All PHIP experiments were performed in 10 mm NMR tubes designed for the implementation of experiments under pressure which were purchased from Sigma Aldrich, together with the corresponding screw caps. In general, the NMR tubes were filled with 5 mg of the chosen catalyst system and between 40 – 100 mg of the substance of interest (with regard to the availability of the substance) inside a glovebox under argon atmosphere in order to avoid deactivation of the catalyst due to ambient oxygen. For experiments with organic solvents, 3 g of solvent was added to the reaction mixture and the NMR tube was sealed with the special standard PASADENA cap containing a thin capillary or the normal screw cap used for ALTADENA experiments under pressure before bringing it outside the glovebox. For ALTADENA or PASADENA experiments under aqueous conditions and pressure, the NMR tubes were sealed with the screw cap before adding the solvent and brought outside the glovebox. Then, D_2O was added to the mixture through the membrane of the screw cap with the help of a needle. The latter way of preparing the sample was also chosen for performing experiments with hollow fibre membranes, but, before starting the experiment the screw cap was changed against a screw cap connected to the membrane setup.

6.4 Calculation of Signal Enhancements

All signal enhancements were calculated by comparing the NMR line integrals or intensities of the recorded PHIP spectrum with a reference spectrum measured in the same sample under the same measurement conditions (same coil, same receiver gain

and same pulse). If more scans than one were necessary for the observation of the thermal peaks in the spectrum, the integrals or intensities of the thermal peaks in the reference had to be divided by the amount of scans. The PHIP and the reference spectra were scaled to the same noise level. As a reference for special pulse sequences like the PH-INEPT+ sequence, no thermal INEPT spectrum was chosen but a standard thermal one pulse ^{13}C spectrum. For calculation of the signal enhancements, the conversion rate of the parahydrogenation reaction at the time point of acquisition (TPA) of a PHIP spectrum is essential. It has to be taken into account for the calculations, that in most cases the conversion rate of the parahydrogenation reaction at the TPA and the one of a reference spectrum recorded after the reaction has stopped is different. Thus, in general the present conversion rates at the TPA were estimated by comparison with the total conversion calculated from the integrals of the NMR peaks of the thermally polarized product at the end of the hydorgenation reaction. If several PHIP spectra were recorded during the parahydrogenation reaction of one sample, the TPA was not taken as the total conversion rate at this point but referred to the reaction proceeding between the single measurements steps.

For the proton NMR spectra, absolute integrals were analyzed in order to compare the PHIP and the reference spectra. Therefore, the absolute integrals of the thermal peaks in the reference spectrum were adjusted to the expected conversion rate at the TPA of the PHIP spectrum. For PASADENA experiments where only the two introduced protons are hyperpolarized, the hyperpolarized peaks were divided by the value of the absolute integral of one thermal proton at the estimated conversion rate. For ALTADENA experiments where the introduced polarization is spread along the scaffold of the molecule, all observed hyperpolarized peaks in the PHIP spectrum were divided by the values of the absolute integrals of the actual amount of protons the thermal peaks stem from.

For the carbon spectra, the signal enhancements were calculated simply by comparing the amplitudes of the NMR lines of the hyperpolarized and thermally polarized compounds. For ALTADENA experiments, a thermal spectrum was recorded with several scans immediately after the ^{13}C polarization was destroyed by the read out pulse of the formerly applied experiment. This served as a reference for all hyperpolarized ^{13}C spectra taken of equal samples under the same conditions during the experiment, representing the amount of thermally polarized peaks for the assumed conversion rate. For PASADENA experiments using hollow fibre membranes, the reference spectrum

was recorded after the reaction was complete and no further polarized peaks but the thermal peaks of the products were visible in the spectrum. The time needed for the total conversion was taken as the basis to estimate the value of conversion rate which took place during 1 minute of the experiment. Also the fact, that at the beginning and at the end of the hydrogenation lower conversion rates are present was taken into account. These spectra were excluded from the signal enhancement calculations. Thus, only the time frame in the middle of the hydrogenation reaction, where the conversion rate was nearly stable was taken for the calculations. Therefore, the recorded reference spectrum after total hydrogenation of 100% was not only divided by the recorded scans, but also normalized to the assumed amount of generated product in the time frame between two recorded spectra.

6.5 T_1 Measurements

The executed spin-lattice relaxation-time measurements in this work were performed as so-called "inversion-recovery experiments". At time $\tau = 0$ the magnetization is inverted by a 180° pulse bringing magnetization vector into the direction of the negative z-axis. This inverted magnetization is then allowed to relax for a time τ. After time τ, a 90° pulse is applied, whereby the present magnetization M_z is rotated into the detectable x,y-direction and the resulting FID is observed and Fourier transformed to give a spectrum. To calculate T_1 several experiments have to be performed for different time frames τ. By plotting the left side of Equation 6.1 against τ, the value of T_1 can be obtained.

$$ln\frac{S(\tau) + S(0)}{2S(0)} = -\tau/T_1 \tag{6.1}$$

In practice, 5 mm NMR tubes were filled with 30 mg of the substance of interest, in general with the pure product of the considered hydrogenation and 1 ml of the corresponding solvent. For the proton measurements, inversion times ranging from 0.2 to 60 seconds and a repetition time of 40 – 150 seconds were applied depending on the investigated substance. The carbon T_1 relaxation times were measured with times of 2 to 80 seconds and a repetition time of 320 – 380 seconds was also chosen in dependency of the regarded molecule. The corresponding T_1 times were calculated by the Bruker Topspin 2.1 T_1-calculation software.

6.6 Synthesis of Model Compounds

6.6.1 5-Methyl-5-propenyl-barbituric acid

1. Step 2-methylmalonic acid diethyl ester (1)

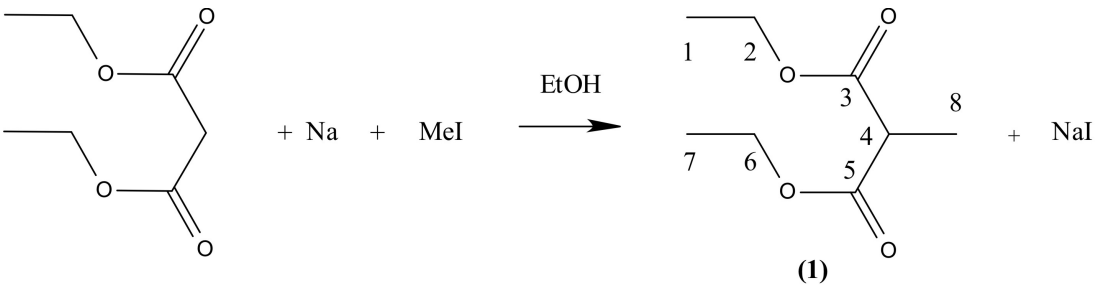

160.17 g/mol 22.99 g/mol 141.94 g/mol 174.19 g/mol 149.89 g/mol

Batch:	21.67 g	(135.29 mmol)	malonic acid diethyl ester
	19.47 g	(137.17 mmol)	methyl iodide
	3.20 g	(139.19 mmol)	sodium
	170 ml		abs. Ethanol
	140 ml		H_2O
	300 ml		diethyl ether

Procedure [107] [1]: (under argon atmosphere)
By adding absolute ethanol dropwise to present sodium, the latter was diluted carefully. After complete dissolution, diethyl malonate and methyl iodide was added subsequently. The mixture was heated under reflux over night. After cooling, water was added and the resulting mixture was extracted three times with diethyl ether. The organic phase was washed with a saturated solution of NaCl and dried over magnesium sulfate. Than, the solvent was evaporated and the product was obtained via fractional distillation in vacuo.

[1] accomplished by M. Feige

Yield: 18.77 g (107.76 mmol) equivalent 79.6% of theory

Characterization: yellow liquid
^{1}H NMR ($CDCl_3$, 250 MHz): δ / ppm = 1.12 - 1.22 (6 H, m, 3 x H(1), 3 x H(7)), 1.30 - 1.33 (3 H, m, 3 x H(8)), 3.23 – 3.38 (1 H, m, 1 x H(4)), 4.01 - 4.17 (4 H, m, 2 x H(2), 2 x H(6)).

2. Step 2-allyl-2-methylmalonic acid diethyl ester (2)

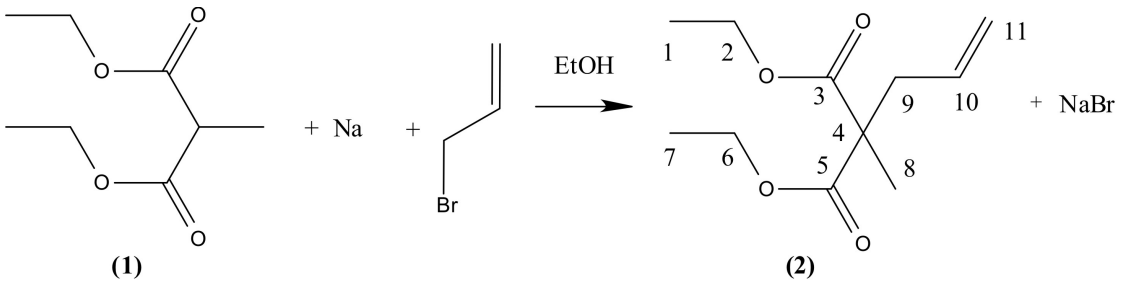

174.19 g/mol 22.99 g/mol 120.98 g/mol 214.26 g/mol 102.89 g/mol

Batch:	4.24 g	(24.34 mmol)	2-methylmalonic acid diethyl ester
	3.21 g	(26.53 mmol)	allyl bromide
	0.65 g	(28.27 mmol)	sodium
	30 ml		abs. Ethanol
	100 ml		H_2O
	10 ml		toluene

Procedure [108] [2]: (under argon atmosphere)
2-Methylmalonic acid diethyl ester was added to a solution of sodium in absolute ethanol. Under cooling, allyl bromide was added dropwise to the mixture. The flask was heated over night under reflux and after cooling, the precipitate (NaBr) was removed by suction and washed with ethanol. The solvent was evaporated in vacuo and the resulting residue was treated with toluene. Undissolved material was filtered off and the organic phase was washed with water and dried over magnesium sulfate. Toluene was evaporated to afford 2-allyl-2-methylmalonic acid diethyl ester.

[2] accomplished by M. Feige

Yield: 4.57 g (21.33 mmol) equivalent 87.6% of theory

Characterization: light yellow liquid
^{1}H NMR ($CDCl_3$, 250 MHz): δ/ ppm = 1.15 - 1.24 (6 H, t, J^2 = 7.1 Hz, 3 x H(1), 3 x H(7)), 1.31 - 1.36 (3 H, s, 3 x H(8)), 2.52 - 2.62 (2 H, m, 2 x H(9)), 4.06 4.19 (4 H, qu, J^2 = 7.1 Hz, 2 x H(2), 2 x H(6)), 4.99 5.11 (2 H, m, 2 x H(11)), 5.51 - 5.75 (1 H, m, 1 x H(10)).

3.Step 5-methyl-5-propenyl-barbituric acid (3)

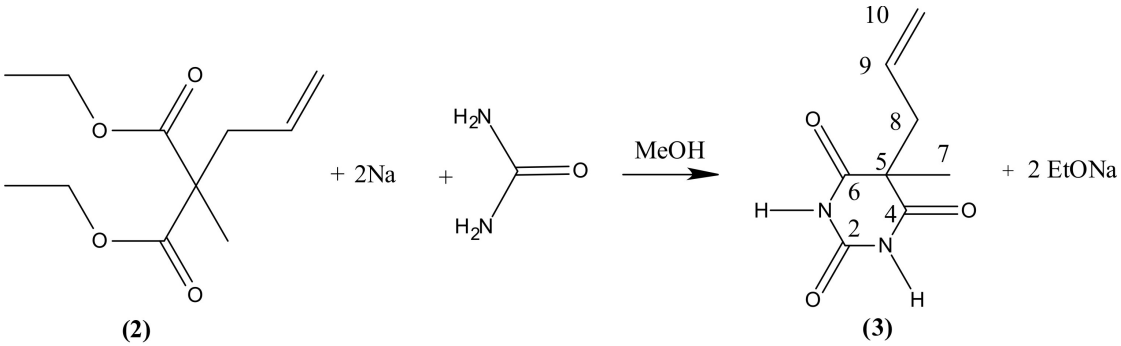

Batch:	4.35 g	(20.30 mmol)	2-allyl-2-methylmalonic acid diethyl ester
	1.43 g	(23.81 mmol)	urea
	1.10 g	(47.85 mmol)	sodium
	30 ml		abs. methanol
	10 ml		H_2O

Procedure [109] [3]: (under argon atmosphere)
Absolute methanol was added dropwise to present sodium in a flask. After complete dissolution, urea and 2-allyl-2-methylmalonic acid diethyl ester was added subsequently to the reaction mixture. The reaction mixture was stirred for 20 minutes at roomtemperature and afterwards it was stirred and heated under reflux for 2 days.

[3] accomplished by M. Feige

After cooling, the solid was extracted by suction and washed with a cooled mixture of methanol/acetone. The resulting product was dryed at 40 °C under vacuo.

Yield: 0.83 g (4.56 mmol) equivalent 22.5% of theory

Characterization: light yellow solid, melting point: 260 °C (defraction)

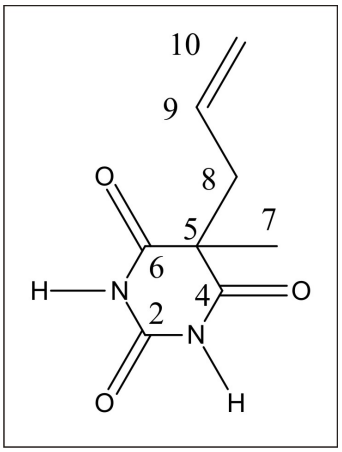

^{1}H NMR (D_2O, 250 MHz): δ/ ppm = 1.20 (3 H, s, 3 x H(7)), 2.45 - 2.47 (2 H, d, J^2 = 7.3 Hz, 2 x H(8)), 5.03 – 5.13 (2 H, m, 2 x H(10)), 5.63 - 5.84 (1 H, m, 1 x H(9)).
^{13}C NMR (D_2O, 63 MHz): δ/ ppm = 19.36 – 24.35 (qu, J^2 = 128.0 Hz, C(7)), 40.70 – 44.16 (t, J^2 = 131.0 Hz, C(8)), 55.46 (s, C(5)), 116.16 – 120.28 (t, J^2 = 155.6 Hz, C(10)), 135.63 – 137.65 (d, J^2 = 151.9 Hz, C(9)), 167.25 Hz, C(2), 183.38 Hz, C(4,6).
MS (FD): m/z (%): 184.9 (16 M^++2), 132.7 (100).

6.6.2 ^{13}C-acetylenedicarboxylic acid dimethyl ester

1.Step ^{13}C-acetylenedicarboxylic acid (4)

a)

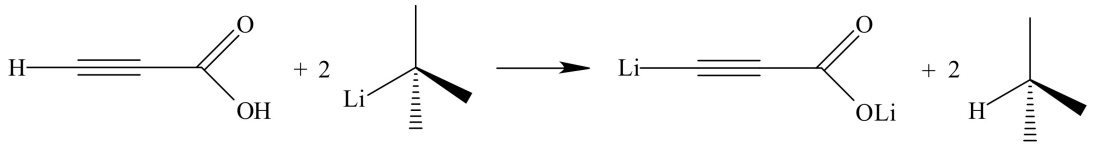

70.05 g/mol 64.05 g/mol 81.91 g/mol 58.12 g/mol

b)

198.32 g/mol 98.08 g/mol 44.99 g/mol 18.02 g/mol 233.39 g/mol

c)

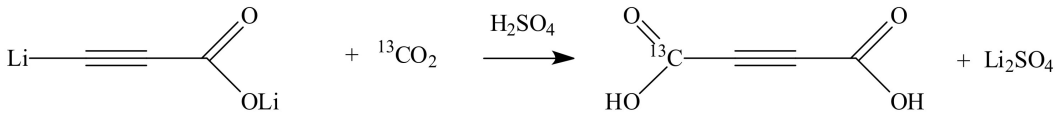

81.91 g/mol 44.99 g/mol 98.08 g/mol 115.04 g/mol 109.95 g/mol

Batch:	a)	35 ml	(59.50 mmol)	tert-butyllithium (1.7 M in pentane)
		1.52 g	(21.70 mmol)	propionic acid
		400 ml		THF
	b)	5.3 g	(26.72 mmol)	^{13}C labeled barium carbonate
		50 ml		H_2SO_4 conc.
	c)	20 ml		10% H_2SO_4

Procedure [91] [4]:
a) Under argon atmosphere, propionic acid was dissolved in dry THF and cooled to -78 °C. Afterwards, tert-butyllithium was added dropwise to the reaction mixture.
b) According to figure 6.3 ^{13}C labeled barium carbonate was put into flask A and the whole system was evacuated. Afterwards, the U-tube B was cooled to -60 °C. The concentrated sulfuric acid was added dropwise to flask A. The generated $^{13}CO_2$ condensed in flask C, whereas the water and acid remained in the cooled U-tube B. To ensure a complete conversion, flask A was heated to 50 °C and flushed with helium gas.
c) The reaction mixture of a) was cooled to -110 °C with liquid nitrogen and carefully transferred to flask C of the apparatus in figure 6.3. Than, the reaction mixture was allowed to warm up until -80 °C and stirred at this temperature for 2 hours. Afterwards, the cooling was removed and the reaction mixture was allowed to warm up until 0 °C and remained at this temperature in an water-ice bath. 10% sulfuric acid was added carefully and the mixture was stirred for 30 more minutes at 0 °C. After warming up, THF was evaporated and the mixture extracted with diethyl ether. The organic layer was dryed and residual solvent was evaporated. Without further characterization, the product was transformed to the dimethylester described in the next step.

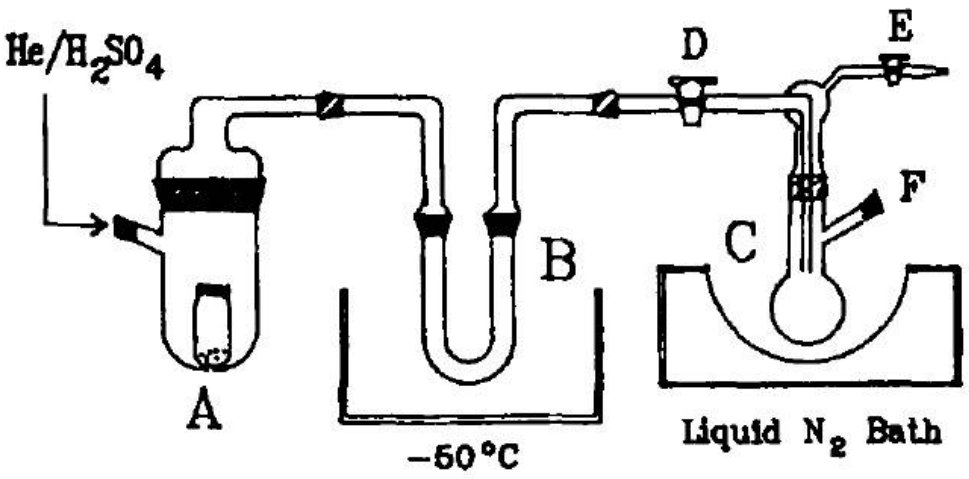

Figure 6.3: Apparatus as described in literature by V. Vijayalakshmi [91].

[4] accomplished by M. Feige

2.Step ^{13}C-dimethyl-acetylenedicarboxylic acid (5)

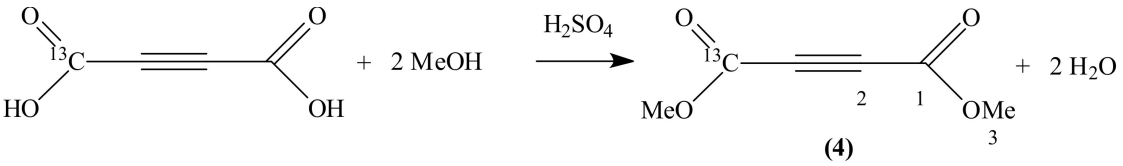

(4)

115.04 g/mol	32.04 g/mol	98.08 g/mol	143.10 g/mol	18.02 g/mol

Batch:	1.45 g	(12.60 mmol)	^{13}C-acetylenedicarboxylic acid
	30 ml		methanol
	4 ml		H_2SO_4 conc.
	75 ml		diethyl ether

Procedure [92] [5]: (under argon atmosphere)
Absolute methanol was diluted with concentrated H_2SO_4 at 0 °C. The ^{13}C-acetylenedicarboxylic acid was dissolved in methanol and given dropwise to the methanol/H_2SO_4 mixture. After stirring for a day at roomtemperature, icewater was added and the reaction mixture was extracted with diethyl ether. The organic layer was washed with icewater, neutralized with a saturated solution of $NaHCO_3$ and dried. Afterwards, the solvent was evaporated and the product was distilled at 8 mbar between 130 °C and 140 °C under vacuo.

Yield: 0.76 g (5.31 mmol) equivalent 42.1% of theory

[5] accomplished by M. Feige

Characterization: light yellow oil

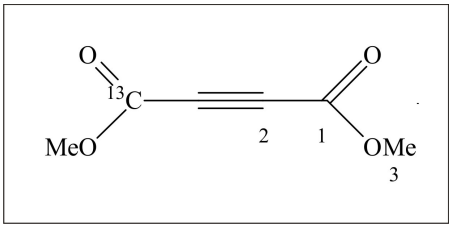

^{1}H NMR(acetone), 250 MHz): δ/ ppm = 3.84 - 3.87 (6 H, t, J^3 = 2.2 Hz, 6 x H(3))
^{13}C NMR (D_2O, 63 MHz): δ/ ppm = 45.83 (C(16)), 71.63 (C(8)), 90.85 (C(7)), 112.02 (C(13)), 115.20 (C(2), 115.54 (C(6)), 118.68 (C(15), 119.13 (C(18), 123.09 (C(11), 125.22 (C(12)), 126.95 (C(5)), 127.08 (C(3)), 131.78 (C(17)), 132.31 (C(14)), 139.16 (C(4)), 140.50 (C(9)), 148.96 (C(10)), 167.74 (C(1)).
IR (KBr): $\tilde{\nu}$ (cm^{-1}):2960 (s) C-H valence vibration of CH_3, 1723 and 1681 (s) C=O valence and ^{13}C=O valence vibration, 1435 $COCH_3$ valence vibration, 1251 and 1218 C-O valence and ^{13}C-O valence vibration.
MS (FD): m/z (%): 143.1 (27 M), 175 (100).

6.6.3 1-Allyl-1-(4-fluorophenyl)-1,3-dihydroisobenzofuran-5-carbonitrile

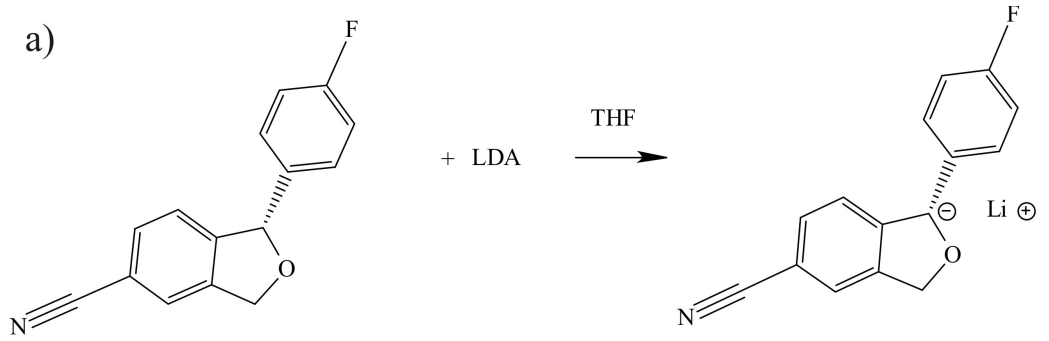

239.07 g/mol 107.12 g/mol 245.08 g/mol

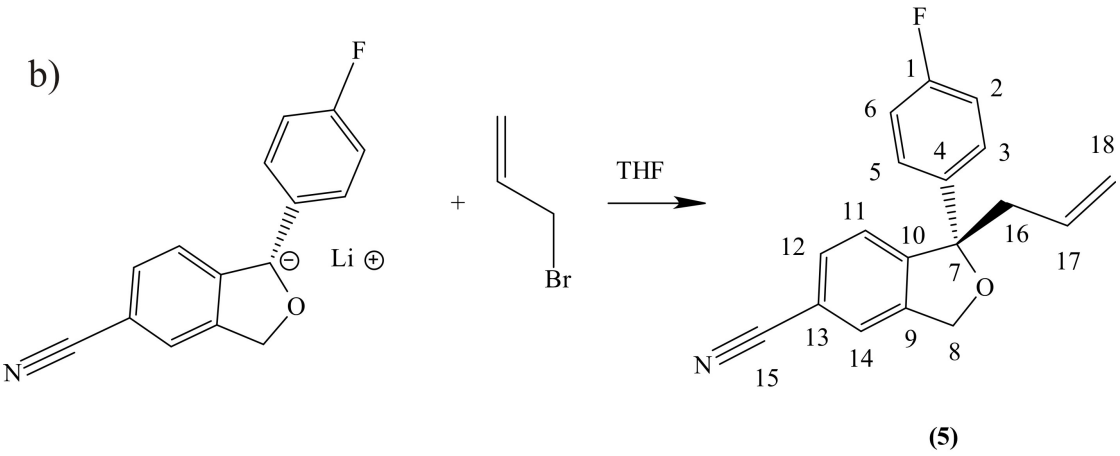

(5)

245.08 g/mol 119,96 g/mol 279.11 g/mol

Batch:	a)	8 ml	(6.4 mmol)	n-butyllithium (0.8 M in pentane)
		1.3 g	(12.8 mmol)	diisopropylamine
		2.4 g	(10.0 mmol)	1-(4-fluorophenyl)-1,3-dihydroisobenzofuran-5-carbonitrile
		25 ml		THF
	b)	1.21 g	(10.1 mmol)	allyl bromide
		13 ml		THF
		75 ml		toluene
		25 ml		H_2O

Procedure [103] [6]: (under argon atmosphere)
Lithium diisopropylamide (LDA) was produced by giving di-isopropylamine dropwise to n-butyllithium in pentan at −30 °C. Afterwards, a solution of 1-(4-fluorophenyl)-1,3-dihydroisobenzofuran-5-carbonitrile in dry THF was added. The reaction mixture was stirred for 10 minutes at −30 °C. Than, a solution of allyl bromide in dry THF was added dropwise and the reaction mixture was allowed to warm up to roomtemperature and stirred over night. Afterwards, reaction mixture was diluted with icewater and the organic layer was extracted with toluol. The organic phase was washed with water, dryed over sodiumsulfate and the solvens was evaporated under vacuo. The product was purified by column chromatography [103].

Yield: 1.58 g (5.66 mmol) equivalent 88.4% of theory

Characterization: yellow oil

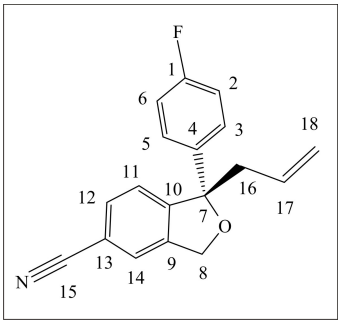

^{1}H NMR($CDCl_3$), 250 MHz): δ/ ppm = 2.79 - 3.03 (2 H, m, 2 x H(16)), 4.97 – 5.20 (4 H, m, 2 x H(8), 2 x H(18)), 5.48 – 5.69, ddt, J^3 = 7.0 Hz, 10.1 Hz, 17.1 Hz, 1 x H(17)), 6.94 – 7.06 (2 H, m, H(2), H(6)), 7.30 – 7.64 (5 H, m, H(3), H(5), H(11), H(12), H(14)).
^{13}C NMR ($CDCl_3O$, 63 MHz): δ/ ppm = 45.83 (C(16)), 71.63 (C(8)), 90.85 (C(7)), 112.02 (C(13)), 115.20 (C(2), 115.54 (C(6)), 118.68 (C(15), 119.13 (C(18), 123.09 (C(11), 125.22 (C(12)), 126.95 (C(5)), 127.08 (C(3)), 131.78 (C(17)), 132.31 (C(14)), 139.16 (C(4)), 140.50 (C(9)), 148.96 (C(10)), 167.74 (C(1)).
MS (FD): m/z (%): 279.2 (45 M), 238.1 (100).

[6] accomplished by M. Feige

6.7 Synthesis of a Water-soluble Ligand System

6.7.1 Tppsm

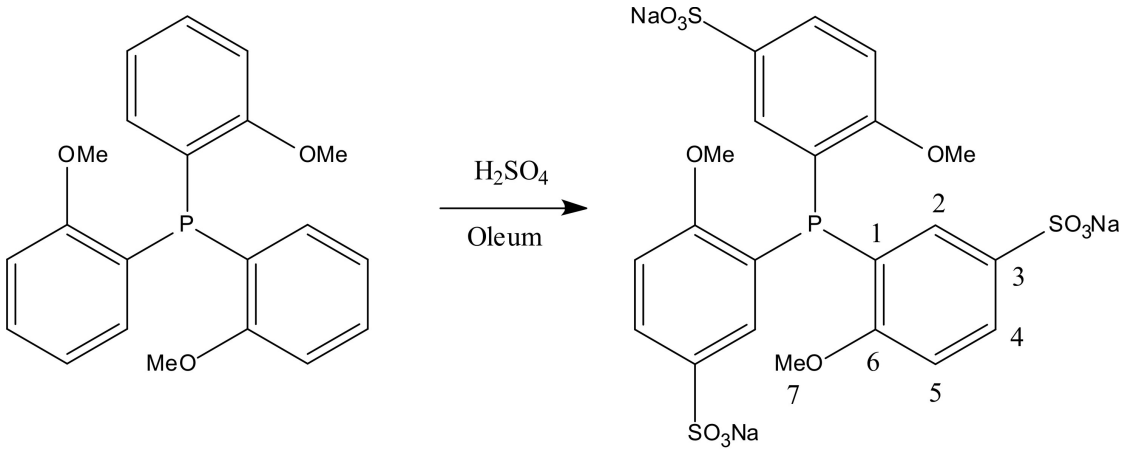

352.12 g/mol 657.94 g/mol

Batch:	0.18 g	(2.91 mmol)	boric acid
	1.15 ml	(96.5 weight %)	H_2SO_4
	0.10 g	(0.28 mmol)	tris(o-methoxyphenyl)phosphine
	2.20 ml	(65 weight %)	oleum
	3.14 ml	(7.24) mmol	triisooctylamine
	7.70 ml		toluene

Procedure [110] [7]: (under argon atmosphere)
Boric acid was dissolved in H_2SO_4 and tris(o-methoxyphenyl)phosphine was added in small portions to the reaction mixture. Afterwards, the mixture was cooled to 5 °C and oleum was added dropwise. Than, the reaction mixture was allowed to warm up to roomtemperature and stirred for 3 days. The reaction mixture was diluted with icewater and stirred for 24 h with toluene and triisooctylamine. Thereby, the sulfonated phosphine passes as an amine salt into the organic layer. Afterwards, the organic compound was isolated and reextracted with a NaOH solution. The aqueous phase was separated and the solvens was evaporated in vacuo.

[7] accomplished by M. Drechsler

Yield: 0.025 g (0.04 mmol) equivalent 13.5% of theory

Characterization: colourless solid

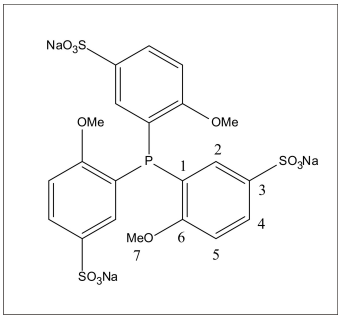

^{1}H NMR(D_2O), 250 MHz): δ/ ppm = 3.78 (9 H, s, 9 x H(7)), 7.20 (3 H, dd, J^4 = 8.9 Hz, J^3 = 4.6 Hz, 3 x H(5), 7.24 (3 H, dd, J^4 = 2.1 Hz, J^3 = 4.6 Hz, 3 x H(4)), 7.93 (3 H, dd, J^4 = 2.1 Hz, J^3 = 9.6 Hz, 3 x H(2).
^{13}C NMR (D_2O, 63 MHz): δ/ ppm = 56.2 C(7), 111.4 C(5), 122.2 C(1), 129.3 C(2), 131.1 C(4), 136.8 C(3), 163.1 C(6).
^{31}P NMR (D_2O, 101 MHz): δ/ ppm = -32.0.

The described experiment serves as a general example for the sulfonation of catalytic ligand systems in order to make these compounds water-soluble. The ligand system dppbs was synthesized according the same procedure.

Bibliography

[1] F. Bloch, W. W. Hansen, M. P. *Phys. Rev.* **1946,** *70,* 474–485.

[2] Purcell, E. M.; Torrey, H. C.; Pound, R. V. *Phys. Rev.* **1946,** *69,* 37–38.

[3] Ardenkjaer-Larsen, J. H.; Fridlund, B.; Gram, A.; Hansson, G.; Hansson, L.; Lerche, M. H.; Servin, R.; Thaning, M.; Golman, K. *P. Natl. Acad. Sci. USA* **2003,** *100,* 10158–10163.

[4] Frydman, L.; Blazina, D. *Nat. Phys.* **2007,** *3,* 415–419.

[5] McCarney, E. R.; Armstrong, B. D.; Lingwood, M. D.; Han, S. *P. Natl. Acad. Sci. USA* **2007,** *104,* 1754–1759.

[6] Münnemann, K.; Bauer, C.; Schmiedeskamp, J.; Spiess, H.; Schreiber, W.; Hinderberger, D. *Appl. Magn. Reson.* **2008,** *34,* 321–330.

[7] Hore, P. J.; Broadhurst, R. W. *Prog. Nucl. Mag. Res. Sp.* **1993,** *25,* 345–402.

[8] Bargon, J.; Kuhn, L. *Helv. Chim. Acta* **2006,** *89,* 2522–2532.

[9] Daviso, E.; Diller, A.; Alia, A.; Matysik, J.; Jeschke, G. *J. Magn. Reson.* **2008,** *190,* 43–51.

[10] Bowers, C. R.; Weitekamp, D. P. *J. Am. Chem. Soc.* **1987,** *109,* 5541–5542.

[11] Pravica, M. G.; Weitekamp, D. P. *Chem. Phys. Lett.* **1988,** *145,* 255–258.

[12] Eisenschmid, T. C.; Kirss, R. U.; Deutsch, P. P.; Hommeltoft, S. I.; Eisenberg, R.; Bargon, J.; Lawler, R. G.; Balch, A. L. *J. Am. Chem. Soc.* **1987,** *109,* 8089–8091.

[13] Natterer, J.; Bargon, J. *Prog. Nucl. Magn. Reson. Spectrosc.* **1997,** *31,* 293–315.

[14] Duckett, S. B.; Sleigh, C. J. *Prog. Nucl. Mag. Res. Sp.* **1999,** *34,* 71–92.

[15] Bowers, C. R. *Encyclopedia of Nuclear Magnetic Resonance, Advances in NMR, vol.9;* John Wiley and Sons. Ltd.: Chichester: 2002.

[16] Aime, S.; Dastru, W.; Gobetto, R.; Viale, A. *Org. Biomol. Chem.* **2005,** *3,* 3948–3954.

[17] Bouchard, L.-S.; Kovtunov, K. V.; Burt, S. R.; Anwar, M. S.; Koptyug, I. V.; Sagdeev, R. Z.; Pines, A. *Angew. Chem. Int. Ed.* **2007,** *46,* 4064–4068.

[18] Bouchard, L.-S.; Burt, S. R.; Anwar, M. S.; Kovtunov, K. V.; Koptyug, I. V.; Pines, A. *Science* **2008,** *319,* 442–444.

[19] Mansson, S.; Johansson, E.; Magnusson, P.; Chai, C.-M.; Hansson, G.; Petersson, J. S.; Stahlberg, F.; Golman, K. *Eur. Radiol.* **2006,** *16,* 57–67.

[20] Golman, K.; Zandt, R.; Lerche, M.; Pehrson, R.; Ardenkjaer-Larsen, J. H. *Cancer Res.* **2006,** *66,* 10855–10860.

[21] Kauczor, H.-U.; Hofmann, D.; Kreitner, K.-F.; Nilgens, H.; Surkau, R.; Heil, W.; Potthast, A.; Knopp, M. V.; Otten, E. W.; Thelen, M. *Radiology* **1996,** *201,* 564–568.

[22] Goodson, B. M. *J. Magn. Reson.* **2002,** *155,* 157–216.

[23] van Beek, E. J. R.; Schmiedeskamp, J.; Wild, J. M.; Paley, M. N. J.; Filbir, F.; Knitz, F.; Mills, G. H.; Woodhouse, N.; Swift, A.; Heil, W.; Wolf, M.; Otten, E. W. *Eur. Radiol.* **2003,** *13,* 2583–2586.

[24] Kastler, A. *Journal de Physique et le Radium* **1950,** 11.

[25] Happer, W. *Reviews of Modern Physics* **1972,** *44,* 169–249.

[26] Colegrove, F. D.; Schearer, L.; Walters, G. *Physical Review* **1963,** *132,* 2561–2572.

[27] Stolz, E.; Meyerhoff, M.; Bigelow, N.; Leduc, M.; Nacher, P.; Tastevin, G. *Applied Physics B-Lasers and Optics* **1996,** *63,* 629–633.

[28] Batz, M.; Baeler, S.; Heil, W.; Otten, E. W.; Rudersdorf, D.; Schmiedeskamp, J.; Sobolev, Y.; Wolf, M. *J. Res. Natl. Inst. Stand. Technol.* **2005,** *110,* 293–298.

[29] Becker, J.; Bermuth, J.; Ebert, M.; Grossmann, T.; Heil, W.; Hofmann, D.; Humblot, H.; Leduc, M.; Otten, E. W.; Rohe, D.; Surkau, R. *Nuclear Instruments and Methods in Physics Research* **1998,** *A 402,* 327–336.

[30] Becerra, L. R.; Gerfen, G. J.; Temkin, R. J.; Singel, D. J.; Griffin, R. G. *Phys. Rev. Lett.* **1993,** *71,* 3561–3564.

[31] Song, C.; Hu, K.-N.; Joo, C.-G.; Swager, T. M.; Griffin, R. G. *J. Am Chem. Soc.* **2006,** *128,* 11385–11390.

[32] Bargon, J. "Lecture in Mainz", 2005.

[33] Bowers, C. R.; Weitekamp, D. P. *Phys. Rev. Lett.* **1986,** *57,* 2645–2648.

[34] Riedel, E. *Anorganische Chemie;* Walter de Gruyter: 1999.

[35] de Vries, J. G.; Elsevier, C. J. *Handbook of Homogeneous Hydrogenation;* Wiley: 2007.

[36] Wedler, G. *Lehrbuch der Physikalischen Chemie;* Wiley-VCH: 1997.

[37] Shriver, D. F.; Atkins, P. W.; Langford, C. H. *Anorganische Chemie;* Wiley-VCH, Weinheim: 1997.

[38] Bradshaw, T. W.; Norris, J. O. W. *Rev. Sci. Instrum.* **1986,** *58,* 83–85.

[39] Woelk, K.; Bargon, J. *Z. Phys. Chem.* **1993,** *180,* 65–93.

[40] Halpern, J.; Okamoto, T.; Zakhariev, A. *J. Mol. Catal.* **1976,** *2,* 65–68.

[41] Schrock, R. R.; Osborn, J. A. *J. Am. Chem. Soc.* **1976,** *98,* 2134–2143.

[42] Halpern, J. *Science* **1982,** *217,* 401–407.

[43] Alario, F.; Amrani, Y.; Colleuille, Y.; Dang, T. P.; Jenck, J.; Morel, D.; Sinou, D. *J. Chem. Soc.* **1986,** *Chem. Commun.,* 202–203.

[44] Thomas, A.; Haake, M.; annd J. Bargon, F. W. G. *Angew. Chem. Int. Ed. Engl.* **1994,** *33,* 755–757.

[45] Kirrs, R. U.; Eisenschmid, T. C.; Eisenberg, R. *J. Am. Chem. Soc.* **1998,** *110,* 8564–8566.

[46] Koptyug, I.; Kovtunov, K.; Burt, S. R.; Anwar, M.; Hilty, C.; Han, S.; Pines, A.; Sagdeev, R. *J. Am. Chem. Soc.* **2007,** *129,* 5580–5586.

[47] Kovtunov, K. V.; Beck, I. E.; Bukhtiyarov, V. I.; Koptyug, I. V. *Angew. Chem. Int. Ed.* **2008,** *47,* 1492–1495.

[48] Ernst, R. R.; Bodenhausen, G.; Wokaun, A. *Principles of Nuclear Magnetic Resonance in One and Two Dimensions;* Clarendon Press: 1987.

[49] Keeler, J. *Understanding NMR Spectroscopy;* Wiley: 2005.

[50] Steigel, A.; Spiess, H. W. *Dynamic NMR Spectroscopy;* Springer-Verlag Berlin Heidelberg New York: 1978.

[51] Warren, W. S.; Jenista, E.; Branca, R. T.; Chen, X. *Science* **2009,** *23,* 1711–1714.

[52] Carravetta, M.; Johannesson, O. G.; Levitt, M. H. *Phys. Rev. Lett.* **2004,** *92,* 153003.

[53] Carravetta, M.; Levitt, M. H. *J. Am. Chem. Soc.* **2004,** *126,* 6228–6229.

[54] Levitt, M. H.; Carravetta, M. *J. Chem. Phys.* **2005,** *122,* 214505–214514.

[55] Vinogradov, E.; Grant, A. K. *J. Magn. Reson.* **2008,** *194,* 46–57.

[56] Eisenschmid, T. C.; McDonald, J.; Eisenberg, R. *J. Am. Chem. Soc.* **1989,** *111,* 7267–7269.

[57] Barkemeyer, J.; Haake, M.; Bargon, J. *J. Am. Chem. Soc.* **1995,** *117,* 2927–2928.

[58] Golman, K.; Axelsson, O.; Johannesson, H.; Mansson, S.; Olofsson, C.; Petersson, J. S. *Magn. Reson. Med.* **2001,** *46,* 1–5.

[59] Goldman, M.; Johannesson, H. *C. R. Physique* **2005,** *6,* 575–581.

[60] Duckett, S. B.; Newell, C. L.; Eisenberg, R. *J. Am. Chem. Soc.* **1993,** *115,* 1156–1157.

[61] Haake, M.; Natterer, J.; Bargon, J. *J. Am. Chem. Soc.* **1996,** *118,* 8688–8691.

[62] Kuhn, L. T.; Bommerich, U.; Bargon, J. *J. Phys. Chem. A* **2006,** *110,* 3521–3526.

[63] Haake, M. Thesis, University of Bonn, 1996.

[64] Bommerich, U. Thesis, University of Bonn, 2005.

[65] Agel, F. Thesis, University of Bonn, 2004.

[66] Dechent, J. F. F. Thesis, Diploma, Johannes Gutenberg University Mainz, 2009.

[67] Hoevener, J. B.; Chekmenev, E. Y.; Harris, K. C.; Perman, W. H.; Robertson, L. W.; Ross, B. D.; Bhattacharya, P. *Magn. Reson. Mater. Phy.* **2009,** *22,* 111–121.

[68] Roth, M.; Bargon, J.; Spiess, H. W.; Koch, A. *Magn. Reson. Chem.* **2008,** *46,* 713–717.

[69] Schröder, L.; Lowery, T. J.; Hilty, C.; Wemmer, D.; Pines, A. *Science* **2006,** *314,* 446–449.

[70] Bowen, S.; Hilty, C. *Angew. Chem. Int. Ed.* **2008,** *47,* 5235–5237.

[71] Gallagher, F. A.; Kettunen, M. I.; Day, S. E.; Hu, D.-E.; Ardenkjaer-Larsen, J. H.; Zandt, R.; Jensen, P. R.; Karlsson, M.; Golman, K.; Lerche, M. H.; Brindle, K. M. *Nature* **2008,** *453,* 940–943.

[72] Wild, J. M.; Paley, M. N. J.; Viallon, M.; Schreiber, W. G.; van Beek, E. J. R.; Griffiths, P. D. *Magn. Reson. Med.* **2002,** *47,* 687–695.

[73] Hu, S.; Lustig, M.; Chen, A. P.; Crane, J.; Kerr, A.; Kelley, D.; Hurd, R.; Kurhanewicz, J.; Nelson, S.; Pauly, J.; Vigneron, D. *J. Magn. Reson.* **2008,** *192,* 258–264.

[74] Mishkovsky, M.; Frydman, L. *ChemPhysChem* **2008,** *9,* 2340–2348.

[75] Baumer, D.; Brunner, E.; Blümler, P.; P.P. Zänker, H. W. S. *Angew. Chem. Int. Ed.* **2006,** *45,* 7282–7284.

[76] Messerle, B. A.; Sleigh, C. J.; Partridge, M. G.; Duckett, S. B. *J. Chem. Soc.* **1999,** 1429–1435.

[77] Korchak, S. E.; Ivanov, K. L.; Yurkovskaya, A. V.; Vieth, H.-M. *Phys. Chem. Chem. Phys.* **2009,** *11,* 11146–11156.

[78] Stephan, M.; Kohlmann, O.; Niessen, H. G.; Eichhorn, A.; Bargon, J. *Magn. Reson. Chem.* **2002,** *40,* 157–160.

[79] Johansson, E.; Olsson, L.; Mnsson, S.; Petersson, J.; Golman, K.; Sthlberg, F.; Wirestam, R. *Magn. Reson. Med.* **2004,** *52,* 1043–1051.

[80] Chen, A. P.; Kurhanewicz, J.; Bok, R.; Xu, D.; Joun, D.; Zhang, V.; Nelson, S. J.; Hurd, R. E.; Vigneron, D. B. *Magn. Reson. Imag.* **2008,** *26,* 721–726.

[81] Bhattacharya, P.; Chekmenev, E. Y.; Perman, W. H.; Harris, K. C.; Lin, A. P.; Norton, V. A.; Tan, C. T.; Ross, B. D.; Weitekamp, D. P. *J. Magn. Reson.* **2007,** *186,* 150–155.

[82] Chekmenev, E. Y.; Norton, V. A.; Weitekamp, D. P.; Bhattacharya, P. *J. Am. Chem. Soc.* **2009,** *131,* 3164-3165.

[83] Sessions, W. V. *J. Am. Chem. Soc.* **1928,** *50,* 1696–1698.

[84] Müller, E.; Huber-Emden, H. *Annalen d. Chemie* **1962,** *660,* 54–59.

[85] James, M. N. G.; Williams, G. J. B. *Acta Crystallographica B30* **1974,** *5,* 1249–1275.

[86] Schleyer, D.; Niessen, H. G.; Bargon, J. *New. J. Chem.* **2001,** *25,* 423–426.

[87] Hoevener, J. B.; Chekmenev, E. Y.; Harris, K. C.; Perman, W. H.; Tran, T. T.; Ross, B. D.; Bhattacharya, P. *Magn. Reson. Mater. Phy.* **2009,** *22,* 123–134.

[88] Chekmenev, E. Y.; Hoevener, J.; Norton, V. A.; Harris, K.; Batchelder, L. S.; Bhattacharya, P.; Ross, B. D.; Weitekamp, D. P. *J. Am. Chem. Soc.* **2008,** *130,* 4212-4213.

[89] Jonischkeit, T.; Bommerich, U.; Stadler, J.; Woelk, K.; Niessen, H. G.; Bargon, J. *J. Chem. Phys.* **2006,** *124,* 201109-01–201109-05.

[90] Haake, M.; Barkemeyer, J.; Bargon, J. *J. Phys. Chem.* **1995,** *99,* 17539–17543.

[91] Somayaji, V. V.; Hall, T. W.; Wiebe, L. I.; Knaus, E. E. *Journal of Labelled Compod and Radiopharmaceutical* **1988,** *15,* 1325–1331.

[92] Huntress, E. H.; Lesslie, T. E.; Bornstein, J. *Organic Syntheses* **1963,** *Coll. Vol. 4,* 329.

[93] Watanabe, M.; Maemura, K.; Kanbara, K.; Tamayama, T.; Hayasaki, H. *Int. Rev. Cytol.* **2002,** *213,* 1–47.

[94] Majumdar, D.; Guha, S. *J. of Mol. Struc.* **1988,** *180,* 125–140.

[95] Roth, M. Thesis, Diploma, Max Planck Institute for polymer research, 2007.

[96] Mutschler, E.; Geisslinger, G.; Kroemer, H. K.; Ruth, P.; Schäfer-Korting, M. *Lehrbuch der Pharmakologie und Toxikologie;* Wiss. Verl.-Ges., Stuttgart: 1991.

[97] Krieglstein, J.; Ahlemeyer, B. *Pharmakologie und Toxikologie: Lehrbuch fr Studierende der Medizin, Pharmazie und Naturwissenschaften;* Schattauer, Stuttgart, New York: 2000.

[98] Kostka, G.; Urbanek, K.; Ludwicki, J. K. *Toxicology* **2007,** *239,* 127–135.

[99] Neves, J. L.; Heitmann, B.; Reiss, T. O.; Schor, H. H. R.; Khaneja, N.; Glaser, S. J. *J. Magn. Reson.* **2006,** *181,* 126–134.

[100] Khaneja, N.; Reiss, T. O.; Kehlet, C.; Schulte-Herbrggen, T.; Glaser, S. J. *J. Magn. Reson.* **2005,** *172,* 296–305.

[101] Roth, M.; Koch, A.; Kindervater, P.; Bargon, J.; Spiess, H. W.; Münnemann, K. *J. Magn. Reson.* **2010,** *204,* 50–55.

[102] Dean, M. *The Human ATP-Binding Cassette (ABC) Transporter Superfamily;* National Library of Medicine (US), NCBI: 2002.

[103] Petersen, H. *International patent* **2001,** *WO 01/68628 A1,* 1–14.

[104] Koch, A.; Bargon, J. *Magn. Reson. Chem.* **2000,** *38,* 216–220.

[105] BASF, "Technical Data Sheet", Technical Report, BASF corporation, Chemical Division, 1997.

[106] Bühler, V. *Excipients for Pharmaceuticals - Povidone, Crospovidone and Copovidone;* Springer: 2005.

[107] Daubinet, A.; Kaye, P. T. *AKRIVOC* **2003,** 93–104.

[108] Warner, D. T. *J. Org. Chem.* **1959,** *24,* 1536–1539.

[109] Bockmühl, M.; Schwabe, R.; Ehrhart, G. *Reichspatentamtschrift* **1931,** *Nr. 526390 Klasse 12p Gruppe 7,* 1–3.

[110] Malmström, T.; Wendt, O. F.; Andersson, C. *J. Chem. Soc., Dalton Trans.* **1999,** 2871–2875.